On Closed-loop Supply Chain and Routing Problems for Hazardous Materials Transportation with Risk-averse Programming, Robust Optimization and Risk Parity

by

Nasrin Mohabbati Kalejahi

A dissertation submitted to the Graduate Faculty of
Auburn University
in partial fulfillment of the
requirements for the Degree of
Doctor of Philosophy

Auburn, Alabama
August 3, 2019

Keywords: Stochastic Optimization, Robust Programming, Multiobjective Mixed Integer Mathematical Model, Risk Parity, Hazardous Materials Routing, Closed-loop Supply Chain Network Design

Approved by

Alexander Vinel, Chair, Assistant Professor of Industrial and Systems Engineering
Jeffrey Smith, Joe W. Forehand Jr. Professor of Industrial and Systems Engineering
Jorge Valenzuela, Philpott-WestPoint Stevens Endowed Distinguished Professor of Industrial and Systems Engineering
Fadel Megahed, Neil R. Anderson Endowed Assistant Professor of Information Systems and Analytics, Miami University
Selen Cremaschi, B. Redd Associate Professor of Chemical Engineering

" تو به دل هستی و این قوم به گِل می جویند   تو به جان هستی و این جمع جهانگرد انند

خود بده درس محبت که ادیان خرد   همه در مکتب توحید تو شاگرد انند "

شهریار

تقدیم به:

پدرم رسول و مادرم فاطمه، به پاس عاطفه ی سرشار، حمایتهای بی دریغ و گرمای امید بخش وجودشان

خواهرم الهام، به پاس مهربانی بی انتها، هم صحبتی های شیرین و راهنمایی های ارزشمندش

همسرم وحید، امید بودنم، دلیل شادی ام، به پاس همه ی حمایتها و عشق پایان ناپذیرش

Abstract

The objective of this dissertation is to develop mathematical optimization models that assist and improve the decision making process in hazardous materials (hazmat) routing and supply chain network design. First, a mathematical model for hazmat closed-loop supply chain network design problem is proposed. The model, which can be viewed as a way to combine a number of directions previously considered in the literature, considers two echelons in forward direction (production and distribution centers), three echelons in backward direction (collection, recovery and disposal centers) and emergency team positioning with objectives of minimizing the strategic, tactical and operational costs as well as the risk exposure on the road network. Since the forward flow of hazmat is directly related to the reverse flow, and since hazmat accidents can occur in all stages of lifecycle (storage, shipment, loading and unloading, etc), it is argued that such a unified framework is essential. The resulting model is a complicated multiobjective mixed integer programming problem. It is demonstrated how it can be solved with a two-phase solution procedure on a case study based on a standard dataset from Albany, NY. Second, the uncertainties of model parameters such as demand and return are considered. With a known distribution for the uncertain data, a two-stage stochastic optimization model is developed, and its performance is studied on the same case study. A robust optimization framework is developed for the same problem in a case where the distributions of demand and return are unknown. The model characteristics and performance are presented based on the Albany case study. Other than the demand and return, risk exposure on the road network during the hazmat transportation can have uncertainty. Third, the risk involved in the hazmat transportation is taken into account, where Risk Parity idea in conjunction with modern risk-averse stochastic optimization (namely coherent measures of risk) are studied. A generalized Risk Parity model is studied, and a combined two stage diversification-risk framework is proposed. The results of a numerical case study on hazmat routing problem under heavy-tailed

distributions of losses are outlined. The model aims to fairly distribute the hazmat shipment amounts on the road network and promote risk equity on the involved communities.

Acknowledgments

My endless appreciations go to my advisor, Dr. Aleksandr Vinel, for his precious instructions, inspirations and invaluable support in every way possible. I would like to sincerely thank Dr. Jeffrey Smith for his valuable advice, directions and continuous support during these years. My deep appreciations go to Dr. Fadel Megahed for his insightful instructions, constant encouragement, and endless support. I would like to thank Dr. Jorge Valenzuela for his valuable counsels and teachings. My appreciations also go to Dr. Selen Cremasch, for her encouragement, help and kindly accepting to serve as my external committee member. Special thanks to my friends, Oguz Toragay, Qiong Hu, Dongjin Cho, Kyongsun Kim, Hyeoncheol Baik, Amir Mehdizadeh and Chanok Han for their amazing friendship, companionship, kindness, and help.

Finally, I wish to express my deepest love and gratitude to my treasured parents, Mr. and Mrs. Rasoul Mohabbati Kalejahi and Fatemeh Sajjadi, and my sister, soon to be Dr. Elham Mohabbati Kalejahi, for their unconditional love, support, encouragement, and inspiration. My deepest appreciations go to my husband, Dr. Vahid Mirkhani, for his endless love, devotion, generosity and the peace and happiness that he has brought into my life.

Contents

List of Figures

List of Tables

Chapter 1

Introduction, Motivation and Contribution

1.1 Decision Making Under Uncertainty

Decision making under uncertainty and risk have been studied in the operations research and management sciences communities for decades. Making decisions without knowing the full effects of uncertain parameters in a problem is challenging. Such problems appear in many application areas such as manufacturing, transportation, energy systems and healthcare. In a deterministic setting, it is assumed that all parameters of the problem are known in advance. In contrary, in an uncertain environment, decision makers have incomplete information about the dynamics of the system and have to deal with probabilistic functions and potential problem-specific characteristics of the problem. Stochastic optimization under uncertainty is a well-known approach to mathematically address such decision making problems. In these models, the uncertainties of the problem are addressed in a way that their effects on the outcome of the problem can be properly be taken into account. In such settings, decisions often be taken in the phase of the unknown. The consequences of the actions then can be fully determined upon the determination of the uncertainty in a later stage. There might be opportunities to revise the actions later as more becomes known.

Classical stochastic optimization problems consider random variables with a known probability distribution. Such information might be approximated by statistical analysis on available historical data or a domain knowledge of an expert. Let x be a decision vector with a feasible region X and random parameter ω. For simplicity assume that the uncertainty only affects the objective function, then the stochastic optimization problem can be presented as follow:

$$\min_{x \in X} \quad E_\omega[f(x, \omega)]. \tag{1.1}$$

Model (1.1) optimizes the expected value of function f with probabilistic occurrence of random parameter ω . Such formulation is used when the decision maker is risk-neutral and interested in the long-run performance of the solution over a large sample. Ignoring the variability of the parameters makes the model less interesting for certain cases where a well performance of the model is expected under the worst-case realization of the random parameter ω. Robust optimization frameworks are employed to find solutions that have a well performance even if the worst-case realization of uncertain parameters happens over an uncertainty set representing all possible values of the random parameters. Let U be the uncertainty set, then the robust formulation of model (1.1) will be:

$$\min_{x \in X} \quad \max_{\omega \in U} f(x, \omega). \tag{1.2}$$

Model (1.2) assumes that the decision maker is a risk-averse and provides a conservative solution, in which too much optimality is given away to achieve a certain level of robustness. Various approaches are introduced in the context of the robust optimization to balance the level of conservatism. Furthermore, risk-averse stochastic optimization frameworks are introduced to capture a wide range of risk attitudes. In such settings, the risk function ρ can be incorporated to the objective function of the model:

$$\min_{x \in X} \quad \rho(f(x, \omega)). \tag{1.3}$$

The model (1.3) minimized the risk associated with the solution x with realization of random parameters ω. Risk measures can also be employed along with other objective functions such as cost. Regardless of the uncertain environment, many of the real world problems consist of multiple criteria and objectives which are mostly contradictory and incomparable, e.g., the price and quality of a product. In countless studies, optimization models developed to deal with such problems include a single objective function. In such cases, the single objective function either considers the most important criterion or incorporates (weighted) summation of various objectives. Since it is difficult to accurately quantify the conflicting goals and their preferred weights, this approach might result in a solution that is not the best possible option. Therefore, multiobjective optimization methods have been developed to help decision makers avoid mixing peerless objectives, and investigate most preferred strategies in managing the optimization problems.

The focus of this research is developing effective risk-averse stochastic programming and robust optimization frameworks for hazardous materials (hazmat) routing and closed-loop supply chain network design. In Section (1.2), the importance of hazmat logistics and the corresponding literature are presented. Then, the motivation of this research based on the gap in the literature is highlighted. Finally, the contributions of current research are presented in Section (1.3).

1.2 Background and Motivation

Hazmat is used in numerous industries, such as petroleum, agriculture, pharmaceutical medicine, industrial water treatment and electronic device manufacturing, etc, and thus, play an important role in today's world. Production of hazmat as well as the generated waste has tremendously increased in recent decades. Accordingly, the volume of hazmat transportation has been expanding due to the increasing demand for different hazmat types at more and more locations. What distinguishes hazmat transportation from general freight applications is the fact that moving hazmat raises an inherent risk for public safety and environment, which requires a more deliberate planning approach.

According to the Pipeline and Hazardous Material Safety Administration (PHMSA) of the U.S. Department of Transportation (US DOT), a hazmat is defined as any substance or material that is toxic, explosive, corrosive, combustible, poisonous, or radioactive. Each year million tons of hazmat with billion dollars of value are being shipped in the U.S. (National Transportation Statistics 2018). Air, highway, rail, water, and pipeline carriers are five means of hazmat transportation. Trucks carry the largest shares by value, tons, and ton-miles of shipments. More than 17,000 incidents were reported in 2018 for the hazmat highway transportation which accounts for 90% of total hazmat incidents and 88% of the total property damages (PHMSA 2018). This explicitly illustrates the importance of effective supply chain and route planning of truck-based hazmat transportation, which is the focus of this study.

To structure the literature review the existing papers are categorized in four classes: hazmat network design, emergency response team location, waste location-routing, and facility location problems. In this section, only papers with focus of single modal highway transportations are reviewed. The literature review codes are given in Table 1.1 and the reviewed papers are characterized in Table 1.2.4.

Table 1.1: Hazmat supply chain network literature review codes.

Category	Detail	Code
Scope	Network Design	ND
	Emergency Response Team Location	ERTL
	Waste Location-Routing	WLR
	Facility Location	FL
Network Type	Forward logistic	F
	Reverse logistic	R
Network Layers	Supplier/Production/Origin	O
	Distribution center	DC
	Collection center	CS
	Recovery center	RC
	Disposal center	DPC
	Emergency response team	ERT
	Customer/Destination	D
Objective Functions	Cost/Distance/Time Minimization	Cost
	Risk Minimization	Risk

1.2.1 Network Design

Selection of routes in hazmat route planning is determined by different objectives of carriers and local governments. The shipment plans of the carriers are typically made without taking into account other factors and, hence, can cause overloaded links in the network. In order to overcome this difficulty, governments and authorities enforce regulations to control the risk induced by hazmat transportation over the population and the environment, and promote equity in the risk distribution over the road network. Hazmat network design problem considers both carriers' and governments' perspectives for producing routing decisions. The hazmat network design routing problem has two main streams of research: network design routing and toll setting.

Kara and Verter (2004) introduced a bi-level programming model for the hazmat network design problem. In their model, outer problem features the authorities' decisions in determining the road links to be included in the network, whereas the inner problem indicates the carriers decisions in selecting roads that are available in the network. Considering Kara and Verter (2004) model as the base framework, other studies solve the hazmat network design problem by introducing new formulations and heuristic approaches (Erkut and Alp 2007a, Erkut and Gzara 2008, Verter and Kara 2008, Bianco et al. 2009, Amaldi et al. 2011, Gzara 2013, Sattarzadeh 2015, Sun et al. 2015, Xin et al. 2015, Sun et al. 2016, Esfandeh et al. 2017, Fontaine and Minner 2018, Yin et al. 2019).

Toll setting is an alternative hazmat regulation policy that governments and authorities use to reduce the traffic congestion and discourage the carriers from overloaded links in the network (Marcotte et al. 2009, Wang et al. 2012, Bianco et al. 2015, Esfandeh et al. 2016). All these studies consider predefined origin-destination pair(s) and aim to regulate the route selection decisions of carriers. More strategic decisions such as locating centers, managing reverse waste flow, and establishing emergency response teams are not considered in these studies.

1.2.2 Emergency Response Team Location

Specially trained and equipped hazmat emergency response teams are required in case of hazmat incidents. Faster service to the affected areas can result in less amount of fatalities, injuries, and damages. It also can expedite the evacuation of the vulnerable areas, containment, and cleanup process. Xu et al. (2013) presented a bi-level framework similar to Kara and Verter

(2004) in which besides the carriers' route selection decisions in the lower level, emergency response department decides to locate emergency service units with the objective of maximizing the total weighted arc length covered.

In another study, Taslimi et al. (2017) considered a policy to open additional road segments along with the decisions about locating the emergency response teams. Saccomanno and Allen (1987) and Berman et al. (2007) adapted the maximum set and arc covering formulation to find the locations of emergency response teams in a predefined network. Hamouda et al. (2004) and Zografos and Androutsopoulos (2008) suggested decision support systems to establish the emergency response teams with aim of minimizing associated risk and response time. List and Turnquist (1998) developed a multiobjective model to find the nondominated routes for each origin-destination pair, flow assignment on routes, and accordingly the location of the emergency response teams. Ma et al. (2015) also presented a multiobjective mathematical model with objectives of maximizing the coverage, minimizing the response time, and minimizing the transportation and fixed opening costs.

All the studies in hazmat emergency response teams location literature consider predetermined network of origin-destination pair(s) and intend to locate emergency response teams in a way that effectively cover the road network in case of incidents. Other features of the networks such as midway operation and center location decisions are not included in these studies.

1.2.3 Waste Location-Routing

Hazardous wastes produced by various industries such as chemical manufacturers, electroplating companies, and petroleum refineries can become an immediate or long-term threat for people's safety and the environment. Large amount of hazmat wastes needs to be transported from the generation sites to the well-equipped treatment, recovery, and disposal centers to be processed, stored, or disposed. Most of the research in the hazmat waste management literature concentrates on a simultaneous waste facility location and routing decisions. List and Mirchandani (1991) proposed a multiobjective model to find the location of the waste management facilities conjointly with the routing decisions of hazmat wastes. For similar studies, see (Zografos and Samara 1989, ReVelle et al. 1991, Stowers and Palekar 1993, Jacobs and Warmerdam 1994, Current and Ratick 1995, Giannikos 1998, Cappanera et al. 2003, Aboutahoun 2012, Boyer et al. 2013, Berglund and Kwon 2014, Zhao and Zhu 2016). Other studies considered technology selection strategies in opening a waste facility, known as waste-technology compatibility constraint, simultaneously with hazmat waste location-routing decisions (Nema and Gupta 1999, 2003, Alumur and Kara 2007, Emek and Kara 2007, Samanlioglu 2013, Zhao and Verter 2015, Zhao et al. 2016, Yu and Solvang 2016, Ardjmand et al. 2016, Yilmaz et al. 2017, Asgari et al. 2017, Rabbani et al. 2018, Asefi et al. 2019).

Zhao and Ke (2017) incorporated the inventory decisions into designing a hazmat waste management system, where they proposed a single period framework to maximize the transportation efficiency through an optimal utilization of vehicles capacity. Rabbani et al. (2019) studied a similar problem and presented a simulation-optimization approach based on a multi-objective evolutionary algorithm to minimize cost and environmental risk.

The majority of the waste management literature considered problems which deal with the challenge of finding one or multiple suited destination locations for hazmat waste treatments and the shipments of hazmat to these destinations. The forward flow of hazmat products is usually disregarded in these studies, meaning that the stream of hazmat products from an origin to processing locations such as distribution centers and to the end customers is not considered.

1.2.4 Facility Location

Besides waste location-routing problems which focus on the reverse flow of hazmat waste, researchers studied the combination of finding the best location of facilities such as distribution centers, warehouses or depots in the forward hazmat network along with the proper routes between these establishments to the customers. Helander and Melachrinoudis (1997) studied hazmat location-routing problem with the objective of minimizing the expected number of hazardous material shipment accidents. Mahmoudabadi and Seyedhosseini (2014) developed a bi-level programming model to determine the locations of distribution centers and the hazmat transportation routes in the network. For similar studies see (Falit-Baiamonte and Osleeb 2000, Zhang et al. 2005, Mahmoudabadi 2015, Tavakkoli-Moghaddam et al. 2015, Mahmoudabadi et al. 2016).

Meiyi et al. (2015) studied a location-scheduling problem on hazardous materials transportation with preselected routes between each depot and customer pair. Wei et al. (2015) studied the capacitated depot location problem in combination with the vehicle routing planning. They proposed a chance-constrained programming model that produced an optimized balance between the transportation risk and cost. Fan et al. (2019) developed an integer linear programming model for the reliable location-routing of hazmat, in which they considered the depot disruption when deciding on depot location. Hu et al. (2019a) introduced a multiobjective optimization method for finding the hazmat warehouse locations and the routes under the constraint of traffic restrictions in inter-city roads. In the hazmat facility location literature, the forward stream of produced products is considered simultaneously with the routing decisions. These studies ignore the backward flow planning of hazmat returns and wastes as well as locating the emergency response teams in the network.

Zhao et al. (2017) proposed three mathematical models for green supply chain management with the aim of minimizing the inherent risks involved in the hazardous materials such as risk of casualties, risk of environmental pollution and risk of property loss. In their model, the stream of hazmat starts with suppliers and continues to manufacturing sites, distribution centers, and to the end customers. The waste is being collected from customers and shipped to recycling, landfill, and incineration centers meaning that there is not any reverse flow of recovered products in the network. Ma and Li (2018) studied the hazmat closed-loop supply chain network design problem. They developed a mathematical model to make decisions about the optimal location of production-recovery sites in the forward supply chain and collection centers in the reverse supply chain. Their model also determines the quantity of hazmat product and waste shipments through the network. For a through review on hazmat risk assessments and problems see Hu et al. (2019b) and Holeczek (2019).

Table 1.2: Taxonomy of the most relevant literature.

Reference	Scope				Network Type		Layers							Objectives	
	ND	ERTL	WLR	FL	F	R	O	DC	CS	RC	DPC	ERT	D	Cost	Risk
Kara and Verter (2004)	✓				✓		✓						✓	✓	✓
Erkut and Alp (2007a)	✓				✓		✓						✓	✓	✓
Erkut and Gzara (2008)	✓				✓		✓						✓	✓	✓
Verter and Kara (2008)	✓				✓		✓						✓		✓
Bianco et al. (2009)	✓				✓		✓						✓		✓
Amaldi et al. (2011)	✓				✓		✓						✓	✓	✓
Gzara (2013)	✓				✓		✓						✓	✓	✓
Sattarzadeh (2015)	✓				✓		✓						✓	✓	✓
Sun et al. (2015)	✓				✓		✓						✓	✓	✓
Xin et al. (2015)	✓				✓		✓						✓	✓	✓
Sun et al. (2016)	✓				✓		✓						✓	✓	✓
Esfandeh et al. (2017)	✓				✓		✓						✓		✓
Fontaine and Minner (2018)	✓				✓		✓						✓	✓	✓
Yin et al. (2019)	✓				✓		✓						✓		✓
Marcotte et al. (2009)	✓				✓		✓						✓	✓	✓
Wang et al. (2012)	✓				✓		✓						✓	✓	✓
Bianco et al. (2015)	✓				✓		✓						✓	✓	✓

Continued on next page

Table 1.2 – *Continued from previous page*

Reference	Scope				Network Type		Layers							Objectives	
	ND	ERTL	WLR	FL	F	R	O	DC	CS	RC	DPC	ERT	D	Cost	Risk
Esfandeh et al. (2016)	✓				✓		✓						✓	✓	✓
Saccomanno and Allen (1987)		✓			✓		✓					✓	✓		✓
List and Turnquist (1998)		✓			✓		✓					✓	✓	✓	✓
Hamouda et al. (2004)		✓			✓		✓					✓	✓		✓
Berman et al. (2007)		✓			✓		✓					✓	✓	✓	
Zografos and Androutsopoulos (2008)		✓			✓		✓					✓	✓	✓	✓
Xu et al. (2013)	✓	✓			✓		✓					✓	✓	✓	✓
Ma et al. (2015)		✓			✓		✓					✓	✓	✓	✓
Taslimi et al. (2017)	✓	✓			✓		✓					✓	✓	✓	✓
Zografos and Samara (1989)			✓			✓					✓		✓	✓	✓
List and Mirchandani (1991)			✓			✓					✓		✓	✓	✓
ReVelle et al. (1991)			✓			✓					✓		✓	✓	✓
Stowers and Palekar (1993)			✓			✓					✓		✓		✓
Jacobs and Warmerdam (1994)			✓			✓					✓		✓	✓	
Current and Ratick (1995)			✓			✓					✓		✓	✓	✓
Giannikos (1998)			✓			✓					✓		✓	✓	✓
Nema and Gupta (1999)			✓			✓					✓		✓	✓	✓
Nema and Gupta (2003)			✓			✓					✓		✓	✓	✓
Cappanera et al. (2003)			✓			✓					✓		✓	✓	

Continued on next page

Table 1.2 – *Continued from previous page*

Reference	Scope				Network Type		Layers							Objectives	
	ND	ERTL	WLR	FL	F	R	O	DC	CS	RC	DPC	ERT	D	Cost	Risk
Alumur and Kara (2007)			✓			✓					✓		✓	✓	✓
Emek and Kara (2007)			✓			✓				✓	✓		✓	✓	
Aboutahoun (2012)			✓			✓					✓		✓	✓	✓
Boyer et al. (2013)			✓			✓				✓	✓		✓	✓	✓
Samanlioglu (2013)			✓			✓				✓	✓		✓	✓	✓
Berglund and Kwon (2014)			✓			✓					✓		✓	✓	✓
Zhao and Verter (2015)			✓			✓					✓		✓	✓	✓
Ardjmand et al. (2016)			✓			✓			✓		✓		✓	✓	✓
Zhao and Zhu (2016)			✓			✓			✓	✓			✓	✓	✓
Zhao et al. (2016)			✓			✓				✓	✓		✓	✓	✓
Yu and Solvang (2016)			✓			✓				✓	✓		✓	✓	✓
Yilmaz et al. (2017)			✓			✓				✓	✓		✓	✓	✓
Asgari et al. (2017)			✓			✓				✓	✓		✓	✓	✓
Rabbani et al. (2018)			✓			✓				✓	✓		✓	✓	✓
Asefi et al. (2019)			✓			✓				✓	✓		✓	✓	
Rabbani et al. (2019)			✓			✓				✓	✓		✓	✓	✓
Helander and Melachrinoudis (1997)				✓	✓		✓	✓					✓		✓
Falit-Baiamonte and Osleeb (2000)				✓	✓		✓	✓					✓		✓
Zhang et al. (2005)				✓	✓		✓	✓					✓	✓	✓

Continued on next page

Table 1.2 – *Continued from previous page*

Reference	Scope				Network Type		Layers							Objectives	
	ND	ERTL	WLR	FL	F	R	O	DC	CS	RC	DPC	ERT	D	Cost	Risk
Mahmoudabadi and Seyedhosseini (2014)				✓	✓		✓	✓					✓	✓	✓
Mahmoudabadi (2015)				✓	✓		✓	✓					✓	✓	✓
Tavakkoli-Moghaddam et al. (2015)				✓	✓		✓	✓					✓	✓	
Wei et al. (2015)				✓	✓		✓	✓					✓	✓	✓
Meiyi et al. (2015)				✓	✓		✓						✓		✓
Mahmoudabadi et al. (2016)				✓	✓		✓	✓					✓	✓	✓
Fan et al. (2019)				✓	✓		✓	✓					✓		✓
Hu et al. (2019a)				✓	✓		✓	✓					✓	✓	✓
Zhao et al. (2017)			✓	✓	✓		✓	✓			✓		✓	✓	✓
Ma and Li (2018)	✓			✓	✓	✓	✓		✓	✓	✓		✓	✓	
This study	✓	✓	✓	✓	✓	✓	✓	✓	✓	✓	✓	✓	✓	✓	✓

Based on the literature outlined above, hazmat network design and facility location problems have been studied widely, and the emergency response team location problem has gained a considerable attention due to the disastrous consequences caused by hazmat incidents. The risk exposure through the hazmat logistics system is not only limited to the shipment process, it similarly affects the settings where hazmat is produced, processed, stored, and disposed. Such sites thereby signify a potential threat to its surroundings since incidents can happen in the facilities and during loading and unloading process (Erkut and Alp 2007b). Therefore, decisions such as the location of establishments in both forward and reverse hazmat supply chain, the amount of forward flow of hazmat products shipments on the road links along with the amount of the backward stream of hazmat waste, and the routing decisions must be made simultaneously. This is because facility locations and customer allocations have a direct impact on both storage risk and transportation risk as well as the establishment, capacity and operational costs. Such decision-making without considering the simultaneous establishment of emergency response teams could incur significant economic losses due to ineffective response times to reach the vulnerable areas in case of incidents.

1.3 Contribution of the Dissertation

The aim of this research is to present a combined optimization model, which incorporates a closed-loop supply chain decision making framework, with simultaneous incorporation of HERT facility location, which has not been considered in the literature before (see, Table 1.2.4). First, based on the gap in the literature of hazardous materials supply chain network design, a multiobjective mixed integer mathematical model is developed for the problem with aim of minimizing associated costs and risks. The model properties and performance are investigated with a case study based on Albany county in the State of New York. Second, the uncertainty of some model parameters with known distributions are studied and a two-stage stochastic model is proposed to deal with the uncertainty. Then, the uncertainty of parameters investigated in a case that the distributions are unknown. The robust optimization counterpart model is developed to deal with such uncertainty for the same case study.

Since the risk exposure on the road network plays an important role in hazmat logistics, governments and authorities concerned with the risk equity of the hazmat shipments. Risk equity in hazmat transportation is mostly studied in the hazmat network design literature, where the mathematical models are developed to open/close road segments or regulate the shipment amounts by toll setting and pricing. Third, a new unified framework is proposed to promote risk equity in hazmat shipments from two class of risk-averse modeling perspectives: a risk-reward framework, which is usually used in engineering stochastic optimization; and methods based on directly promoting diversification such as Risk Parity and Equal Risk Contribution that often employed in financial applications. The aim of the proposed methods are to ensure that the risks associated with hazmat transportation are distributed evenly among the exposed communities while making sure that overall system risk is controlled.

Chapter 2

Multiobjective Mixed Integer Mathematical Model for Hazardous Materials Closed-loop Supply Chain Network Design with Emergency Response Teams Location

2.1 Introduction

Hazmat route planning is a basic problem in hazmat transportation with the aim of safety management to reduce the occurrence of dangerous events. Hazmat route planning considers selecting one or several paths among available ones between an origin and a destination. The selection criteria depend on the different objectives of the decision makers. One of the involved parties in hazmat transportation is the carriers with the objective of minimizing travel time and cost. The other party is regional and local government authorities, who regulate hazmat transportation with the objective of minimizing the total risk and promoting equity in its spatial distribution. Such regulations impose restrictions on transporting through highly populated areas and the amount of traffic over network links.

The supply chain network design problems can be divided into two categories: forward and reverse logistics. In the forward network, the activities and processes such as manufacturing of new products and their distribution to the customers are planned while in the reverse network collection of the returned (used) products, their inspection, recovery and disposal are carried out. Growing attention is given to the reverse logistics due to the concerns about increasing the resource utilization rate by recovering and recycling, and decreasing environmental pollution by properly managing waste. The performance of the forward and reverse logistics are interrelated and managing them separately results in sub-optimal network design. Integration of forward and backward logistics is known in the literature as the closed-loop supply chain network design problem. In this chapter, we studied the hazmat closed-loop supply chain network design problem considering perspectives of both parties: carriers and government authorities. The proposed supply chain network design problem aims to effectively locate the hazmat facilities such as production, distribution, collection, recovery and disposal centers. It also works toward controlling the quantity of shipments considering the cost and imposed risk, and providing minimum cost and risk routes for carriers. We further also include emergency response team placement decisions as part of the problem. Since hazmat incidents can occur in origin during loading, in transit, in transit storage, and at destination during unloading (PHMSA 2018), it is important to take accident response into consideration when planning the supply chain. All these decisions are made simultaneously for both forward and reverse streams of hazmat.

There are two types of integration in supply chain management: horizontal and vertical (Pishvaee et al. 2010). Considering strategic (long term), tactical (medium term) and operational (short term) planning levels separately, while integrating activities in the same planning level is known as the horizontal integration. Combining the decision-making processes across different planning levels is referred to as the vertical integration. In the strategic level, the decisions are associated with the supply chain configuration, such as opening potential facilities. In the tactical level, it is assumed that configuration of the supply chain is established and the aim is to optimize the production quantity, transportation amounts and customer allocation with respect to various costs such as manufacturing, distribution, collection and disposal. Determination of shipment routes among facilities and customers is associated with the operational planning. Combining forward and reverse logistics decisions is an example of horizontal integration.

In this study, a mathematical model is introduced for hazmat closed-loop supply chain network design (HSCND) problem with elements of both vertical and horizontal integration. The proposed model is capable of handling three levels of strategic, tactical and operational planning decisions: facilities and emergency response teams location, the quantity of shipments across the network with capacity settings of facilities, and hazmat route selection. It also combines the forward and reverse flow of hazmat and integrates hazmat shipment decisions with response team placement. The rest of the chapter is organized as follows. The HSCND problem is defined and a mixed integer mathematical model is proposed in Section 2.2. The two-phase solution method is presented in Section 2.3, which can find all of the Pareto optimal solutions for the problem. Computational results for a case study in Albany county in the State of New York are provided in Section 2.4. Finally, concluding remarks are discussed in Section 2.5.

The main contribution of this chapter is in developing an optimization model, which: a) introduces a new framework for managing hazmat on road networks by considering both carriers and governments perspectives b) integrates hazmat forward and backward logistics to efficiently satisfy customer demands as well as managing hazmat waste, c) integrates the decisions of locating emergency response team to the flow optimization and facility location and capacity decisions, d) selects the best set of routes for hazmat shipments within the network. This study is an effort to bridge the four sides of literature outlined above by introducing a new bi-objective mathematical model, which is capable of handling three levels of decisions: location, flow, and routing. The model and solution procedure are presented in the next sections.

2.2 Problem Definition

A single period, single product, multi-echelon forward-reverse hazmat supply chain network design problem is considered with production and distribution centers in the forward flow and collection, recovery and disposal centers in the backward flow. Hazmat emergency response teams location problem is also included, placing them in such a way that they can effectively respond to the incidents that happen in the facilities, during the loading and unloading as well as shipment. This problem is more complex than regular hazmat network design considering only forward or backward network flows at a time, thereby it requires more effort to model and solve.

The proposed model considers the following assumptions: a) potential locations of production, distribution, collection, recovery and disposal centers as well as the emergency response teams are known a priori; b) customer locations are predetermined and fixed; c) there are no flows between similar facilities e.g. one distribution center to another; d) hazmat demands and returns are deterministic and known. Note that the assumption on deterministic nature of the demand and return (and hence shipment quantities) is fairly restrictive, and a stochastic case should be considered in a future study.

One of the involved parties in hazmat transportation is the carriers with objective of minimizing travel time and cost. Besides the carriers, there are regional and local government authorities, who want to regulate the hazmat transportation with objective of minimization of the total risk and promoting equity in the spatial distribution of risk. Such regulations impose restrictions in transporting high populated areas and the amount of traffic over the network links.

Both parties' perspectives are considered in this model by including two objective functions. First objective function attempts to minimize the total cost of the system and consequently, maximize the profit. The second one seeks to minimize the risk by distributing the shipments on the road segments with lower risk exposure. The decision maker should deal with the trade-offs between these two objectives since they are conflicting, and, in general, incomparable. The purpose of this problem is to determine the optimal number of facilities (e.g. production, distribution, collection, recovery and disposal) to be opened, their optimal locations and capacity, and the optimal quantity of the product and waste flows among facilities and customers. It also determines the optimal number and locations of hazmat emergency response teams. On the operational level, a set of best routes are determined considering the cost and risk objective functions.

2.2.1 Model formulation

The general structure of the proposed closed-loop supply chain is illustrated in Figure 2.1. Production facilities are responsible for providing new products and shipping them to the distribution centers. These products are then shipped to the customers to satisfy their demand through a pull system in the forward direction. The backward flow consists of the returned products from customers, which are then transferred to the collection centers for inspection and testing. The high quality returned products have a capability of entering to the recovery process, i.e. re-manufacturing. Recoverable products are shipped to the production facilities to perform recovery process. Then, they are inserted to the forward flow as recovered products.

The scrap products are transferred from collection centers to the disposal centers in a push system. The hazmat waste will be shipped directly from customers to the disposal centers. The average disposal rate of the returned products is associated with the quality of the returned products.

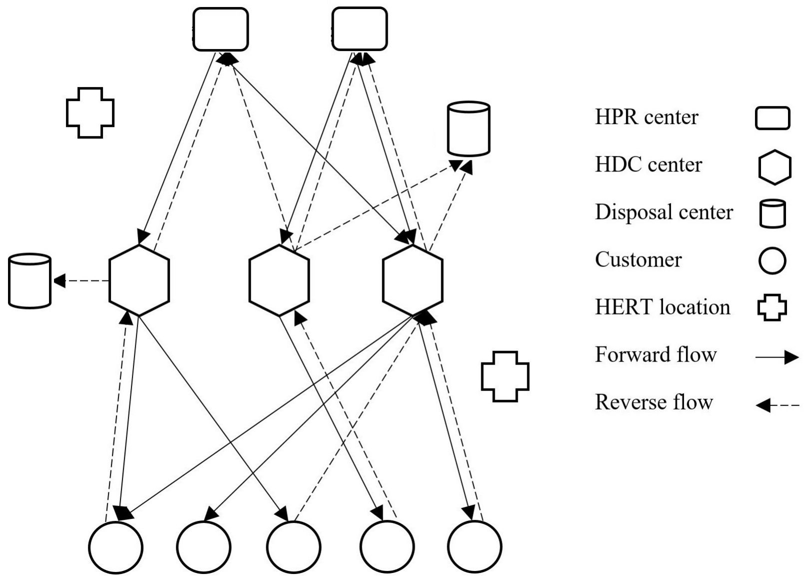

Figure 2.1: Hazmat closed-loop supply chain network structure.

Production facilities can apply any required procedures on the recoverable products and insert them to the forward flow. Therefore, it is assumed that a production and a recovery center can be opened at the same location. Following convention in the literature (Lee and Dong 2008, Hatefi and Jolai 2014) having hybrid production and recovery (HPR) centers are considered. Similarly, distribution and collection centers are considered to be established in the same locations with the name of hybrid distribution and collection (HDC) centers. This strategy results in the cost saving and pollution reduction since the facilities are sharing infrastructure, space, staff, and material handling equipment.

A path-based formulation is used, in which it is assumed that the decision-maker predetermines a set of available paths between each potential center and customer locations. In the case study below, this set is calculated as k shortest paths, but these can be determined in any way. It is also assume that hazmat transportation risk on each arc is pre-evaluated. One of the most popular strategies for risk estimation is based on expected consequence, which combines incident probability (e.g., fixed probability per mile traveled) with an estimate of exposed population (see more details in Section 2.4).

The following notations are defined to formulate the hazmat integrated forward-reverse network design. Equations (2.1)–(2.33) provide problem formulation.

Sets

I	Index set of fixed locations of HPR centers, $i \in I$
J	Index set of potential locations of HDC centers, $j \in J$
K	Index set of potential locations of disposal centers, $k \in K$
M	Index set of potential locations of emergency response team, $m \in M$
L	Index set of fixed locations of customers, $l \in L$
N	Index set of nodes in the network $a, b, c, d \in N$

Parameters

d_l	Quantity of demand of customer *l*
r_l	Return rate of the used products from customer *l*
δ	Average disposal rate of returned products
$MCPC_i$	Maximum production capacity available for HPR center *i*
$MCPR_i$	Maximum recovery capacity available for HPR center *i*
$MCDC_j$	Maximum distribution capacity available for HDC center *j*
$MCDR_j$	Maximum collection capacity available for HDC center *j*
MCK_k	Maximum capacity available for disposal center *k*
f_i	Fixed cost of opening a HPR center *i*
g_j	Fixed cost of opening a HDC center *j*
h_k	Fixed cost of opening disposal center *k*
e_m	Fixed cost of locating hazmat emergency response team *m*

α_i	Manufacturing cost per unit of new products at HPR center *i*
ρ_i	Recovery cost per unit of recoverable products at HPR center *i*
β_j	Distribution cost per unit of products at HDC center *j*
η_j	Collection and sorting cost per unit of returned products at HDC center *j*
γ_k	Disposal cost per unit of scrap products at disposal center *k*
CP_i	Capacity cost per unit of new products at production center *i*
CPC_i	Capacity cost per unit of recoverable products at recovery center *i*
CD_j	Capacity cost per unit of products at distribution center *j*
CDC_j	Capacity cost per unit of returned products at collection center *j*
CK_k	Capacity cost per unit of scrap products at disposal center *k*
TC_{ab}	Transportation cost per unit of products from node *a* to node *b*
D_{ab}	Distance from node *a* to node *b*
Risk_{ab}	Transportation risk on the arc from node *a* to node *b*
P_{ab}	The number of available paths from node *a* to node *b*
KS_{abcdp}	A binary parameter equals to 1 if the arc (*a*,*b*) is used in the *p*-th path of traveling from *c* to *d*
ϕ	Percentage of the nodes that emergency response teams should cover
RT	The risk threshold in the network
RET	The emergency response team's response threshold based on quantity of shipments
CT	The coverage threshold of emergency response teams based on distance
BM	A large number

Decision Variables

Q_i	Binary variable equals to 1 if HPR *i* is opened, 0 otherwise
T_j	Binary variable equals to 1 if HDC center *j* is opened, 0 otherwise
U_k	Binary variable equals to 1 if disposal center *k* is open, 0 otherwise
G_m	Binary variable equals to 1 if emergency response team locates at location *m*, 0 otherwise
X_{ijp}	Quantity of new products shipped from production *i* to distribution *j* on path *p*
E_{ijp}	Quantity of recovered products shipped from production *i* to distribution *j* on path *p*
Y_{jlp}	Quantity of products shipped from distribution *j* to customer *l* on path *p*
Z_{ljp}	Quantity of products returned from customer *l* to collection *j* on path *p*
V_{jip}	Quantity of recoverable products shipped from collection *j* to recovery *i* on path *p*
W_{jkp}	Quantity of returned products shipped from collection *j* to disposal center *k* on path *p*
pc_i	Production capacity of HPR center *i*
pcr_i	Recovery capacity of HPR center *i*
dc_j	Distribution capacity of HDC center *j*
dcr_j	Collection capacity of HDC center *j*
zc_k	Disposal capacity of disposal center *k*
B_{ab}	Quantity shipped on arc (*a*,*b*)
C_{mb}	Binary variable equals to 1 if emergency response team *m* covers node *b*
CC_{mab}	Binary variable equals to 1 if emergency response team *m* covers arc (*a*,*b*)
NC_b	Binary variable equals to 1 if node *b* is covered by at least one emergency response team

$$\min \quad \sum_{i\in I}(f_iQ_i + CP_ipc_i + CPC_ipcr_i) + \sum_{j\in J}(g_jT_j + CD_jdc_j + CDC_jdcr_j)$$
$$+ \sum_{k\in K}(h_kU_k + CK_kzc_k) + \sum_{m\in M} e_mG_m + \sum_{i\in I}\sum_{j\in J}\sum_{p\in P_{ij}} \alpha_iX_{ijp} + \sum_{i\in I}\sum_{j\in J}\sum_{p\in P_{ij}} \rho_iE_{ijp}$$
$$+ \sum_{j\in J}\sum_{l\in L}\sum_{p\in P_{jl}} \beta_jY_{jlp} + \sum_{l\in L}\sum_{j\in J}\sum_{p\in P_{lj}} \eta_jZ_{ljp} + \sum_{j\in J}\sum_{k\in K}\sum_{p\in P_{jk}} \gamma_kW_{jkp} + \sum_{a\in N}\sum_{\substack{b\in N\\ b\neq a}} TC_{ab}B_{ab} \tag{2.1}$$

$$\min \quad \sum_{a\in N}\sum_{\substack{b\in N\\ b\neq a}} Risk_{ab}B_{ab} \tag{2.2}$$

$$\text{s. t.} \quad \sum_{j\in J}\sum_{p\in P_{jl}} Y_{jlp} = d_l, \quad \forall l \in L \tag{2.3}$$

$$\sum_{j\in J}\sum_{p\in P_{lj}} Z_{ljp} = r_ld_l, \quad \forall l \in L \tag{2.4}$$

$$\sum_{i\in I}\sum_{p\in P_{ij}} (X_{ijp} + E_{ijp}) = \sum_{l\in L}\sum_{p\in P_{jl}} Y_{jlp}, \quad \forall j \in J \tag{2.5}$$

$$\sum_{k\in K}\sum_{p\in P_{jk}} W_{jkp} = \delta\sum_{l\in L}\sum_{p\in P_{lj}} Z_{ljp}, \quad \forall j \in J \tag{2.6}$$

$$\sum_{i\in I}\sum_{p\in P_{ji}} V_{jip} = (1-\delta)\sum_{l\in L}\sum_{p\in P_{lj}} Z_{ljp}, \quad \forall j \in J \tag{2.7}$$

$$\sum_{j\in J}\sum_{p\in P_{ji}} V_{jip} = \sum_{j\in J}\sum_{p\in P_{ij}} E_{ijp}, \quad \forall i \in I \tag{2.8}$$

$$\sum_{j\in J}\sum_{p\in P_{ij}} X_{ijp} \leq pc_i, \quad \forall i \in I \tag{2.9}$$

$$pc_i \leq MCPC_iQ_i, \quad \forall i \in I \tag{2.10}$$

$$\sum_{j\in J}\sum_{p\in P_{ij}} X_{ijp} \leq Q_iBM, \quad \forall i \in I \tag{2.11}$$

$$\sum_{j\in J}\sum_{p\in P_{ji}} V_{jip} \leq pcr_i, \quad \forall i \in I \tag{2.12}$$

$$pcr_i \leq MCPR_iQ_i, \quad \forall i \in I \tag{2.13}$$

$$\sum_{j\in J}\sum_{p\in P_{ji}} V_{jip} \leq Q_iBM, \quad \forall i \in I \tag{2.14}$$

$$\sum_{l \in L} \sum_{p \in P_{jl}} Y_{jlp} \leq dc_j, \quad \forall j \in J \tag{2.15}$$

$$dc_j \leq MCDC_j T_j, \quad \forall j \in J \tag{2.16}$$

$$\sum_{l \in L} \sum_{p \in P_{jl}} Y_{jlp} \leq T_j BM, \quad \forall j \in J \tag{2.17}$$

$$\sum_{l \in L} \sum_{p \in P_{lj}} Z_{ljp} \leq dcr_j, \quad \forall j \in J \tag{2.18}$$

$$dcr_j \leq MCDR_j T_j, \quad \forall j \in J \tag{2.19}$$

$$\sum_{l \in L} \sum_{p \in P_{lj}} Z_{ljp} \leq T_j BM, \quad \forall j \in J \tag{2.20}$$

$$\sum_{j \in J} \sum_{p \in P_{jk}} W_{jkp} \leq zc_k, \quad \forall k \in K \tag{2.21}$$

$$zc_k \leq MCK_k U_k, \quad \forall k \in K \tag{2.22}$$

$$\sum_{j \in J} \sum_{p \in P_{jk}} W_{jkp} \leq U_k BM, \quad \forall k \in K \tag{2.23}$$

$$\begin{aligned}
&\sum_{j \in J} \sum_{l \in L} \sum_{p \in P_{jl}} KS_{abjlp} Y_{jlp} + \sum_{l \in L} \sum_{j \in J} \sum_{p \in P_{lj}} KS_{abljp} Z_{ljp} + \sum_{j \in J} \sum_{k \in K} \sum_{p \in P_{jk}} KS_{abjkp} W_{jkp} \\
&+ \sum_{j \in J} \sum_{i \in I} \sum_{p \in P_{ji}} KS_{abjip} V_{jip} + \sum_{i \in I} \sum_{j \in J} \sum_{p \in P_{ij}} KS_{abijp} E_{ijp} \\
&+ \sum_{i \in I} \sum_{j \in J} \sum_{p \in P_{ij}} KS_{abijp} X_{ijp} = B_{ab}, \quad \forall a, b \in N
\end{aligned} \tag{2.24}$$

$$D_{mb} C_{mb} \leq CT, \quad \forall m \in M, \forall b \in N \tag{2.25}$$

$$C_{mb} \leq G_m, \quad \forall m \in M, \forall b \in N \tag{2.26}$$

$$\sum_{m \in M} C_{mb} \leq NC_b BM, \quad \forall b \in N \tag{2.27}$$

$$\sum_{m \in M} C_{mb} \geq NC_b, \quad \forall b \in N \tag{2.28}$$

$$\sum_{b \in N} NC_b \geq N\phi \tag{2.29}$$

$$(B_{ab} + B_{ba}) - RET \leq BM \sum_{m \in M} CC_{mab}, \quad \forall a, b \in N \tag{2.30}$$

$$C_{ma} + C_{mb} - 1 \leq CC_{mab}, \quad \forall m \in M, \forall a, b \in N \tag{2.31}$$

$$\frac{1}{2}(C_{ma} + C_{mb}) \geq CC_{mab}, \quad \forall m \in M, \forall a, b \in N \tag{2.32}$$

$$Q_i, T_j, U_k, G_m, C_{mb}, CC_{mab}, NC_b \in \{0, 1\}, \quad \forall i, \forall j, \forall k, \forall l, \forall m, \forall a, b,$$

$$X_{ijp}, E_{ijp}, Y_{jlp}, Z_{ljp}, W_{jkp}, V_{jip}, B_{ab} \geq 0, \quad \forall i, \forall j, \forall k, \forall l, \forall p, \forall a, b,$$

$$pc_i, pcr_i, dc_j, dcr_j, zc_k \geq 0, \quad \forall i, \forall j, \forall k. \tag{2.33}$$

The first objective function (2.1) seeks to minimize three categories of cost: a) the fixed cost of establishing hybrid production/recovery (HPR) centers, hybrid distribution/collection (HDC) centers and disposal centers as well as locating emergency response teams in the network, b) the variable costs including manufacturing cost in the production sites, re-manufacturing cost for recoverable products in the recovery facilities, operating cost in distribution centers, collection and sorting costs for the returned products in the collection centers, and c) related transportation costs of shipments. The other objective function (2.2) aims to minimize the risk of exposure on the network with respect to the associated quantity of shipments on each arc.

Constraints are classified into four categories: a) *Network Flow Balance* constraints which refer to balancing the forward and backward flows in order to fulfill customers' demand, b) *Capacity* constraints which define optimal capacities for each center and guarantee that the network flow does not exceed the maximum available capacity of centers, c) *Arc Flow* constraint defines the amount of shipments on each arc in the network since each arc, d) *Coverage* constraints which assure that centers are covered by emergency response teams and the arcs with shipment amounts larger than a threshold are covered by at least one emergency response team.

Network Flow Balance constraints are presented in equations (2.3) to (2.8). Constraint (2.3) states that the quantity of the products shipped from the distribution centers to each customer using available paths between these centers and customers should be equal to the demand of that specific customer. This constraint guarantees that the demand of each customer is fully satisfied. Constraint (2.4) addresses the quantity of the returned products. Constraint (2.5) assures that both new and recovered products are shipped to customers to satisfy their demands.

Constraints (2.6) and (2.7) refer to the quality of the returned products and state that a proportion of the returned products, i.e., scrap products are shipped to the disposal centers, and the rest transfered to the HPR centers for recovery using available paths between centers and customers. Constraint (2.8) guarantees that all the recoverable products that are shipped to production centers will be inserted into the forward flow after re-manufacturing.

Capacity constraints are enforced with equations (2.9) to (2.23). Constraints (2.9), (2.10) and (2.11) define the production capacity needed in each HPR center and guarantee that the capacity needed to produce new products does not exceed the maximum available capacity for the center. Constraints (2.12), (2.13) and (2.14) define the same conditions for HPR centers. Constraints (2.15), (2.16) and (2.17) determine the distribution capacity of each HDC center and imply that the forward flow from an HDC center should not exceed maximum available capacity. Constraints (2.18), (2.19) and (2.20) determine the collection capacity of each HDC center and state that the reverse flow to a HDC center should not exceed maximum available capacity. Constraints (2.21), (2.22) and (2.23) define the disposal capacity of each disposal center and impose the capacity restriction of each disposal center in receiving the returned materials i.e., scrap products and hazmat waste from customers.

Arc Flow constraint (2.24) determines the cumulative amount of shipments on each arc in the road network. *Coverage* constraints are described with equations (2.25) to (2.32). Coverage can be defined in a number of different ways. Here, a global parameter , referred to as *coverage threshold (CT)*, is defined which corresponds to the coverage radius of a response team, i.e, defines the reach of a response team, within which it can effectively respond to an incident. Note that it can easily be modified to be dependent on the location of the response team. it is also assumed that an arc in the network is covered if nodes at both ends of the arc are within the coverage threshold of a response team. With that, the following requirements for response team placement are considered: a) at least ϕ nodes in the network should be within CT of a response team; b) all arcs with sufficiently large amount of shipped hazmat (exceeding a value referred to as *response threshold, RET*) have to be covered by a team. Constraint (2.25) defines the coverage of nodes in the network by emergency response teams. Specifically, it is assumed that a node is covered if it is within a given threshold from an established response team. Constraint (2.26) states that an emergency response team can cover a node only if it is established. Constraints (2.27), (2.28) and (2.29) guarantee that ϕ percent of the network is covered by the emergency response teams. Constraint (2.30) assures that if a cumulative shipment amount on an arc exceed a threshold, at least one emergency response team should cover that arc. Constraints (2.31) and (2.32) indicate that an arc is covered by an emergency response team if both nodes of the arc are covered by the same team. Constraint (2.33) refers to the binary and non-negativity restrictions on the corresponding decision variables.

2.3 Solution Approach: Two-Phase Method

Our proposed model contains two objective functions, minimization of cost and risk, as well as integer variables. For this reason, solution to the problem consists of a set of discrete non-dominated points located on the Pareto front. Note that due to presence of integer variables, Pareto front is not necessarily convex. Multiobjective optimization methods can often be classified into Criteria Space Search (CSS) approaches (see, among others Haimes 1971, Ulungu and Teghem 1995) and Decision Space Search (DSS) algorithms (see, among others Stidsen et al. 2014, Stidsen and Andersen 2018).

Criteria Space Search (CSS) algorithms and Decision Space Search (DSS) algorithm are two categories of main approaches to solve multiobjective mixed integer programming (MOMIP) models. The CSS algorithms are iterative processes in which extra constraints are added to the base MOMIP model's criteria space to create a series of single-objective optimization models and find the Pareto optimal solutions. The Pareto optimal solutions are nondominated solutions which cannot be improved in one objective function without deteriorating their performance in at least one of the other objectives. The set of Pareto optimal solutions shape a Pareto front. The ϵ-constraint method and the two-phase method are two effective CSS algorithms widely used to solve various MOMIP models. The ϵ-constraint method finds lexicographic points by optimizing one of the objective functions at a time and restricting the rest of the objectives as constraints within user-specific values. The drawback of this method is that it might not find all the solutions in the Pareto front. The two-phase method starts with the two supported extreme nondominated points and finds all the points of the Pareto front by solving a series of single-objective models.

DSS algorithms are basically branch-and-bound algorithms, modified to handle more than one objective. Various types of branching, probing, and fathoming strategies are studied for MOMIP problems. Most of the general branch and bound algorithms for MOMIP models in the literature allow only two objective functions and require the integer variables to be binary, and the continuous variables occur in only one of the two objectives (Parragh and Tricoire (2018)), which cause a restriction in implementation on cases that do not follow such structure. Also, such approaches are computationally inefficient for large scale problems.

In order to obtain solutions to the proposed model, the two-phase method introduced by Ulungu and Teghem (1995) as an effective CSS algorithm is employed. The specific structure of the solution methodology is adapted from Stidsen et al. (2014). The two-phase method starts with obtaining two nondominated supported (located on the convex hull of the Pareto front) extreme solutions named as the upper left (z^{UL}) and the lower right (z^{LR}) points, respectively. These two points are associated with the minimum cost ($z_1(x, y)$) and minimum risk ($z_2(x, y)$) solutions in our bi-objective model. The rest of the supported extreme nondominated points in between of these two points are usually found using a parametric optimization problem. To do so, a search direction λ is defined and then the following parametric optimization problem is solved:

$$\begin{aligned} \min \quad & z_\lambda(x, y) = \lambda z_1(x, y) + z_2(x, y) \\ \text{s. t.} \quad & (x, y) \in \mathbb{X}, \end{aligned} \tag{2.34}$$

where $\lambda \in \mathbb{R}_+$ and $\mathbb{X}$ is a set of feasible solutions for the bi-objective model. The search stops when all possible combination of consecutive points are considered. Algorithm 1 demonstrates the steps in the first phase. Phase two is employed to find all the nondominated supported nonextreme and nondominated unsupported solutions as in Algorithm 2.

Phase two starts with the list of sorted (based on z_1) nondominated solutions attained in phase one, creating a set of triangles using two sequential points and a local nadir point to be searched iteratively. The search for the rest of the nondominated points in this triangle can be carried out by adding a set of constraints to (2.34):

$$\begin{aligned}
\min \quad & z_\lambda(x, y) = \lambda z_1(x, y) + z_2(x, y) \\
\text{s. t.} \quad & z_1(x, y) \leq z_1^- \\
& z_2(x, y) \leq z_2^+ \\
& z_\lambda(x, y) \leq UB \\
& z_\lambda(x, y) \geq LB \\
& \sum_{j=1}^{n} \{x_j | x_j^+ = 0\} + \sum_{j=1}^{n} \{1 - x_j | x_j^+ = 1\} \geq 1 \\
& \sum_{j=1}^{n} \{x_j | x_j^- = 0\} + \sum_{j=1}^{n} \{1 - x_j | x_j^- = 1\} \geq 1
\end{aligned} \tag{2.35}$$

The last two constraints are know as no-good , which are added as cuts to the search space to eliminate the previously found solutions. The search continues until all the triangles have been investigated and all the nondominated solutions have been found. Providing all Pareto solutions, the decision maker can select the most preferred solution among all.

Algorithm 1: Two Phase Method - Phase I

Data: $z^{UL} := (z_1^{UL}, z_2^{UL})$ and $z^{LR} := (z_1^{LR}, z_2^{LR})$.

Result: $\varphi :=$ nondominated supported extreme points.

begin

- $\varphi \longleftarrow \{z^{UL}, z^{LR}\}$
- $z^+ \longleftarrow z^{UL}$; $z^- \longleftarrow z^{LR}$
- **while** $z^+ \neq z^{LR}$ **do**
  - $\lambda \longleftarrow \lambda(z^+, z^-)$
  - solve (2.34) such that (x^*, y^*) is the optimal solution
  - **if** $z_\lambda(x^*, y^*) < \lambda z_1^+ + z_2^+$ **then**
    - add $z^* = (z_1(x^*, y^*), z_2(x^*, y^*))$ to φ between z^+ and z^-
  - **else**
    - $z^+ \longleftarrow z^-$; $z^- \longleftarrow Next(\varphi, z^+)$

Algorithm 2: Two Phase Method - Phase 2

Data: φ and z^{UL}, z^{LR} first and last pints in φ.

Result: $\vartheta :=$ all nondominated points.

begin

$\vartheta \longleftarrow \varphi$

$z^{+} \longleftarrow z^{UL}$; $z^{-} \longleftarrow Next(\varphi, z^{+})$

for $i \leftarrow 1$ *(to numbe of points in φ)-1* **do**

$\lambda \longleftarrow \lambda(z^{+}, z^{-})$

$LB \longleftarrow \lambda z_1^{+} + z_2^{+}; UB \longleftarrow \lambda z_1^{-} + z_2^{+}$

while $LB \neq UB$ **do**

solve (2.35)

if *finds optimal solution (x^{*}, y^{*})* **then**

add $z^n = (z_1(x^*, y^*), z_2(x^*, y^*))$ to ϑ if it is nondominated

else

return

add a no-good constraint corresponding to z^n

$LB \longleftarrow \lambda z_1^n + z_2^n$

$z^{+} \longleftarrow z^{-}; z^{-} \longleftarrow Next(\varphi, z^{+})$

2.4 Computational Results: A Case Study

To study the behavior of the hazmat closed-loop supply chain network design problem and evaluate the performance of the proposed model, a case study is performed. The study is based on a case presented in Toumazis et al. (2013), based on the area around Albany, NY. The region, shown in Figure 2.2, includes seven interstate highways, and is a key junction of major hazmat transportation activity (Kang et al. 2014). Results are presented from the computational experiments based on a network with 90 nodes and 148 arcs with potential spots for four HPR, five HDC, three disposal centers, three emergency response teams, and ten predefined customers. Certain parameters are randomly generated based on uniform distribution functions presented in Table 2.1. The average disposal rate is considered to be 20% and the 20 shortest paths from each potential centers to other destination nodes are extracted using Yen's k-shortest path algorithm (Yen 1971).

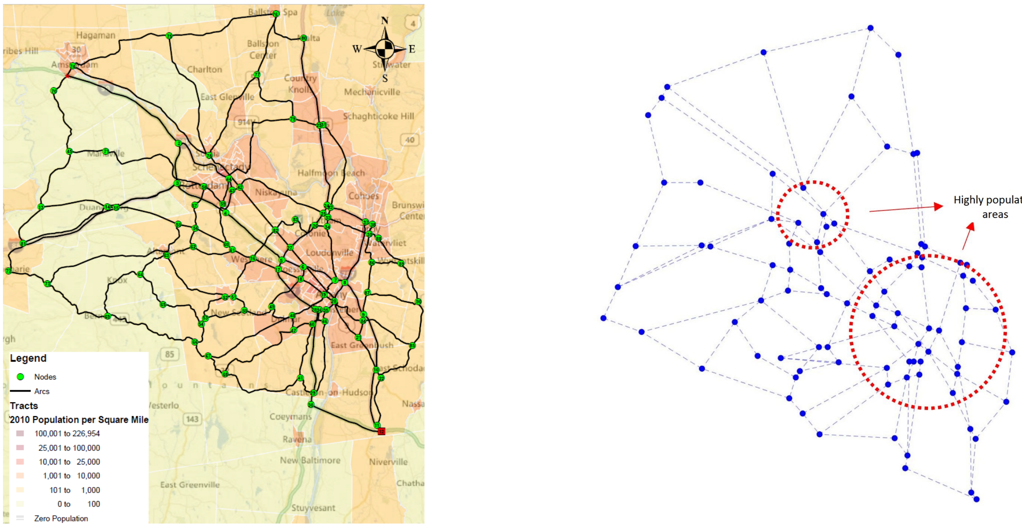

a) Actual network with population densities (Toumazis 2015)

b) Simplified representation

Figure 2.2: Alternative Representations of the Albany network.

Table 2.1: Source of model parameters generation.

Parameter	Random distribution	Parameter	Random distribution
d_m	∼Uniform (150,230)	α_i	∼Uniform (0.003,0.005)
r_m	∼Uniform(0.1,0.3)	ρ_i	∼Uniform (0.002,0.004)
$MCPC_i$	∼Uniform(800,1000)	β_j	∼Uniform (0.002,0.004)
$MCPR_i$	∼Uniform (250,450)	η_j	∼Uniform (0.002,0.003)
$MCDC_j$	∼Uniform (550,850)	γ_k	∼Uniform (0.003,0.004)
$MCDR_j$	∼Uniform (200,400)	CP_i	∼Uniform (50,70)
MCK_k	∼Uniform (450,650)	CPC_i	∼Uniform (25,45)
f_i	∼Uniform (400,450)	CD_j	∼Uniform(30,65)
g_j	∼Uniform (200,250)	CDC_j	∼Uniform(10,40)
h_k	∼Uniform (150,200)	CK_k	∼Uniform(25,40)
e_m	∼Uniform (60,200)	TC_{ab}	∼Uniform(0,0.02)

Knowing the accident probabilities and potential consequences is important in order to calculate the risk parameter on each arc of the network. The human health aspect of a hazmat accident is quantified by estimating the number of individuals that can suffer the consequences of a dangerous materials release. The average population density in the neighborhood of a road segment is the critical factor in calculating the accident consequences. In this case study, the risk and distance parameters are initiated using real data presented by Toumazis (2015).

The effect of certain parameter changes in designing hazmat supply chain network is investigated, namely: a) ϕ, b) CT, and c) RET. These parameters can be initialized by the decision maker (mostly governments and local authorities) based on their strategy in dealing with the problem. In this case study, it is considered setting the percentage of the nodes covered by emergency response teams as $\phi = \{1, 0.8\}$ corresponding to full and partial coverage of the network by emergency response teams. Other parameters such as the coverage threshold of emergency response teams depends on ϕ and the distance between pairs of emergency response teams and different centers and customers (D_{ma}). Note that for a fixed value ϕ there exists a value, which is denoted as $Dmin$, such that if $CT < Dmin$, then the problem becomes infeasible, since there is a limited number of potential response team locations. This value can be calculated with the following optimization problem:

$$\begin{aligned} \min \quad & Dmin \\ \text{s. t.} \quad & D_{ma}X_{ma} \leq Dmin, \quad \forall m \in M, \forall a \in N \\ & \sum_{m \in M} X_{ma} \leq NC_a BM, \quad \forall a \in N \\ & \sum_{m \in M} X_{ma} \geq NC_a, \quad \forall a \in N \\ & \sum_{a \in N} NC_a \geq N\phi \\ & Dmin \geq 0; \quad X_{ma} \in \{0,1\}, \quad \forall m \in M, a \in N, \end{aligned} \tag{2.36}$$

where X_{ma} is defined as a binary variable equal to 1 if emergency response team m covers node a knowing that there is a distance threshold $Dmin$. For all cases first this problem is solved in order to determine appropriate range of parameter CT.

All computations were performed on a 3.50GHz Intel(R) Xeon(R) computer system with 64.0GB RAM. AMPL with Gurobi solver and AMPL API in Matlab2018b are used to run mathematical model instances and implementation of the two phase method. The computation time for solving a single-objective version of the full HSCND model (Phase I) was 4.48 seconds in average. Extracting the full Pareto front for each instance of the problem using two phase method takes 117.32 seconds in average. Two separate cases are considered depending on the value of parameter ϕ.

2.4.1 Case 1: $\phi = 1$

For case 1, the full network coverage by emergency response teams with $\phi = 1$ is considered. Using the model provided in (2.36) the $Dmin = 22.2$ is achieved, which is the lower bound for CT parameter. Setting $CT_{LB} = 22.2$ means that each node of the network is in the reach of at least one emergency response team. Therefore, the upper bound for CT here is 42.7, which allows all nodes to be in reach of all potential emergency response teams. In this case, since all nodes are required to be covered, all arcs are covered as well, and hence parameter RET does not affect the solution. The Pareto fronts for thee sets of associated parameters are demonstrated in Figure 2.3.

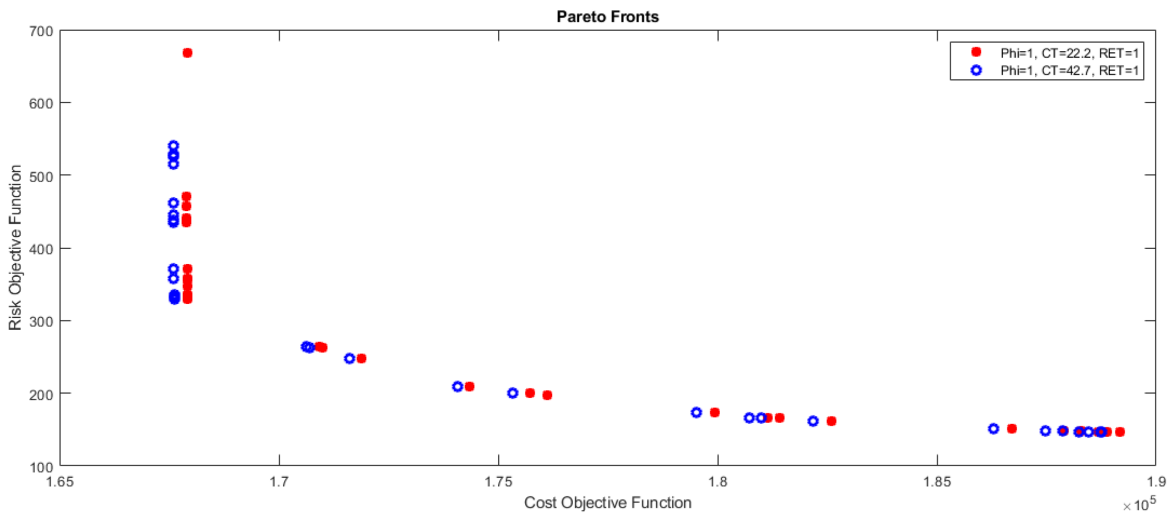

Figure 2.3: Pareto front for various instances of the HSCND problem with $\phi = 1$.

Based on the results presented in Figure 2.3, changing the CT parameter does not change the Pareto front significantly. The slight difference between two Pareto fronts are based on different locations of emergency response teams and their associated costs. For this case, three notable points are investigated on the Pareto front of the instance with the lower bound of parameter CT, i.e., $CT = 22.2$. These three critical points of the Pareto front of Figure 2.3 are: a) upper left point associated with the minimum cost solution, b) maximum curvature associated with the middle point where the slope changes dramatically, c) lower right point associated with minimum risk solution. Comparing points (a) and (b) indicates that a slight increase in the cost objective function results in a huge decrease in risk objective, i.e., 0.01% cost increase, 30% risk decrease. The minimum cost network has a cost objective function value of 167899.6 units with highest imposed risk of 470.7 units. The Pareto front achieved by our proposed model suggests a better network design with a very similar cost of 167915.8 units but a considerably lower imposed risk of 330.4 units. Comparing points (a) and (c) shows 11% increase in cost function and 69% decrease in risk objective value. While a decision maker should select the most preferred network among the suggested ones based on budget restrictions or risk regulations, it must be noted that in this case the only viable solutions are between points b) and c). Three resulted network configurations corresponding to points (a), (b), and (c) with the locations of centers and emergency response teams as well as the routing decisions are presented in Figure 2.4. Throughout the Albany network presentations, the green nodes indicate production/recovery facilities location, the blue nodes show distribution/collection centers, the purple nodes demonstrate disposal centers, the orange nodes are for customer locations, and the red pentagrams show establishment of the emergency response teams.

Networks presented in the Figure 2.4 demonstrate how the location and routing decisions change between the solutions on the Pareto front. The minimum risk network avoids populated areas to open facilities and route the shipments. Comparing solutions (a) and (c) the location of hybrid production/recovery facilities, hybrid distribution/collection facilities, disposal centers and emergency response teams change. Using the Yen's k-shortest path algorithm, 20 routes are available between each facility-to-facility pair and facility-to-customer pairs. In solution (a), 43% of the routes are the first shortest paths and 84% of routes are first, second, third and

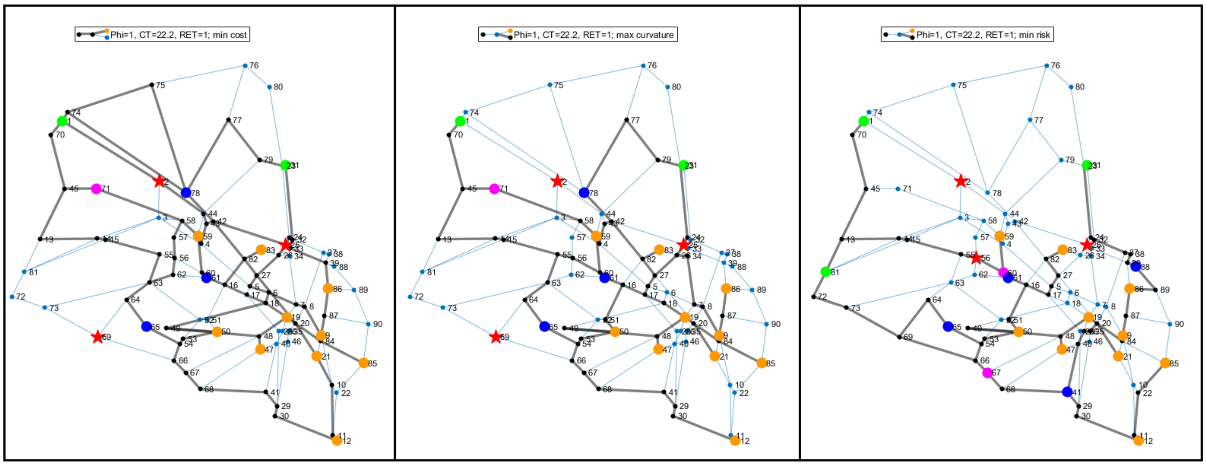

Figure 2.4: Minimum cost, maximum curvature, and minimum risk closed-loop supply chain designs for $\phi = 1$. Green nodes indicate production/recovery facilities, blue nodes indicate distribution/collection centers, purple nodes indicate disposal centers, orange nodes indicate customer locations, and red pentagrams indicate the emergency response teams.

forth shortest paths among the centers and customers since the objective is to minimize the cost. In solution (c), 54% of the routes are the first shortest paths, and 72% of routes are first, second, third and forth shortest paths. This indicates that the minimum risk solution is still reasonable for the carriers to be selected in terms of the transportation cost and time. Also, routes with longer distances (up to 17th best route) are selected to avoid the highly populated areas.

2.4.2 Case 2: $\phi = 0.8$

Setting ϕ to any value rather than 1 will result in different optimal solutions and affect the structure of the defined network as well as the cost and imposed risk, which highlights the importance of making location decisions of the emergency response teams simultaneously with the forward and reverse logistics. With $\phi = 0.8$, the minimum distance to cover all 80% of the network nodes is determined to be $Dmin = 12.2$ using model (2.36). Accordingly, the quantity of shipments on each road segments becomes important to determine coverage. In order to achieve a feasible solution the lower bound for RET is determined as $RET_{LB} = 98$. The problem converges to the same Pareto front for large values of RET since such values relax the RET related constraints. Figure 2.5 demonstrate a set of Pareto solutions considering $\phi = 0.8, CT = 12.2$, and varying the RET parameter.

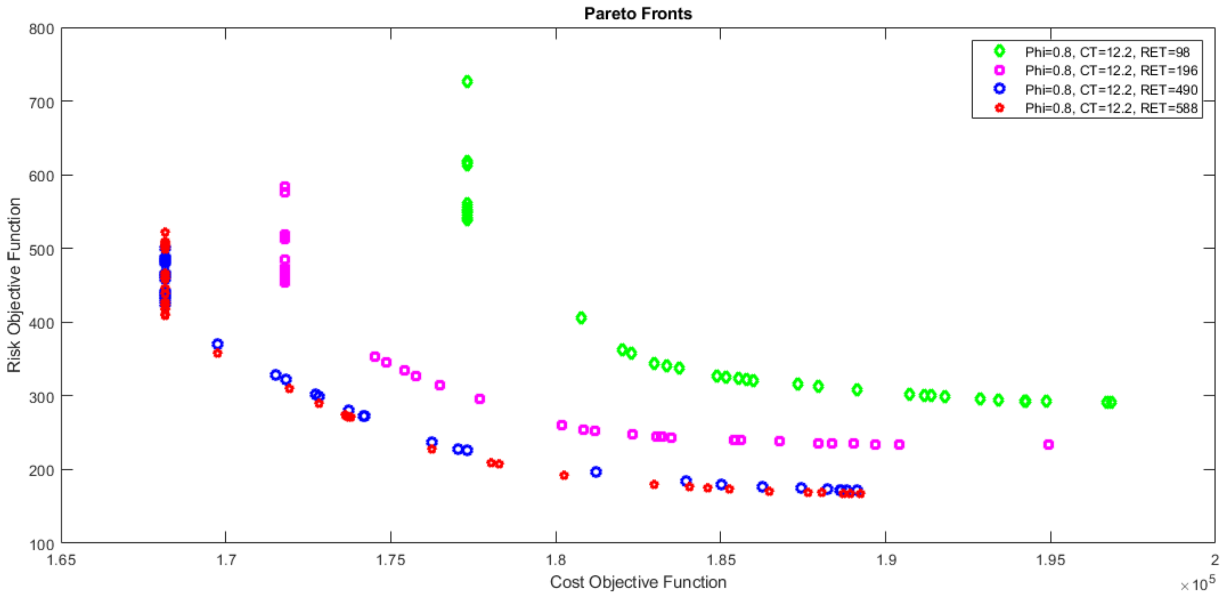

Figure 2.5: Pareto front for various instances of the HSCND problem with $\phi = 0.8, CT = 12.2$ and varying RET.

The resulted Pareto fronts presented in Figure 2.5 show how changing the strategies of the decision maker can cause different networks with wide range of cost and imposed risk. RET parameter can be regulated by government and local authorities to control the overloaded segments across the road network. Results also demonstrate that an appropriate set of parameters can decrease the associated cost and risk and present a better network. Each Pareto front in Figure 2.5 also has three critical points: a) upper left point associated with the minimum cost solution, b) maximum curvature associated with the middle point where the slope changes dramatically, c) lower right point associated with minimum risk solution. The shape and slope of the Pareto fronts demonstrate how slightly increasing the cost objective value can result in a remarkable reduction of the risk objective.

The effect of varying CT in case of $\phi = 0.8$ is also investigated. Figure 2.6 shows the Pareto fronts for two different instances of the problem considering $CT = 12.2$ and $CT = 24.4$ (double the $Dmin$ value). As we discussed before, the $RET_{LB} = 98$ for the first case. Doubling the CT results in $RET_{LB} = 1$, meaning that it relaxes the corresponding constraints.

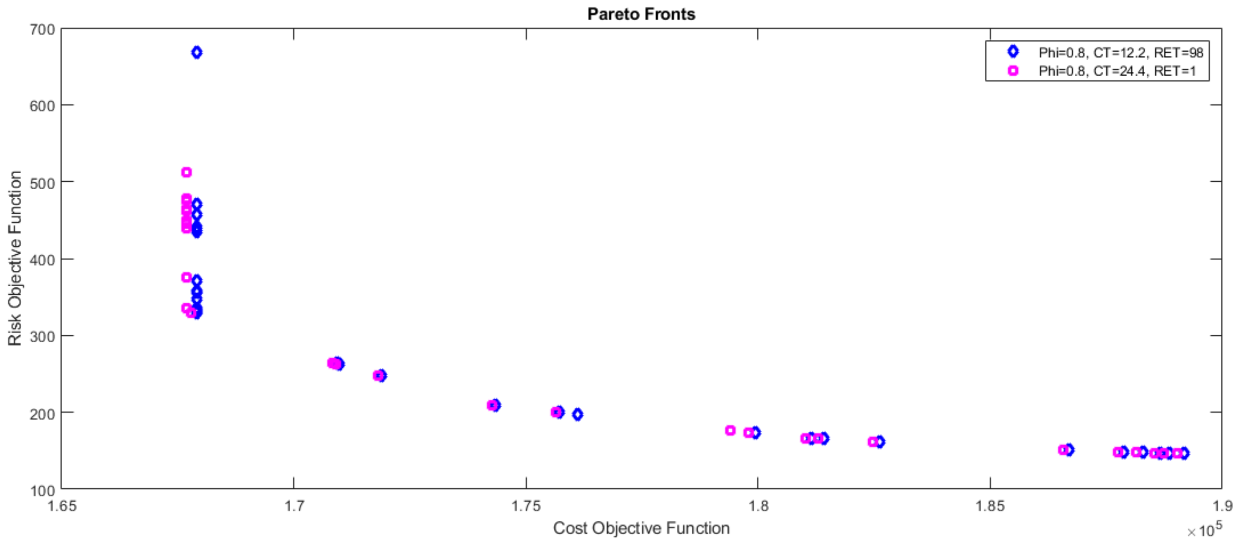

Figure 2.6: Pareto front for various instances of the HSCND problem with $\phi = 0.8$ and varying CT.

Results in Figure 2.6 show that increasing the lower bound of parameter CT relaxes the effect of RET parameter. Any increase in RET parameter doesn't influence the Pareto front significantly. It is possible to compare the supply chain network designs of instances with $\phi = 0.8$ on Figure 2.7. The first two network designs (I and II) refer to the minimum cost and minimum risk networks in the case of $CT = 12.2$ corresponding to the green Pareto front in Figure 2.5. The second two network designs (III and IV) are associated with the minimum cost and minimum risk networks in the case of $CT = 24.4$ corresponding to the blue Pareto front in Figure 2.6.

Figure 2.7 demonstrates how the location and routing decisions change through the solutions on different Pareto fronts. The first two network designs (i.e., I and II) are very restricted and do not allow for much avoidance of the populated areas. Although the routing decisions are different in each network. For network (I) 48% of the routes are the first shortest paths, and 80% of the routes are first, second, third and forth shortest paths among the centers and customers while network (II) has 30% of the first shortest paths, meaning that it ships along longer routes to reduce the imposed risk. The second two network designs (i.e., III and IV) provide better solutions in comparison to networks (I) and (II) and have similar behavior to the case 1 where $\phi = 1$. The routing planning in network (IV) shows well avoidance of highly populated areas using 65% of the first shortest paths. This means the model provides reasonable solution for carriers in respect to cost of transportation while ensuring minimum risk exposure. Network (III) used the first shortest paths 88% of the time.

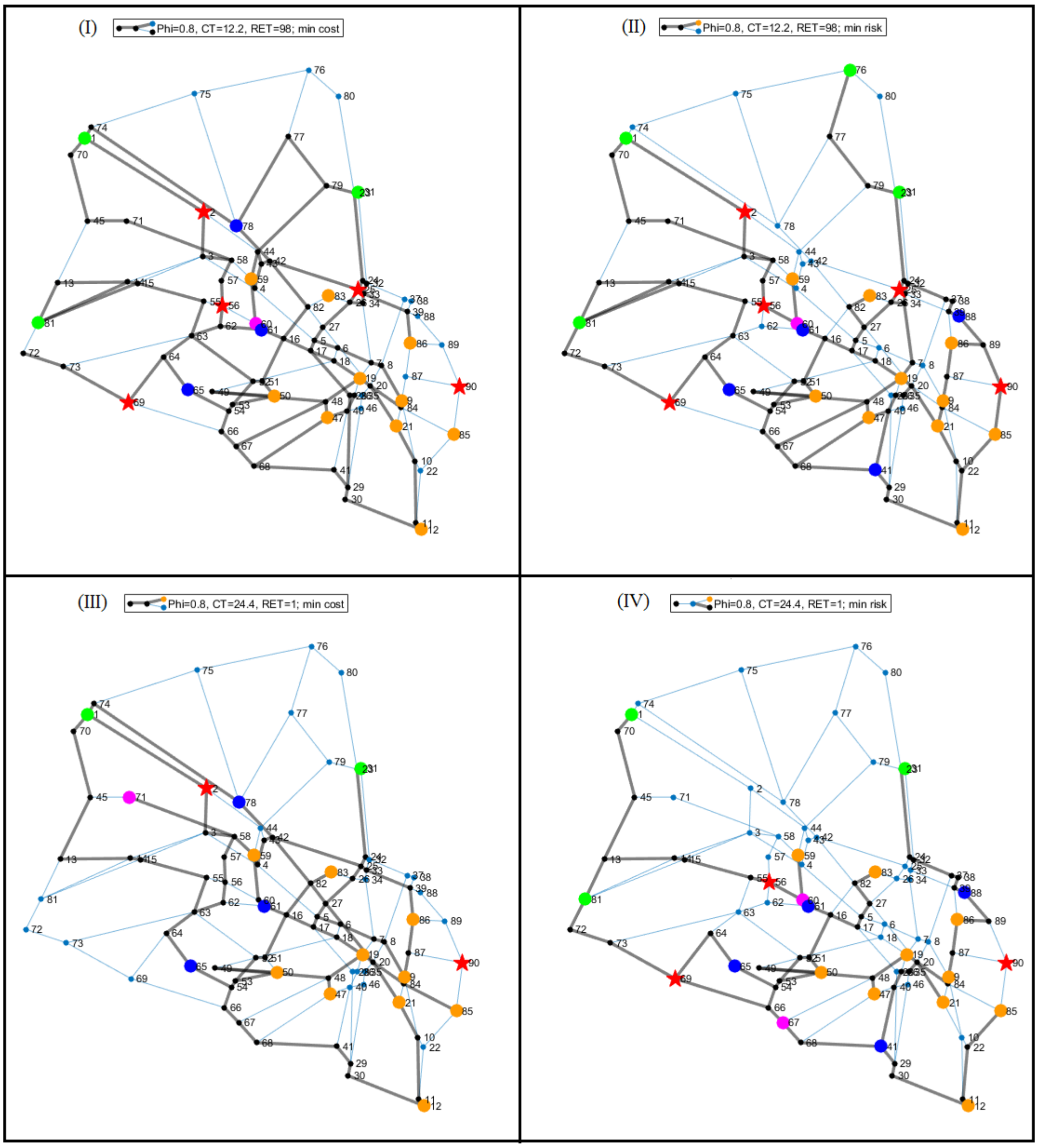

Figure 2.7: Minimum cost and minimum risk closed-loop supply chain designs for various instances of $\phi = 0.8$. Green nodes indicate production/recovery facilities, blue nodes indicate distribution/collection centers, purple nodes indicate disposal centers, orange nodes indicate customer locations, and red pentagrams indicate the emergency response teams.

To sum up, the Pareto front can depend heavily on the choice of parameters. Further, the cost and risk values are dependent on where on the Pareto front the solution in question is located. At the same time, t in all tested cases Pareto fronts exhibit similar shape. Specifically, compared to the overall minimum cost solution, it is always possible to sacrifice a little bit of cost for a large improvement in risk up to a point after which the relationship reverses, i.e., smaller improvement in risk can only be bought with larger increase in costs. Hence, a decision maker may be directed to only consider the points between maximum curvature and minimum risk points.

2.5 Conclusion

Increases of hazmat product and waste shipments, as well as environmental concerns, have been attracting a growing attention to hazmat return logistics management in addition to traditionally considered forward logistics. The risk involved in hazmat transportation makes the hazmat supply chain network design different and more challenging than the regular networks due to a larger number of components that need to be incorporated into the design. In this chapter, the hazmat closed-loop supply chain network design problem is investigated considering two echelons in forward direction (production and distribution centers) and three echelons in backward direction (collection, recovery and disposal centers). Cost is a critical factor in establishing hazmat supply chain and consists of fixed costs of opening centers, operational cost in these centers, and transportation costs. Risk is another important factor in hazmats logistics, which is a measure of accident occurrence probability and the consequence of such accidents. A bi-objective mixed integer mathematical model is proposed that is able to jointly address the importance of cost and risk factors in building the hazmat closed-loop supply chain network. The proposed model helps with making strategic and tactical decisions such as the number and locations of the facility establishments and their capacity settings. In reality, separating the routing from facility siting is not efficient, since selection of the centers implies selection of routes in a sense that there must exist appropriate routes from an origin to a destination for the flow of products and waste. In addition, to move the solution method closer to the practical application, multiple paths between every possible origin-destination pair is considered and the model is allowed to find optimal sets for route planning.

In order to have an effective system, the model makes the decisions regarding the required number of emergency response teams and their locations simultaneously with other strategic decisions. The reason is that the facility locations directly influence the routing decisions, where both affect the location of emergency response teams. The Albany county network in the State of New York is employed to illustrate the application of the developed model. The effect of certain parameters on the hazmat supply chain network design is investigated and the associated solutions are presented. The effects of uncertainty in demand and return parameters are investigated in Chapter 3. In an stochastic environment risk-averse approaches such as Conditional Value-at-Risk (CVaR) can be employed to study the uncertainty of the risk parameter in designing the hazmat routing and supply chain, which more explained in Chapter 4.

Chapter 3

Stochastic and Robust Optimization of Hazmat Closed-loop Supply Chain Network Design with Emergency Response Teams Location

3.1 Introduction

In the previous chapter, a deterministic mixed integer programming model for hazmat closed-loop supply chain network design is introduced. Under this setting, it is assumed that all the parameters such as demand and return are known. Therefore, the best decision is to ship exactly the demand and return quantities to fulfill customers' needs and minimize associated costs and risk.

In practice, some decisions should be made before realization of some parameters. Consider a case where the facility placement decisions should be made before the realization of the demand and return. One possible way to proceed this problem is to view demand and return as random variables. It is possible to assume that the probability distribution of demand and return are known, where the distributions can be estimated from historical data. Therefore, the expected value of the total cost and risk can be calculated which rely on the placement decisions and shipment quantities by utilizing stochastic optimization framework. Such formulation approaches the problem by minimizing the total cost and risk on average, meaning that by the Law of Large Numbers, for a fixed placement decisions, the average of the total cost and risk, over many repetitions will converge to the expected value and the solution will be optimal on average.

To apply such framework to hazmat closed-loop supply chain network design problem, a two-stage stochastic optimization model is presented. In the first stage, the decisions regarding the placement of centers and their capacities are made before a realization of demand and return become known. At the second stage, with realization of demand and return, the decision maker takes recourse action of shipping the required quantities to fully satisfy the demand and return on an extra cost. In case of finitely many scenarios, it is possible to model the stochastic program as a deterministic optimization problem by writing the expected value as the weighted sum of probabilities multiplied to the associated values. In the two-stage programming, the second-stage problem is feasible for every possible realization of the random data.

On the other hand, there might be cases in practice, where a new product is introduced or a new market is exploited. Therefore, there is not enough historical data to estimate the distribution of demand and return. Robust optimization is used where the probability distribution of the uncertain data is unknown. It assumes that the uncertain data resides in the an uncertainty set. Classic robust programming does not allow constraint violation for any realization of the data in the uncertainty set. Robust optimization models are computationally tractable for many classes of uncertainty sets and problem types, which makes them attractive for various real-world applications.

The rest of this chapter is organized as follow. In Section (3.2) a two-stage stochastic optimization model for HSCND with uncertainty in demand and return is presented. The model performance on the Albany case study is analyzed. In Section (3.3) first the necessary background and definitions in robust optimization are presented. Then, a robust optimization model for HSCND is introduced and sensitivity analysis on involved parameters based on Albany case study is done to determine the model effectiveness.

3.2 Two-Stage Stochastic Optimization Approach

In this section, a two-stage stochastic optimization model is introduced for hazmat closed-loop supply chain network design (HSCND) problem, which addresses an integration of strategic, tactical and operational planning levels. Strategic decisions include finding the best locations for establishing facilities and defining their capacities The tactical decisions are defining quantity of shipments across the network. The operational decisions refer to the transportation routing decisions based on the associated transportation costs and risks. The proposed model contains two objective functions to fulfill both governments' and carries' goals in designing the hazmat network. The model considers two echelons in forward direction and three echelons in backward direction, i.e., hybrid production-recovery (HPR), hybrid distribution-collection (HDC) centers and disposal centers. The hazmat emergency response teams (HERT) location decisions are made simultaneously with both forward and reverse logistics design.

The uncertainties in demand and return are considered with known probabilities (scenarios) in this section. In the first stage, strategic decisions such as location and capacities of facilities are determined before realizing any uncertain parameter. In the second stage, tactical and operational decisions such as network flows and routings are made after the realization of uncertain parameters. The decision of establishing the emergency response teams is made simultaneously with the flow and routing decisions in the second stage. Followings show the notations and the proposed model.

Sets

I	Index set of potential locations of HPR centers, $i \in I$
J	Index set of potential locations of HDC centers, $j \in J$
K	Index set of potential locations of disposal centers, $k \in K$
M	Index set of potential locations of emergency response team, $m \in M$
L	Index set of fixed locations of customers, $l \in L$
N	Index set of nodes in the network $a, b, c, d \in N$
S	Index set of transportation risk scenarios $s \in S$

Parameters

d_{ls}	Demand of customer *l* in scenario *s*
r_{ls}	Return rate of customer *l* in scenario *s*
δ	Average disposal rate of returned products
$MCPC_i$	Maximum production capacity available for HPR center *i*
$MCPR_i$	Maximum recovery capacity available for HPR center *i*
$MCDC_j$	Maximum distribution capacity available for HDC center *j*
$MCDR_j$	Maximum collection capacity available for HDC center *j*
MCK_k	Maximum capacity available for disposal center *k*

f_i Fixed cost of opening a HPR center *i*

g_j Fixed cost of opening a HDC center *j*

h_k Fixed cost of opening disposal center *k*

e_m Fixed cost of locating hazmat emergency response team *m*

α_i Manufacturing cost per unit of new products at HPR center *i*

ρ_i Recovery cost per unit of recoverable products at HPR center *i*

β_j Distribution cost per unit of products at HDC center *j*

η_j Collection and sorting cost per unit of returned products at HDC center *j*

γ_k Disposal cost per unit of scrap products at disposal center *k*

CP_i Capacity cost per unit of new products at production center *i*

CPC_i Capacity cost per unit of recoverable products at recovery center *i*

CD_j Capacity cost per unit of products at distribution center *j*

CDC_j Capacity cost per unit of returned products at collection center *j*

CK_k Capacity cost per unit of scrap products at disposal center *k*

TC_{ab} Transportation cost per unit of products from node *a* to node *b*

D_{ab} Distance from node *a* to node *b*

$Risk_{ab}$ Transportation risk on the arc from node *a* to node *b* in scenario *s*

pr_s Probability of scenario s

P_{ab} The number of available paths from node *a* to node *b*

KS_{abcdp} A binary parameter equals to 1 if the arc (*a*,*b*) is used in the *p*-th path of traveling from *c* to *d*

ϕ Percentage of the nodes that emergency response teams should cover

RET The emergency response team's response threshold based on quantity of shipments

CT The coverage threshold of emergency response teams based on distance

BM A large number

Decision Variables

Q_i	Binary variable equals to 1 if HPR *i* is opened, 0 otherwise
T_j	Binary variable equals to 1 if HDC center *j* is opened, 0 otherwise
U_k	Binary variable equals to 1 if disposal center *k* is open, 0 otherwise
G_{ms}	Binary variable equals to 1 if ERT *m* is established in scenario s, 0 otherwise
X_{ijps}	Quantity of new products shipped from HPR *i* to HDC *j* on path *p* in scenario *s*
E_{ijps}	Quantity of recovered products shipped from HPR *i* to HDC *j* on path *p* in scenario *s*
Y_{jlps}	Quantity of products shipped from HDC *j* to customer *l* on path *p* in scenario *s*
Z_{ljps}	Quantity of products returned from customer *l* to HDC *j* on path *p* in scenario *s*
V_{jips}	Quantity of recoverable products from HDC *j* to HPR *i* on path *p* in scenario *s*
W_{jkps}	Quantity of returned products from HDC *j* to disposal center *k* on path *p* in scenario *s*
pc_i	Production capacity of HPR center *i*
pcr_i	Recovery capacity of HPR center *i*
dc_j	Distribution capacity of HDC center *j*
dcr_j	Collection capacity of HDC center *j*
zc_k	Disposal capacity of disposal center *k*
B_{abs}	Quantity shipped on arc (*a*,*b*) in scenario *s*
C_{mbs}	Binary variable equals to 1 if ERT *m* covers node *b* in scenario s
CC_{mabs}	Binary variable equals to 1 if ERT *m* covers arc (*a*,*b*) in scenario s
NC_{bs}	Binary variable equals to 1 if node *b* is covered by at least one ERT in scenario s

$$\min \quad \sum_{i\in I}(f_iQ_i + CP_ipc_i + CPC_ipcr_i) + \sum_{j\in J}(g_jT_j + CD_jdc_j + CDC_jdcr_j)$$

$$+ \sum_{k\in K}(h_kU_k + CK_kzc_k) + E[Q(x,\xi)] \tag{3.1}$$

$$\text{s. t.} \quad pc_i \leq MCPC_iQ_i, \quad \forall i \in I \tag{3.2}$$

$$pcr_i \leq MCPR_iQ_i, \quad \forall i \in I \tag{3.3}$$

$$dc_j \leq MCDC_jT_j, \quad \forall j \in J \tag{3.4}$$

$$dcr_j \leq MCDR_jT_j, \quad \forall j \in J \tag{3.5}$$

$$zc_k \leq MCK_kU_k, \quad \forall k \in K \tag{3.6}$$

$$Q_i, T_j, U_k, pc_i, pcr_i, dc_j, dcr_j, zc_k \geq 0, \forall i, \forall j, \forall k \tag{3.7}$$

where $E[Q(x,\xi)]$ denotes the recourse function with decision variables symbolized by x and uncertainty associated to the model ξ. For the given scenario ξ_s, the $Q(x,\xi)$ represents the Pareto optimal values for two objective functions of the second stage problem (3.8)-(3.35):

$$\min \quad \sum_{i\in I}\sum_{j\in J}\sum_{p\in P_{ij}}\sum_{s\in S}\alpha_iX_{ijps} + \sum_{i\in I}\sum_{j\in J}\sum_{p\in P_{ij}}\sum_{s\in S}\rho_iE_{ijps} + \sum_{j\in J}\sum_{l\in L}\sum_{p\in P_{jl}}\sum_{s\in S}\beta_jY_{jlps}$$

$$+ \sum_{l\in L}\sum_{j\in J}\sum_{p\in P_{lj}}\sum_{s\in S}\eta_jZ_{ljps} + \sum_{j\in J}\sum_{k\in K}\sum_{p\in P_{jk}}\sum_{s\in S}\gamma_kW_{jkps} + \sum_{a\in N}\sum_{\substack{b\in N\\ b\neq a}}\sum_{s\in S}TC_{ab}B_{abs}$$

$$+ \sum_{m\in M}e_mG_{ms} \tag{3.8}$$

$$\min \quad \sum_{a\in N}\sum_{\substack{b\in N\\ b\neq a}}\sum_{s\in S}Risk_{ab}B_{abs} \tag{3.9}$$

$$\text{s. t.} \quad \sum_{j \in J} \sum_{p \in P_{jl}} Y_{jlps} = d_{ls}, \quad \forall l \in L, \forall s \in S \tag{3.10}$$

$$\sum_{j \in J} \sum_{p \in P_{lj}} Z_{ljps} = r_{ls} d_{ls}, \quad \forall l \in L, \forall s \in S \tag{3.11}$$

$$\sum_{i \in I} \sum_{p \in P_{ij}} (X_{ijps} + E_{ijps}) = \sum_{l \in L} \sum_{p \in P_{jl}} Y_{jlps}, \quad \forall j \in J, \forall s \in S \tag{3.12}$$

$$\sum_{k \in K} \sum_{p \in P_{jk}} W_{jkps} = \delta \sum_{l \in L} \sum_{p \in P_{lj}} Z_{ljps}, \quad \forall j \in J, \forall s \in S \tag{3.13}$$

$$\sum_{i \in I} \sum_{p \in P_{ji}} V_{jips} = (1 - \delta) \sum_{l \in L} \sum_{p \in P_{lj}} Z_{ljps}, \quad \forall j \in J, \forall s \in S \tag{3.14}$$

$$\sum_{j \in J} \sum_{p \in P_{ji}} V_{jips} = \sum_{j \in J} \sum_{p \in P_{ij}} E_{ijps}, \quad \forall i \in I, \forall s \in S \tag{3.15}$$

$$\sum_{j \in J} \sum_{p \in P_{ij}} X_{ijps} \leq pc_i, \quad \forall i \in I, \forall s \in S \tag{3.16}$$

$$\sum_{j \in J} \sum_{p \in P_{ij}} X_{ijps} \leq Q_i BM, \quad \forall i \in I, \forall s \in S \tag{3.17}$$

$$\sum_{j \in J} \sum_{p \in P_{ji}} V_{jips} \leq pcr_i, \quad \forall i \in I, \forall s \in S \tag{3.18}$$

$$\sum_{j \in J} \sum_{p \in P_{ji}} V_{jips} \leq Q_i BM, \quad \forall i \in I, \forall s \in S \tag{3.19}$$

$$\sum_{l \in L} \sum_{p \in P_{jl}} Y_{jlps} \leq dc_j, \quad \forall j \in J, \forall s \in S \tag{3.20}$$

$$\sum_{l \in L} \sum_{p \in P_{jl}} Y_{jlps} \leq T_j BM, \quad \forall j \in J, \forall s \in S \tag{3.21}$$

$$\sum_{l \in L} \sum_{p \in P_{lj}} Z_{ljps} \leq dcr_j, \quad \forall j \in J, \forall s \in S \tag{3.22}$$

$$\sum_{l \in L} \sum_{p \in P_{lj}} Z_{ljps} \leq T_j BM, \quad \forall j \in J, \forall s \in S \tag{3.23}$$

$$\sum_{j \in J} \sum_{p \in P_{jk}} W_{jkps} \leq zc_k, \quad \forall k \in K, \forall s \in S \tag{3.24}$$

$$\sum_{j \in J} \sum_{p \in P_{jk}} W_{jkps} \leq U_k BM, \quad \forall k \in K, \forall s \in S \tag{3.25}$$

$$\sum_{j\in J}\sum_{l\in L}\sum_{p\in P_{jl}} KS_{abjlp}Y_{jlps} + \sum_{l\in L}\sum_{j\in J}\sum_{p\in P_{lj}} KS_{abljp}Z_{ljps} + \sum_{j\in J}\sum_{k\in K}\sum_{p\in P_{jk}} KS_{abjkp}W_{jkps}$$
$$+ \sum_{j\in J}\sum_{i\in I}\sum_{p\in P_{ji}} KS_{abjip}V_{jips} + \sum_{i\in I}\sum_{j\in J}\sum_{p\in P_{ij}} KS_{abijp}E_{ijps}$$
$$+ \sum_{i\in I}\sum_{j\in J}\sum_{p\in P_{ij}} KS_{abijp}X_{ijps} = B_{abs}, \quad \forall a,b \in N, \forall s \in S \tag{3.26}$$

$$D_{mb}C_{mbs} \leq CT, \quad \forall m \in M, \forall b \in N, \forall s \in S \tag{3.27}$$

$$C_{mbs} \leq G_{ms}, \quad \forall m \in M, \forall b \in N, \forall s \in S \tag{3.28}$$

$$\sum_{m\in M} C_{mbs} \leq NC_{bs}BM, \quad \forall b \in N, \forall s \in S \tag{3.29}$$

$$\sum_{m\in M} C_{mbs} \geq NC_{bs}, \quad \forall b \in N, \forall s \in S \tag{3.30}$$

$$\sum_{b\in N} NC_{bs} \geq N\phi \quad \forall s \in S \tag{3.31}$$

$$(B_{abs} + B_{bas}) - RET \leq BM \sum_{m\in M} CC_{mabs}, \forall a,b \in N, \forall s \in S \tag{3.32}$$

$$C_{mas} + C_{mbs} - 1 \leq CC_{mabs}, \quad \forall m \in M, \forall a,b \in N, \forall s \in S \tag{3.33}$$

$$\frac{1}{2}(C_{mas} + C_{mbs}) \geq CC_{mabs}, \quad \forall m \in M, \forall a,b \in N, \forall s \in S \tag{3.34}$$

$$G_{ms}, C_{mbs}, CC_{mabs}, NC_{bs} \in \{0,1\}, X_{ijps}, E_{ijps}, Y_{jlps}, Z_{ljps}, W_{jkps}, V_{jips}, B_{abs} \geq 0,$$
$$\forall i \in I, \forall j \in J, \forall k \in K, \forall m \in M, \forall l \in L, \forall p \in P, \forall s \in S, \forall a,b \in N. \tag{3.35}$$

The first stage objective function (3.1) aims to minimize the fixed cost of locating hybrid production/recovery (HPR) centers, hybrid distribution/collection (HDC) centers and disposal centers in the road network. It also minimizes the capacity costs of establishing different centers. Constraint sets (3.2) to (3.6) guarantee that if a center is decided to be established, the capacity assigned to that center will not exceed the maximum available capacity. Constraint (3.7) indicates non-negativity of the first stage decision variables.

The second stage objective function (3.8) minimizes the operational cost of different centers, transportation cost on the road network, and the cost of establishing emergency response teams. The objective function (3.9) minimizes the risk exposure on the network with respect to the associated risk measure and quantity of shipments on each arc. Similar to the deterministic model, network flow balance constraints are presented in equations (3.10) to (3.15). These constraints ensure that the customers' demand and return are satisfied and the hazmat product and waste flows are addressed accordingly. Constraints (3.16) and (3.25) guarantee that the shipments do not exceed the assigned capacities of the corresponding centers in the first stage. Arc flow constraint (3.26) determines the cumulative amount of shipments on each arc in the road network, which is important in risk and transportation cost calculations.

Constraint (3.27) defines the coverage of nodes in the network by emergency response teams in a way that if the distance between an emergency response team and a node is less than a specific distance, the emergency response team would be cover the center in case of an incident. Constraint (3.28) states that an emergency response team can cover a node if it is established. Constraints (3.29), (3.30) and (3.31) guarantee that ϕ percent of the network is covered by the emergency response teams considering a node is covered if at least one emergency response team covered the node.

Constraint (3.32) assures that if a cumulative shipment amount on an arc exceed a threshold, at least one emergency response team should cover that arc. Constraints (3.33) and (3.34) indicate that an arc is covered by an emergency response team if both nodes of the arc are covered by the same team. Constraint (3.35) refers to the binary and non-negativity restrictions on the corresponding decision variables.

The above model shows the sequence of events in the recourse problem where first stage decisions are made in the presence of demand and return uncertainties. After a realization of these uncertain parameters, the recourse decisions such as shipment amounts and the routing decision are made. First-stage decisions are, however, chosen by taking their future effects into account. These future effects are measured by the value function or recourse objective function, which computes the expected value of taking first stage decisions.

It is possible to combine all the cost objective functions in both stages and write them as a single objective function with the assigned probabilities of each scenario, and combine all the constraint into a single optimization model. Such representation is called deterministic equivalent program of the two-stage stochastic model. The deterministic equivalent model is used to investigate the performance of the model.

3.2.1 Computational Results: A Case Study

The main concern of this chapter is to design an effective hazmat supply chain in the presence of uncertainty. Two different sources of uncertainty are considered in this chapter: demand quantities and return quantities. The demand and return amounts could be affected by unexpected events such as appearance of new competitors, new products, or change in customers' use patterns. The proposed two-stage stochastic model determines the locations of the centers and their capacities at the first stage decisions in realization of the recourse forward and reverse network flows to meet the demand and return. In this section, the same Albany case study that was presented in Chapter 2, is used to showcase the proposed model's performance. Since the parameter setting effects are investigated in Chapter 2, here we don't focus on different parameter settings and instead we study the stochastic model performance under different scenarios. The parameters are set to $\phi = 1, CT = 22.2, RET = 1$ for all the computations in this chapter. Total 7 different scenarios are considered for demand. It should be noted that the return is a proportion of demand, consequently, it will have uncertainty too. The average scenario equals to the nominal values in deterministic model. Based on the economical growth, three scenarios are considered for cases with 10%, 20% and 30% lower values than the nominal demand and three other scenarios are for cases with 10%, 20% and 30% growth of the nominal demand. It is assumed that all the scenarios occur with equal probability.

Adding scenario index to the second stage formulation significantly increases the number of decision variables and constraints, whereby, makes the stochastic model computationally more difficult. Although, it is impossible to find a solution that is ideal under all scenarios, decisions in the stochastic model are hedged against various circumstances. In order to evaluate the two-stage stochastic model solutions, two values are employed from the literature (Birge and Louveaux 2011): a) the expected value of perfect information (EVPI), and b) the value of the stochastic solution (VSS).

The EVPI measures the maximum amount a decision maker would be ready to pay in return for complete information about the uncertain data. It is computed as the difference between the objective function of the deterministic problem (know as wait-and-see approach) with the expected value of the stochastic solution (known as the here-and-now approach). In cases where no further information about the future is available the VSS becomes more practically relevant. Table 3.1 shows the EVPI for Albany case study for two solutions on the Pareto front: a) minimum cost and its associated risk, b) minimum risk and its associated cost. First, we assume that we know which scenario will happen for sure and therefore, solve the deterministic model using the corresponding demand and return quantities. The solutions of such assumption is presented in table 3.1 for each scenario. Since in an stochastic environment we will never know for sure which scenario will happen a simple way to plan the system is to consider the mean of all the solutions we found for each scenario. If we use this mean solution for the problem there will be a loss of profit due to presence of uncertainty. The EVPI measures the amount that is worth to pay for the perfect information.

Table 3.1: Demonstrating EVPI for two solutions on the Pareto front by comparing stochastic model solutions with the average performance of seven scenarios.

	Scenarios							Mean	Stochastic Solution	EVPI (%)
	1 (-30%)	2 (-20%)	3 (-10%)	4 (nominal)	5 (+10%)	6 (+20%)	7 (+30%)			
min cost	112616.90	131044.17	149471.56	167912.82	187240.93	207521.12	228950.77	169251.18	228915.42	26.06
risk	309.38	359.35	406.87	667.81	568.18	613.37	616.62	505.94	555.80	8.97
cost	132292.14	150468.49	167958.01	189179.48	210264.72	231471.09	252283.64	190559.65	252279.07	24.46
min risk	94.30	110.94	127.58	146.77	166.78	187.16	210.00	149.08	149.08	0.00

The results in Table 3.1 indicate that if the decision maker uses the mean solution of scenarios instead of considering the uncertainty in the system, they'll lose 26.06% of the total profit in case of the minimum cost network design and 24.46% of the total profit in case of the minimum risk network design. These values show the importance of considering uncertainty of the system and solving the stochastic model to avoid huge costs and profit lost.

Due to computational difficulties of solving stochastic optimization models, a simpler approach can be replacing all random variables by their expected values. The associated problem is known as the expected value (EV) problem. Thereby, the deterministic model is solved with mean values of demand or return scenarios. The solution obtained from the model is called the expected value solution. Then, the expected result of using the EV solution is defined by placing the deterministic first stage results into the stochastic model and obtaining the expected value with respect to the scenarios. The solution is called the EEV measure. Then the VSS can be measured by calculating the difference between EEV and two-stage stochastic model's solution (SS). Therefore, the VSS measures the goodness of the expected solution value when the expected values are replaced by the random values for the input variables. On other words, VSS measures the possible again from solving the stochastic model.

For the hazmat supply chain network design case study under 7 different scenarios of demand and return uncertainties, the VSS values for minimization of cost and risk objective functions are calculated. In order to do so, the deterministic model solution with the average of all seven scenarios is solved. In the case where the aim is to find a solution with minimum cost, the placements are: HPR = $\{1, 31\}$, HDC=$\{61, 65, 78\}$ and disposal center= $\{71\}$. For scenarios 1, 2 and 3 where the demand expected to be -30%, -20% and -10% of the nominal demand, respectively, the same placement of centers work. Demand quantities in scenario 4 are the average (nominal) values. For scenarios 5, 6, and 7 where the demand expected to be +10%, +20% and +30% of the nominal demand, respectively, the deterministic solution does not work. In these scenarios there is a need for extra centers to be opened to fulfil the demand. For these cases, we consider a penalty to the objective function value for adding extra capacity. For cost minimization case, VSS is as follow:

$$VSS = EEV - SS = 254811.98 - 228915.42 = 25896.56 \tag{3.36}$$

This value measures possible again from solving the stochastic model. In the case where the aim is to find a solution with minimum risk, the deterministic model with average of all scenarios opens extra centers to route shipments in a way that avoids highly populated areas. This centers are not fully used up to their maximum capacities in this solution. But, for scenarios 5,6, and 7 the same solution works since there are enough established centers to fulfill the demand. The placements for this case are : HPR = {1, 31, 81}, HDC={41, 61, 65, 88} and disposal center= {60, 67}. This solution work for all the scenarios, therefore, there is no penalty for any extra capacity. The EEV for minimum risk case has the same value as the stochastic model, therefore, VSS is zero. The reason the VSS is zero for this case is that the first stage solutions are similar for both EV and SS problems. It is argued that even though increasing the number of centers will add to the computational runtime significantly, it can allow more room for altering the first stage decisions and, therefore, make VSS a positive value.

For the sake of comparison the Pareto solutions obtain from deterministic model with nominal demand and two-stage stochastic model in cases of demand and return uncertainties are demonstrated in Figure 3.1.

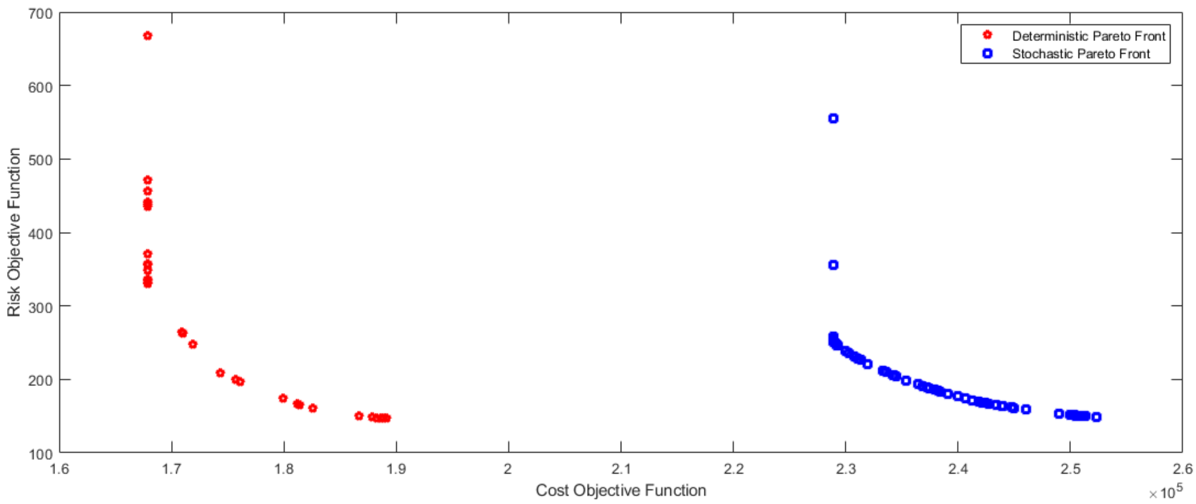

Figure 3.1: Comparing Pareto fronts obtained from the deterministic model with nominal demand and two-stage stochastic model with demand and return uncertainties and $\phi = 1, CT = 22.2, RET = 1$.

The Pareto fronts in Figure 3.1 show how two-stage stochastic model finds solutions that address all involved scenarios. Therefore, the objective function values are higher than the deterministic model as it is expected.

3.3 Robust Programming Approach

In deterministic programming it is always assumed that the input parameters are precisely known for developed optimization models. Even in a case that data can happen to have uncertainty, the model parameters might be approximated by their nominal values (e.g. if the real distribution of the data is known or assumed to be known). In practice, input data uncertainty is inevitable due to the their random nature, measurement errors, or scarcity of information. Data uncertainty can influence the quality and feasibility of the model. If input data take values different than the known or nominal ones, the deterministic optimal solution might no longer be optimal and even it might not be feasible due to violation of some constraints. The robust optimization approach was introduced to immunize the optimization models from the data uncertainty. Robust optimization is used in applications such that the infeasibility of the solution is not tolerable, the parameter uncertainty is not stochastic, or the distributional information for the data is unavailable. The aim of the robust optimization approach is to accept suboptimal solutions for the nominal values of the data in order to ensure that the solution remains feasible and near optimal when data change. In the robust optimization framework, first a deterministic data set is defined within the uncertain space, then the best solution is obtained for the corresponding optimization problem (called robust counterpart optimization problem) with uncertain data. This solution is feasible for any realization of the data uncertainty in the given set.

Since the quantities of demand and return are critical factors in making strategic decisions in hazmat supply chain, depending solely on a stationary or probabilistic distribution can not guarantee the efficiency of the system. Therefore, robust optimization framework is employed to formulate the uncertainty related to demand and return. In this section, first set-induced robust counterpart optimization techniques and related uncertainty sets are presented. Then, a robust optimization model for hazmat closed-loop supply chain network design is introduced.

3.3.1 Uncertainty set-induced robust optimization

In this subsection, the set-induced robust counterpart optimization techniques are presented. The uncertain data are assumed to be varying in a given uncertainty set in the set-induced robust optimization. The aim is to find the best solution among those that are feasible in case of data perturbations in a given uncertainty set. Let matrix A be the coefficient matrix of the constraints with i rows and j columns. Consider the linear optimization problem in (3.37), in which the left hand side (LHS) constraints coefficients are subject to uncertainty:

$$\begin{aligned} \min \quad & cx \\ \text{s. t.} \quad & \sum_j \tilde{a}_{ij} x_j \le b_i, \quad \forall i, \\ & x_j \in X, \quad \forall j, \end{aligned} \tag{3.37}$$

where X indicates a bounded feasible space and $\tilde{a}_{ij}$ represents the true value of the parameters which are subject to uncertainty. It is assumed that the uncertainty affecting each constraint is independent of others. Consider a particular row i of the model constraints, and let J_i represent the subset of variables in row i whose corresponding coefficients are subject to uncertainty. Let $\hat{a}_{ij}$ expresses maximum deviation from the nominal values for the corresponding parameters. The uncertainties for LHS parameters are defined as (3.38):

$$\tilde{a}_{ij} = a_{ij} + \xi_{ij} \hat{a}_{ij}, \quad \forall j \in J_i, \tag{3.38}$$

where ξ_{ij} are independent random variables called the aggregated scaled deviation of uncertain parameters which are distributed in the range of $[-1, 1]$. Under the set-induced robust optimization framework with a predefined uncertainty set U, it is aimed to find a robust solution for the model in (3.37) where the feasibility of the constraints is maintained for any realization of the random variables ξ_{ij}. With definitions in (3.38), the original model in (3.37) can be remodeled as follow:

$$\begin{aligned} \min \quad & cx \\ \text{s. t.} \quad & \sum_j a_{ij}x_j + \max_{\xi \in U}\{\sum_{j \in J_i} \xi_{ij}\hat{a}_{ij}x_j\} \le b_i, \quad \forall i, \\ & x_j \in X, \quad \forall j. \end{aligned} \tag{3.39}$$

3.3.2 Uncertainty Sets

The set-induced robust counterpart formulations in (3.39) depend on the selection of the uncertainty set U. Several uncertainty sets are developed such as box, ellipsoidal, and polyhedral uncertainty sets. The box uncertainty set is defined using the ∞-norm of the uncertain data for each constraint i:

$$U_\infty = \{\xi | \, ||\xi||_\infty \le \Theta\} = \{\xi_{ij} | \, |\xi_{ij}| \le \Theta_i, \quad \forall j \in J_i\} \tag{3.40}$$

where Θ is the adjustable non-negative parameter which controls the size of the uncertainty set. If each data element $\tilde{a}_{ij}$ is modeled as a bounded and independent random variable taking value in an interval $[a_{ij} - \hat{a}_{ij}, a_{ij} + \hat{a}_{ij}]$, then the uncertainty can be represented in form of $\tilde{a}_{ij} = a_{ij} + \xi_{ij}\hat{a}_{ij}, \forall j \in J_i$ as it is presented in (3.38). This is known as the interval uncertainty set which is a special case of box uncertainty set with $\Theta = 1$ (i.e., $U_\infty = \{\xi_{ij} | \, |\xi_{ij}| \le 1, \forall j \in J_i\}$). To obtain a bounded uncertainty, the adjustable parameter is suggested to acquire a rang as $\Theta \le 1$ for the box uncertainty set.

Considering the box uncertainty set, the corresponding robust counterpart constraint in model (3.39) is equivalent to (see Li et al. 2011 for proof):

$$\sum_j a_{ij}x_j + [\Theta_i\{\sum_{j \in J_i} \hat{a}_{ij}|x_j|\}] \le b_i, \quad \forall i. \tag{3.41}$$

Notice that the robust counterpart formulation is constructed constraint by constraint and different parameter values can be applied for different constraints. Constraint (3.41) contains absolute value term $|x_j|$. If the variable is positive, the absolute value operator can be directly removed. Otherwise, it can be further equivalently transformed to the following constraints because their corresponding feasible sets are identical:

$$\begin{cases} \sum_j a_{ij}x_j + [\Theta_i\{\sum_{j\in J_i} \hat{a}_{ij}u_j\}] \leq b_i, \quad \forall i \\ -u_j \leq x_j \leq u_j, \quad \forall j, \\ u_j \geq 0, \quad \forall j. \end{cases} \tag{3.42}$$

The robust formulation proposed by Soyster (1973) employed the same concept with $\Theta_i = 1$ which is known as the most conservative approach and so-called "worst case scenario" robust model for bounded uncertainty. Formulation (3.43) shows Soyster's robust counterpart model:

$$\begin{aligned} \min \quad & cx \\ \text{s. t.} \quad & \sum_j a_{ij}x_j + \sum_{j\in J_i} \hat{a}_{ij}u_j \leq b_i, \quad \forall i \\ & -u_j \leq x_j \leq u_j, \quad \forall j, \\ & x_j \in X, u_j \geq 0, \quad \forall j. \end{aligned} \tag{3.43}$$

The solution of (3.43) remains feasible (i.e., "robust") for every possible realization of the uncertain data $\tilde{a}_{ij}$. To show that, let x^* be the optimal solution of model (3.43). At optimality, $y_j = |x_j^*|$, which reforms the robust counterpart constraint in (3.43) as:

$$\sum_j a_{ij}x_j^* + \sum_{j\in J_i} \hat{a}_{ij}|x_j^*| \leq b_i, \quad \forall i \tag{3.44}$$

With the above definitions, for every possible realization of the uncertain data $\tilde{a}_{ij}$:

$$\sum_j \tilde{a}_{ij}x_j^* = \sum_j a_{ij}x_j^* + \sum_{j\in J_i} \xi_{ij}\hat{a}_{ij}x_j^* \leq \sum_j a_{ij}x_j^* + \sum_{j\in J_i} \hat{a}_{ij}|x_j^*| \leq b_i, \quad \forall i \tag{3.45}$$

For every i-th constraint, the term $\sum_{j\in J_i} \hat{a}_{ij}|x_j|$ gives the necessary protection of the constraint by maintaining a gap between $\sum_j a_{ij}x_j^*$ and b_i. Therefore, this approach provides the highest protection of constraint violations. The robust formulation proposed by Soyster (1973) is too conservative meaning that it assumes all the uncertain data will meet their worst cases which is unlikely to happen in practice. By using such formulation too much of optimality is given up compare to the nominal problem in order to ensure robustness (i.e. the robust solution has worse objective function than the nominal problem).

Ben-Tal and Nemirovski (2000) proposed a robust optimization model with ellipsoidal uncertainty set which is less conservative than the Soyster's approach. The ellipsoidal uncertainty set is defined using the 2-norm of the uncertain data for each constraint i:

$$U_2 = \{\xi | \, ||\xi||_2 \leq \Omega\} = \{\xi_{ij} | \sqrt{\sum_{j \in J_i} \xi_{ij}^2} \leq \Omega_i\}, \tag{3.46}$$

where Ω is the adjustable parameter controlling the bounds of the uncertainty set. In order to have a bounded uncertainty, the adjustable parameter is suggested to acquire a rang as $\Omega \leq \sqrt{|J_i|}$, where $|J_i|$ is the cardinality of the set J_i. Considering the ellipsoidal uncertainty set , the corresponding robust counterpart constraint in model (3.39) is equivalent to:

$$\sum_j a_{ij} x_j + \left[\Omega_i \sqrt{\sum_{j \in J_i} \hat{a}_{ij}^2 x_j^2} \right] \leq b_i, \quad \forall i. \tag{3.47}$$

The robust formulation proposed by Ben-Tal and Nemirovski (2000), employed the ellipsoidal uncertainty set to deal with the level of conservatism:

$$\begin{aligned} \min \quad & cx \\ \text{s. t.} \quad & \sum_j a_{ij} x_j + \sum_{j \in J_i} \hat{a}_{ij} u_{ij} + \Omega_i \sqrt{\sum_{j \in J_i} \hat{a}_{ij}^2 v_{ij}^2} \leq b_i, \quad \forall i \\ & - u_{ij} \leq x_j - v_{ij} \leq u_{ij}, \quad \forall i, j, \\ & x_j \in X, u_{ij} \geq 0, \quad \forall i, j. \end{aligned} \tag{3.48}$$

They showed that the probability that the i-th constraint is violated is at most exp($\Omega_i^2/2$). Every feasible solution of this model is a feasible solution for Soyster's model. The ellipsoidal uncertainty set creates a nonlinear model which is computationally more complex.

Polyhedral uncertainty set is defined using 1-norm of the uncertain data vector for each constraint i:

$$U_1 = \{\xi | \, ||\xi||_1 \leq \Gamma\} = \{\xi_{ij} | \sum_{j \in J_i} |\xi_{ij}| \leq \Gamma_i\}, \tag{3.49}$$

where Γ is the adjustable parameter controlling the size of the uncertain set. The suggested range for having a bounded uncertainty space is defined as $\Gamma \leq |J_i|$. Considering the polyhedral uncertainty set, the corresponding robust counterpart constraint in model (3.39) is equivalent to:

$$\begin{cases} \sum_j a_{ij} x_j + \Gamma_i p_i \leq b_i, \\ p_i \geq \hat{a}_{ij} |x_j|, \quad \forall j \in J_i. \end{cases} \tag{3.50}$$

By replacing the absolute value term $|x_j|$ with auxiliary variable u_j an equivalent robust formulation for (3.50) can be obtained by:

$$\begin{cases} \sum_j a_{ij} x_j + \Gamma_i p_i \leq b_i, \\ p_i \geq \hat{a}_{ij} u_j, \quad \forall j \in J_i, \\ -u_j \leq x_j \leq u_j, \quad \forall j, \\ u_j \geq 0, \forall j \end{cases} \tag{3.51}$$

An upper bound is introduced for each of the above mentioned uncertainty sets to achieve a bounded uncertainty space. When the value of the adjustable parameters is equal to the upper bound, the bounded uncertain space is entirely covered by the corresponding uncertainty set. Therefore, further increase of the parameter's value could lead to a more conservative solution and will not improve the solution robustness (Li et al. 2011). Figure 3.2 shows the box, ellipsoidal, and polyhedral uncertainty sets for a single constraint with two uncertain coefficients.

Bertsimas and Sim (2004) introduced a robust optimization framework that employs the polyhedral uncertainty set to flexibly adjust the level of conservatism of the robust solutions in terms of probabilistic bounds of constraint violations. They defined a parameter Γ_i (known as the budget of uncertainty) as the number of coefficients in constraint i that might acquire values different than their nominal ones. The proposed approach ensures the feasibility of the solution

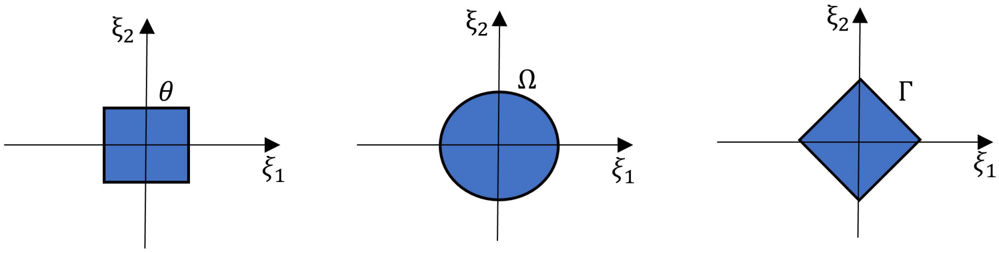

Figure 3.2: Uncertainty sets: a) box uncertainty set, b) ellipsoidal uncertainty set, c) polyhedral uncertainty set.

if less than Γ_i uncertain coefficients change. If more than Γ_i uncertain parameters change the solution will stay feasible with high probability. In other words, they provided deterministic and probabilistic guarantees against constraints violation.

For every i-th constraint of (3.37), the parameter Γ_i is defined to take values in the interval $[0, |J_i|]$. The aim is to protect the robust solution against all cases in which up to Γ_i of the coefficients are allowed to change. Let Γ_i be an integer, then the robust counterpart model in (3.39) can be reformulated as (3.52), where only Γ_i subset of coefficients in J_i are subject to change:

$$\begin{aligned} \min \quad & cx \\ \text{s. t.} \quad & \sum_j a_{ij}x_j + \max_{\{S_i | S_i \subseteq J_i, |S_i| = \Gamma_i\}} \{\sum_{j \in S_i} \hat{a}_{ij} u_j\} \\ & -u_j \leq x_j \leq u_j, \quad \forall j, \\ & u_j \geq 0, \quad \forall j. \end{aligned} \tag{3.52}$$

For constraint i, the $\beta_i(x, \Gamma_i) = \max_{\{S_i | S_i \subseteq J_i, |S_i| = \Gamma_i\}} \{\sum_{j \in S_i} \hat{a}_{ij} u_j\}$ is called the protection function that adjust the robustness against the level of conservatism. If $\Gamma_i = 0, \rightarrow \beta_i(x, \Gamma_i) = 0$, the constraints are equivalent to that of the nominal problem meaning that no changes happen in the coefficients. In this case, there is no protection against uncertainty. On the contrary, if $\Gamma_i = |J_i|$, the problem is equivalent to the Soyster's formulation where all the coefficients are subject to change. In this case, the constraint i is fully protected against the worst-case realization of uncertain coefficients. Therefore, varying $\Gamma_i \in [0, |J_i|]$ provides the flexibility for the decision maker to adjust the robustness (i.e., the level of protection against the constraint violation) against the level of conservatism (i.e., cost of the solution). With $\Gamma_i \in [0, |J_i|]$ and polyhedral uncertainty set, for each constraint i, the J_i subset of variables whose corresponding coefficients are subject to uncertainty is presented as: $J_i = \{\tilde{a}_{ij} | \tilde{a}_{ij} = a_{ij} + \xi_{ij}\hat{a}_{ij}, \forall j, \forall \xi \in \Xi\}$, where $\Xi = \{\xi_{ij} | \sum_j |\xi_{ij}| \leq \Gamma_i, \xi_{ij} \leq 1\}$.

In order to linearize the model (3.52), first the inner maximization is transfered to dual and then the dual problem is incorporated into the original one. For a given vector x^*, the value of the protection function in (3.52) is equal to the objective function for the following problem:

$$\begin{aligned} \beta_i(x^*, \Gamma_i) = \max \quad & \sum_{j \in J_i} \xi_{ij}\hat{a}_{ij}x_j^* \\ \text{s. t.} \quad & \sum_{j \in J_i} \xi_{ij} \leq \Gamma_i, \qquad \forall i \\ & 0 \leq \xi_{ij} \leq 1, \qquad \forall j \in J_i. \end{aligned} \tag{3.53}$$

Now, the inner maximization problem is transfered to its conic dual by introducing dual variables λ_i and μ_{ij} as in (3.54):

$$\begin{aligned} \min \quad & \Gamma_i\lambda_i + \sum_{j \in J_i} \mu_{ij}, \\ \text{s. t.} \quad & \lambda_i + \mu_{ij} \geq \hat{a}_{ij}x_j^*, \qquad \forall i, \forall j \in J_i, \\ & \lambda_i \geq 0, \mu_{ij} \geq 0, \qquad \forall i, \forall j \in J_i. \end{aligned} \tag{3.54}$$

Then, applying the dual (3.54) to the model (3.52) the following robust counterpart formulation is achieved, which is the proposed robust model by Bertsimas and Sim (2004):

$$\begin{aligned} \min \quad & cx \\ \text{s. t.} \quad & \sum_j a_{ij}x_j + \lambda_i\Gamma_i + \sum_{j \in J_i} \mu_{ij} \leq b_i, \quad \forall i, \\ & \lambda_i + \mu_{ij} \geq \hat{a}_{ij}u_j, \quad \forall i, j \in J_i, \\ & -u_j \leq x_j \leq u_j, \quad \forall j, \\ & u_j \geq 0, \lambda_i \geq 0, \mu_{ij} \geq 0, \quad \forall i, j. \end{aligned} \tag{3.55}$$

3.3.3 Robust Optimization Model

In this part, a robust optimization framework for the hazmat closed-loop supply chain network design is introduced with uncertainties in demand and return using polyhedral uncertainty sets. Since return quantities are proportions of demand quantities the formulations are conducted accordingly. The robust optimization structures are adapted from Bertsimas and Sim (2004) and Keyvanshokooh et al. (2016).

In the robust counterpart formulation, the demand uncertainty is allowed to deviate from a nominal scenario toward a worst-case realization within a polyhedral uncertainty set with budget of uncertainty constraints. Please note that the nominal scenario is equivalent to deterministic optimization framework for the problem. To develop the uncertainty set, first the positive and negative deviation percentages from nominal scenario for demand are defined. The positive deviation is in case that the true value of the parameter is greater than the nominal value. The negative deviation is in case the true value of the parameter is smaller than the nominal value. The definition for the demand is presented as (3.56).

$$\xi_l^{d+} = \frac{\tilde{d}_l - d_l}{\hat{d}_l^{+}}, \qquad \xi_{ls}^{d-} = \frac{d_l - \tilde{d}_l}{\hat{d}_l^{-}}, \quad \forall l \in L. \tag{3.56}$$

Using the (3.56) equation, the uncertainty set of demand is presented as follow:

$$JD = \{\tilde{d}_l | \tilde{d}_l = d_l + \xi_l^{d+} \times \hat{d}_l^{+} - \xi_l^{d-} \times \hat{d}_l^{-}, \quad \forall l \in L, \forall \xi_l^{d+}, \xi_l^{d-} \in \Xi_d\}, \tag{3.57}$$

where:

$$\Xi_d = \{\xi_l^{d+}, \xi_l^{d-} | 0 \leq \xi_l^{d+} \leq 1, 0 \leq \xi_l^{d-} \leq 1, \sum_{l \in L} (\xi_l^{d+} + \xi_l^{d-}) \leq \Gamma^d\}. \tag{3.58}$$

Using the budget of uncertainty, it is possible to limit the number of cases in which the demand or return may deviate from its nominal values. In the proposed mathematical deterministic model, allowing for such uncertainty might cause violations of constraints (2.3) and (2.4) which relate to fully satisfying demand and return. Therefore, these constraints are relaxed and their violations are considered in the objective function as a penalty. Thereby, the aim is to minimize the worst-case costs associated with the violations of constraints (2.3) and (2.4). The corresponding penalty is a parameter which can be adjusted by the decision maker based on the importance of satisfying all demands and returns in a competitive or free marketplaces. The following parameters are added to the deterministic framework parameters set:

New Robust Parameters	
PED	Penalty cost per unit of non-satisfied demands of customers
PER	Penalty cost per unit of exceed amount of flow over returns collected from customers
SUD	Surplus cost per unit of exceed amount of flow over demands received by customers
SCR	Scrap cost per unit of uncollected returns of customers

In order to incorporate the robust counterpart constraints (3.57) in the optimization model, the objective functions (2.1) and (2.2) are kept as well as constraints (2.5)-(2.33), but constraints (2.3) and (2.4) are removed. Instead of two last mentioned constraints, an equation is developed which calculates the violation of random demand and return satisfaction based on the penalty, surplus and scrap costs defined:

$$\begin{aligned} WCV = \sum_{l \in L}[\max[(\tilde{d}_l - \sum_{j \in J}\sum_{p \in P_{jl}} Y_{jlp}) \times PED, (\sum_{j \in J}\sum_{p \in P_{jl}} Y_{jlp} - \tilde{d}_l) \times SUD]] \\ + \sum_{l \in L}[\max[(r_l\tilde{d}_l - \sum_{j \in J}\sum_{p \in P_{jl}} Z_{ljp}) \times SCR, (\sum_{j \in J}\sum_{p \in P_{jl}} Z_{ljp} - r_l\tilde{d}_l) \times PER]] \end{aligned} \tag{3.59}$$

Equation (3.59) can be added to the cost objective function of the deterministic optimization model to adjust the demand and return decisions. Since the equation is nonlinear, for the sake of computation the linear equivalent model can be express as follows:

$$\min \quad WCV = \sum_{l \in L}(ZD_l + ZR_l) \tag{3.60}$$

$$\text{s. t.} \quad (\tilde{d}_l - \sum_{j \in J}\sum_{p \in P_{jl}} Y_{jlp}) \times PED \leq R1_l, \quad \forall \tilde{d}_l \in JD, \forall l \in L, \tag{3.61}$$

$$(\sum_{j \in J}\sum_{p \in P_{jl}} Y_{jlp} - \tilde{d}_l) \times SUD \leq R1_l \quad \forall \tilde{d}_l \in JD, \forall l \in L, \tag{3.62}$$

$$(r_l\tilde{d}_l - \sum_{j \in J}\sum_{p \in P_{jl}} Z_{ljp}) \times SCR \leq R2_l, \quad \forall \tilde{d}_l \in JD, \forall l \in L, \tag{3.63}$$

$$(\sum_{j \in J}\sum_{p \in P_{jl}} Z_{ljp} - r_l\tilde{d}_l) \times PER \leq R2_l, \quad \forall \tilde{d}_l \in JD, \forall l \in L, \tag{3.64}$$

$$ZD_l, ZR_l \geq 0, \forall l \in L. \tag{3.65}$$

The constraints (3.61)-(3.65) should be satisfied for all the realizations of the uncertain demands and returns within the defined uncertainty sets. Therefore, the robust counterpart of each constraint is formulated. Starting with the constrain (3.61), using the definitions in (3.57), the equivalent robust counterpart constraint is as follow:

$$\max[(\tilde{d}_l - \sum_{j \in J}\sum_{p \in P_{jl}} Y_{jlp}) \times PED] \leq ZD_l, \quad \forall l \in L, \tag{3.66}$$

which can be reformulated as (3.67) giving the deviations:

$$(d_l - \sum_{j \in J}\sum_{p \in P_{jl}} Y_{jlp}) \times PED + \max_{\xi_l^{d+}, \xi_l^{d-} \in \Xi_d} \{(\xi_l^{d+} \times \hat{d}_l^{+} - \xi_l^{d-} \times \hat{d}_l^{-}) \times PED\} \leq ZD_l, \forall l \in L. \tag{3.67}$$

In robust counterpart constraint (3.67) we optimize over the positive and negative deviation percentages from nominal scenario for uncertain demands. In order to linearize the constraint (3.67), first the inner maximization (protection function) is formulated for each $l \in L$ as the following model with using the definitions of budget of uncertainty:

$$
\begin{aligned}
\max \quad & \xi_l^{d+} \times \hat{d}_l^{+} - \xi_l^{d-} \times \hat{d}_l^{-} \\
\text{s. t.} \quad & \xi_l^{d+} \leq 1, \\
& \xi_l^{d-} \leq 1, \\
& (\xi_l^{d+} + \xi_l^{d-}) \leq \Gamma_l^d, \\
& \xi_l^{d-}, \xi_l^{d+} \geq 0.
\end{aligned} \tag{3.68}
$$

Then, the above model is transformed to its dual as follow:

$$
\begin{aligned}
\min \quad & \Gamma_l^d \lambda_l^d + \mu_l^1 + \mu_l^2 \\
\text{s. t.} \quad & \lambda_l^d + \mu_l^1 \geq \hat{d}_l^{+}, \\
& \lambda_l^d + \mu_l^2 \geq -\hat{d}_l^{-}, \\
& \lambda_l^d, \mu_l^1, \mu_l^2 \geq 0.
\end{aligned} \tag{3.69}
$$

The second constraint is the above model is redundant. Therefore, the dual variable μ_l^2 is removed from the dual formulation. Finlay, the dual is incorporated in the original constraint (3.67) and the linear robust counterpart constraint set is obtained as follow:

$$
\begin{aligned}
& PED \times [(d_l - \sum_{j \in J} \sum_{p \in P_{jl}} Y_{jlp}) + \Gamma_l^d \lambda_l^1 + \mu_l^1] \leq ZD_l, \quad \forall l \in L, \\
& \lambda_l^1 + \mu_l^1 \geq \hat{d}_l^{+}, \quad \forall l \in L, \\
& \lambda_l^1, \mu_l^1 \geq 0, \quad \forall l \in L.
\end{aligned} \tag{3.70}
$$

The same process is applied on constraint (3.62) to find its robust counterpart equivalence. The corresponding linear robust counterpart constraint for (3.62) is obtained as follows:

$$
\begin{aligned}
& SUD \times [(\sum_{j \in J} \sum_{p \in P_{jl}} Y_{jlp} - d_l) + \Gamma_l^d \lambda_l^2 + \mu_l^2] \leq ZD_l, \quad \forall l \in L, \\
& \lambda_l^2 + \mu_l^2 \geq \hat{d}_l^{-}, \quad \forall l \in L, \\
& \lambda_l^2, \mu_l^2 \geq 0, \quad \forall l \in L.
\end{aligned} \tag{3.71}
$$

Since return is a proportion of demand for each costumer, constrain (3.63) can be reformulated as (3.72) giving the deviations:

$$\begin{aligned}&(r_l d_l - \sum_{j\in J}\sum_{p\in P_{lj}} Z_{ljp}) \times SCR \\ &\quad + \max_{\xi_l^{d+},\xi_l^{d-}\in \Xi_d} \{(\xi_l^{d+} \times r_l \hat{d}_l^{+} - \xi_l^{d-} \times r_l \hat{d}_l^{-}) \times SCR\} \leq ZR_l, \quad \forall l \in L.\end{aligned} \tag{3.72}$$

where r_l is a constant and can be written out of the max equation. Therefore, we have the same equation as in (3.68), which has the dual model as in (3.69). Using this model, the robust counterpart equivalence of constraint (3.63) is as follow:

$$\begin{aligned}&SCR \times [(r_l d_l - \sum_{j\in J}\sum_{p\in P_{lj}} Z_{ljp}) + r_l \Gamma_l^d \lambda_l^1 + r_l \mu_l^1] \leq ZR_l, \quad \forall l \in L, \\ &\lambda_l^1 + \mu_l^1 \geq \hat{d}_l^{+}, \quad \forall l \in L, \\ &\lambda_l^1, \mu_l^1 \geq 0, \quad \forall l \in L.\end{aligned} \tag{3.73}$$

In (3.73) the last two constraints are redundant since we had them in the demand robust counterpart before. The same process is applied for constraint (3.64) and the robust counterpart is presented as follow:

$$PER \times [(\sum_{j\in J}\sum_{p\in P_{lj}} Z_{ljp} - r_l d_l) + r_l \Gamma_l^d \lambda_l^2 + r_l \mu_l^2] \leq ZR_l, \quad \forall l \in L, \tag{3.74}$$

The equation (3.60) is added to the cost objective function of the deterministic model as the associated cost of demand and return violations. Furthermore, the total number of $6 \times |L|$ constraints are added to the deterministic model as the corresponding robust constraints of (3.61), (3.62), (3.63) and (3.64). In these constraints, considering all the uncertainty sources at their worst case scenario would lead to an over conservative solution. To avoid this case, the parameters Γ_l^d is adjustable to conform the robustness against the level of conservatism of the solution. This parameter restricts the number of times that demand and return quantities deviate from the nominal scenario in their polyhedral uncertainty sets. Higher values of these parameters increase the level of robustness as the expense of worse objective function value.

3.3.4 Computational Results: A Case Study

The Albany case study is used with the same parameter as the nominal values to assess the performance of proposed framework. Then, uncertainty sets for demand and return are developed. Knowing the nominal demand and return as the deterministic model parameters, maximum positive and negative deviations from the nominal case are determined. Various sensitivity analysis are applied on the most important parameters such as the level of deviation and the budget of uncertainty in order to verify the performance of the proposed model.

The effects of uncertainty on demand and return are studied simultaneously since return is a proportion of demand. First the level of deviation (LD) of uncertain parameter is defined with respect to its nominal value and the value is set to $LD = \{10\%, 20\%, 30\%\}$. For example, $LD = 10\%$ means that the true value for the uncertain demand can be realized within an interval where the floor is 10% less than the nominal demand and the ceiling is 10% more than the nominal demand. Therefore, the LD parameter is used to change the radius of the polyhedral uncertainty set for demand and return.

Furthermore, the parameters Γ_l^d is varied from 1 to its maximum value $|L|$ by 1 in order to investigate its effect on the model performance. It should be noted that $\Gamma_l^d = 0$ refers to the nominal case which is equivalent to the deterministic optimization solution. Also, $\Gamma_l^d = |L|$ refers to the worst case scenario where all the demand and return quantities are subject to the uncertainty.

Since the influence of model parameters such as ϕ, CT and RET is investigated in Chapter 2, the focus is not to analyze such parameter changes in this chapter. The same trend is expected in the performance of the robust model. Thus, the concentration here is to investigate robust programming parameters. For the rest of the computational results the parameters are set as $\phi = 1$, $CT = 22.2$ and $RET = 1$. Considering $LD = 10\%$, different Pareto solutions are compared in a case where the demand and return are subject to uncertainty. Figure 3.3 presents the Pareto fronts achieved from the deterministic model with $\sum_l \Gamma_l^d = 0$ as the nominal front, the Pareto front obtained by setting $\sum_l \Gamma_l^d = 5$ as the average case and the Pareto front for the worst case with $\sum_l \Gamma_l^d = |L| = 10$.

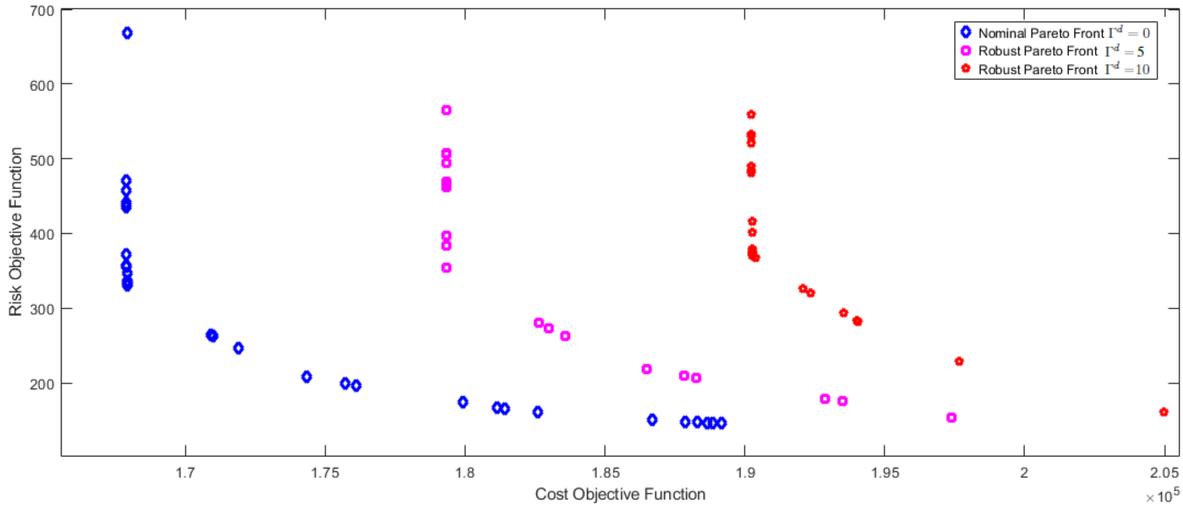

Figure 3.3: Comparing Pareto solutions for various budget of uncertainty values: $\sum_l \Gamma_l^d = \{0, 5, 10\}$.

Results in Figure 3.3 demonstrate the fact that the robust model solutions have higher objective functions since robust formulation protects the solutions against infeasibility caused by perturbations of the uncertain parameters. The worst case scenario with $\sum_l \Gamma_l^d = |L|$ has the highest objective function values since it is a conservative approach which gives up too much optimality for the solution's robustness. The effect of level of uncertainty for various amounts of budget of uncertainty on the cost and risk objective functions are also analyzed. Two cases are considered where the cost objective function is minimized and the case where the risk objective function is minimized. In other words only the upper left and lower right points of the associated Pareto fronts are considered in this comparison. For three levels of uncertainty $LD = \{10\%, 20\%, 30\%\}$, Figure 3.4 shows how objective functions changes with increase of budget of uncertainty $\sum_l \Gamma_l^d$.

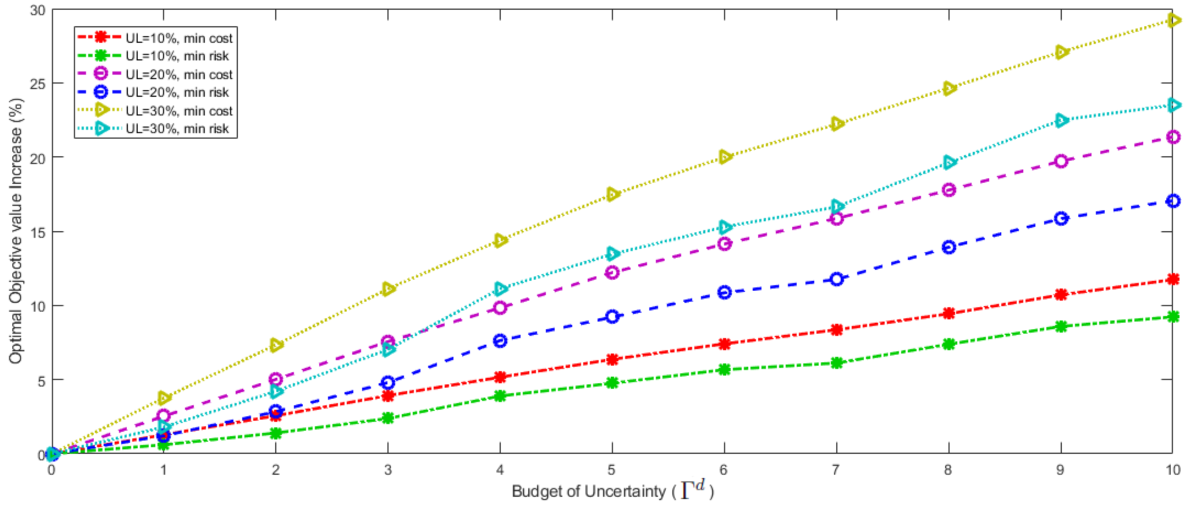

Figure 3.4: Comparing risk and cost objective function changes for various UL values in case of demand and return uncertainties.

The values in Figure 3.4 are calculated by using the nominal case as the base solution and compare the results of robust solutions by increasing the budget of uncertainty. Results indicate that both risk and cost objective function values are increased by enlarging of the budget of uncertainty for demand. As expected, the risk and cost objective values increase with the growth in level of uncertainty since the model guarantees robust solutions in cases of different data perturbations. Also, increases in the number of customers with uncertain demand and return changes the magnitude of the objective functions. Since these values are highly rely on the demand and return satisfaction levels they are subject to increase.

As it is mentioned before, robust models result in higher objective values in return of keeping the feasibility of the model in case of data uncertainty. Therefore, knowing the probability of constraint violation is critical. It is also possible to calculate the bounds on the probability of violation of each constraint using following equation presented by Bertsimas and Sim (2004):

$$pr(\sum_j a_{ij}x_j^* < b_i) \leq 1 - F(\frac{(\Gamma_i - 1)}{\sqrt{|J_i|}}) \tag{3.75}$$

where F refers to the standard normal cumulative distribution function. Using equation (3.75) a bound on the probability of constraint violation is computed under the assumption of symmetric distributions for independent demand quantities. The constraint violation bounds for each case are presented in Figure 3.5 as a function of Γ^d.

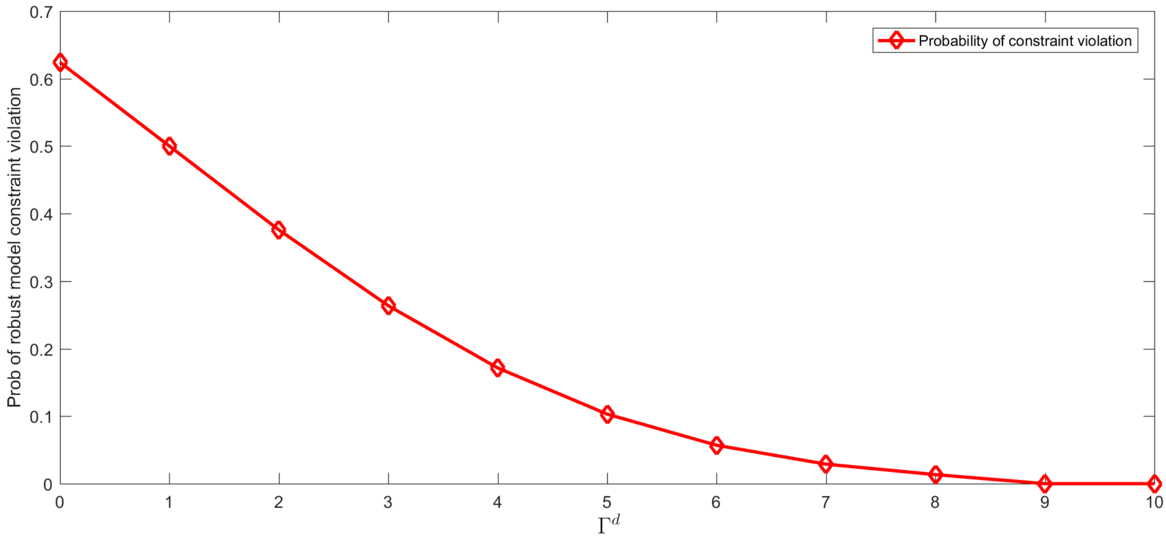

Figure 3.5: Robust model constraint violation probabilities considering various budgets of uncertainty.

The result in Figure 3.5 shows that when the lowest objective function values are obtained (deterministic case) the solutions are not robust with respect to volatility of uncertain parameters. By increasing the budget of uncertainty from 0 to 5 the violation probability decreases substantially. For the case with higher budgets of uncertainty the probability of robust model constraint violation is close to zero. This case is known as the most conservative robust optimization framework where the solution is feasible even the worst case realization of the random parameters happens.

We are also interested in analyzing the corresponding decision variables for demand satisfaction such as the quantity of shipments and routings. In Figure 3.6 the Albany supply chain network solutions achieved by deterministic model are compared with robust programming solutions. For the robust network, the demand and return have uncertainties with $UL = 10\%$ and $\Gamma^d = 10$.

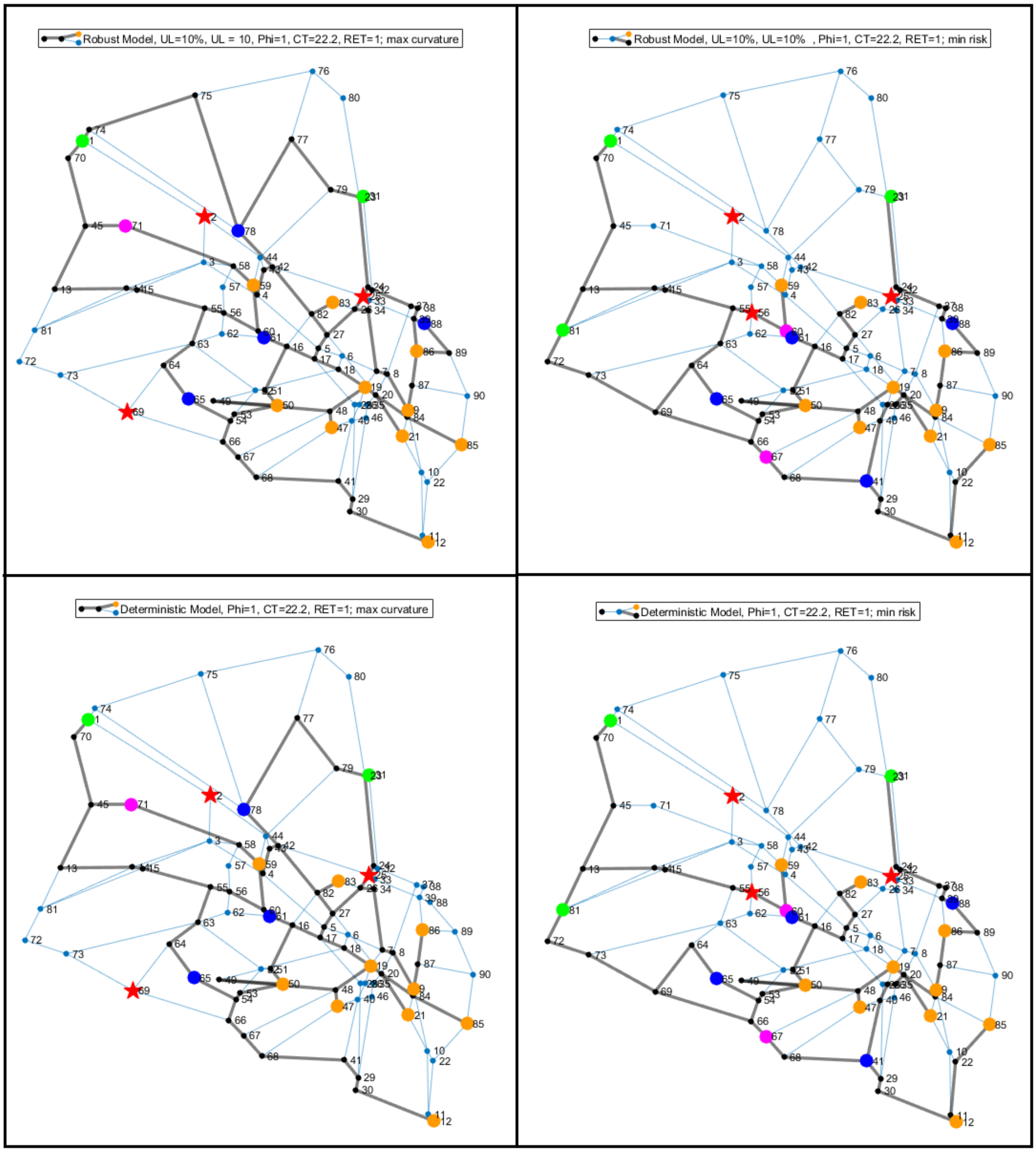

Figure 3.6: Comparing robust model networks with deterministic networks for two solutions of maximum curvature and minimum risk. Green nodes indicate production/recovery facilities, blue nodes indicate distribution/collection centers, purple nodes indicate disposal centers, orange nodes indicate customer locations, and red pentagrams indicate the emergency response teams.

Demand and return uncertainties result in increases in the capacities of the centers and shipping larger volumes of hazmat on road segments. Results in Figure 3.6 indicate that for maximum curvature solution the location of hybrid distribution/collection centers and the routings are different. The robust model also adds routes and increases the shipment quantities on the road segments. In case of the risk minimization, the robust model provides a network design similar to the deterministic model which avoids highly populated areas while guarantying feasibility of the design in the worst case realization of demand and return quantities.

3.4 Conclusion

In this chapter, the hazmat supply chain network design is studied under uncertainty of demand and return parameters. In practice, these parameters are not known for sure and therefore, their uncertainty should be taken into account in designing the associated network. First, a case is investigated where the distributions of uncertain parameters are known. A two-stage stochastic programming model is developed to address such uncertainty. In the first stage the decisions corresponding to the facilities location and capacity as well as emergency response teams placing are made. In the second stage, decisions regarding the shipment amounts and routing are made based on the realization of the uncertain parameters. There might be a case in practice where the parameter uncertainty is not stochastic, or the distributional information for the data is unavailable. A robust optimization approach is presented for such problem which aims to accept a suboptimal solutions for the nominal values of the data in order to ensure that the solution remains feasible and near optimal when data changes. The computational results of both models are presented based on the Albany case study, which provide an effective framework to design hazmat supply chain network under uncertainty.

Besides demand and return, the risk parameter in the hazmat shipment can also be subject to uncertainty. The associated risk on the road network depends on various factors such as the material type, nature of the area around the release, weather conditions, and the released quantity. These factors are subject to uncertainty. on the other hand, hazmat accidents have catastrophic consequences. With a heavy-tailed distribution of losses it can expected to observe future costs far exceeding anything seen previously. Therefore, addressing such risk is important in the hazmat transportation. The next chapter is devoted to study and present methodologies that can help promoting risk equity on hazmat road network.

Chapter 4

A Generalized Risk-averse Stochastic Optimization Framework for Risk Parity with Coherent Risk Functions with Application in Hazardous Material Routing

4.1 Introduction and Background

The standard risk-reward model for decision-making (see, for example, Krokhmal et al. 2011, for a review) aims to deliver decisions that are explicitly optimal considering combination of risk and reward. At the same time, especially in financial portfolio management literature, it has been observed that in some conditions, an indirect approach based on improving diversification may yield better results. In this case, the decision maker is concerned with selecting a decision without direct regard to an objective function, and instead distributes her/his resources to achieve maximum diversity, consequently, avoiding excessive losses. These approaches are not mutually exclusive, as risk-reward objective tends to indirectly promote diversification and vice versa.

Intuitively, decisions made with explicit goal of maximum diversity may be less dependent on the underlying stochastic model. Indeed, even if the stochastic model turns out to be inappropriate and the future realization is observed to be very different from the considered scenarios, a diverse decision vector may still be adequate and not overexposed to any specific source of risk. On the other hand, risk-reward optimization may suffer from over-fitting to a specific stochastic model. This issue can be particularly important in distributions that exhibit catastrophic behavior (Cooke and Nieboer 2011). In a heavy-tailed or fat-tailed distribution of loss, one can expect to observe future costs far exceeding anything seen previously, which can be difficult to account for in a risk-reward framework.

The concept of Risk Parity (RP) for a financial portfolio was proposed by Qian (2005). Here the goal is to create a portfolio of financial assets, such that each equally contributes to the total portfolio variance. While in finance, Risk Parity condition has a very straightforward interpretation for engineering or operations research applications it is possible to use a number of other possible interpretation. Risk Parity can be used for improving robustness of the solution, i.e., protecting against overfitting to a specific stochastic model. Alternatively, Risk Parity condition can be interpreted as enforcing fairness of the decision. Indeed, in this case, a decision vector can be considered where each member is weighted proportionally to its risk contribution, hence allowing us to distribute some resource while taking into account risk exposure. Finally, Risk Parity portfolio can be imagined as a way to balance between a number of candidate solutions. For example, if candidate solutions represent paths in a network, it is possible to enforce Risk Parity over these paths in order to ensure that no single part of the network is overexposed.

4.1.1 Risk Parity and Equal Risk Contribution

Maillard et al. (2010) provided an introduction to analytics of Risk Parity, referred to as Equal Risk Contribution (ERC) in financial portfolio optimization, as well as established a number of important properties. The authors developed and studied theoretical properties of an optimization model for variance-based ERC. The RP and ERC portfolios were studied from analytical and numerical perspectives in various articles and their performance compared to the existing methods such as Equally Weighted, minimum variance and mean variance portfolios (Stefanovits 2010, Chaves et al. 2011, Fisher et al. 2012, Choueifaty et al. 2013, Lohre et al. 2014, Roncalli and Weisang 2016), showing promising results in different case studies.

A number of algorithms have been developed to generate variance-based ERC portfolios and find asset weights in the portfolios such as Newton's Method (Chaves et al. 2012), cyclical coordinate descent algorithm (Griveau-Billion et al. 2013) and second-order conic programming (SOCP) model (Mausser and Romanko 2014).

Cesarone and Tardella (2016) introduced a closely related concept of Equal Risk Bounding (ERB), in which only a subset of assets is included in the final portfolio. They developed a non-convex Quadratic Programming framework for ERB and studied its properties. Their results showed that if short selling is allowed, ERB coincides with RP solution on a subset of assets with the lowest variance. Feng and Palomar (2016) introduced an iterative solving procedure based on successive convex approximation for selecting a subset of assets and finding RP portfolio.

Some attempts were made to develop generalized RP and risk budgeting frameworks for portfolio construction (Haugh et al. 2015, Feng and Palomar 2015). Reviews of investment theory and problems, RP, and risk budgeting can be found in (Bruder and Roncalli 2012, Roncalli 2013, Kolm et al. 2014).

In addition to variance, other risk measures such as Value-at-Risk (VaR) and Conditional-Value-at-Risk (CVaR) were employed in RP and ERC portfolio generation. Cherny and Orlov (2011) proved that linear risk contribution exists and is unique for the Weighted VaR class, as a coherent risk measure. Boudt et al. (2012) tested for the equality of the Sharpe ratios between the minimum CVaR (concentration) and minimum standard deviation portfolios. Cesarone and Colucci (2017) studied the performance of minimum CVaR and RP portfolios considering different datasets with equities, bonds and mixed assets.

The existing studies mostly considered variance-based RP for financial portfolio management, and a number of promising results have been observed in a variety of case studies. A few studies discussed the idea of generalized RP approaches, especially to CVaR and VaR measures. However, such approaches have not received a significant attention in the operations research community. The current study differs from the existing studies in that it attempts to establish a comprehensive analysis of the ways to define generalized RP model based on the optimization framework. This then allows us easily develop the corresponding solution procedures and embed this concept into larger optimization-based decision making models.

4.1.2 Risk Measures Classification

A thorough review of risk measure theory can be found in Krokhmal et al. (2011). Here some major definitions are presented for the sake of completeness. Two of the most widely used in practice risk measures are Value-at-Risk (VaR) and Conditional-Value-at-Risk (CVaR). VaR, defined as the quantile of the loss distribution at the appropriate confidence level, is often used in applications (see, for example, JP Morgan 1994, Jorion 1997, Duffie and Pan 1997, and references therein) and can also be studied from the perspective of chance constraints (Charnes et al. 1958, Prékopa 1995, Birge and Louveaux 1997, Shapiro et al. 2014). At the same time, it possesses certain undesired properties, such as non-convexity and discontinuity with respect to confidence level, and is often characterized as not being a proper modeling approach (Artzner 1997, Artzner et al. 1999). CVaR was introduced in Rockafellar and Uryasev (2000, 2002) as a way to circumvent these issues. It is defined as the average loss exceeding VaR and is a de-facto standard approach in many application areas.

The concept of coherent measures of risk was introduces by Artzner (1997) (see also, Artzner et al. 1999). The aim was to define a class of risk functions that can be viewed as proper measures of risk. For the sake of completeness, the definitions associated with concepts of coherency, as discussed in Krokhmal et al. (2011), are presented as we will rely on them later on.

Convex Risk Measures. A lower semicontinuous function $\rho : \mathcal{X} \mapsto \bar{\mathbb{R}} = \mathbb{R} \cup \{+\infty\}$, where $\mathcal{X}$ refers to the space of random losses is said to be a *convex measure of risk* if it satisfies the following axioms:

(A1) *Monotonicity*: $\rho(X) \leq \rho(Y)$ for all $X \leq Y$;

(A2) *Convexity*: $\rho(\lambda X + (1-\lambda)Y) \leq \lambda\rho(X) + (1-\lambda)\,\rho(Y), \quad \lambda \in [0, 1]$;

(A3) *Translation invariance*: $\rho(X + a) = \rho(X) + a$, $a \in \mathbb{R}$.

Coherent Risk Measure. Function ρ is called a *coherent risk measure of risk* if it satisfies axioms (A1) – (A3), and additionally:

(A4) Positive homogeneity: $\rho(\lambda X) = \lambda\rho(X)$, $\lambda > 0$.

Pflug (2000) proved that CVaR is a coherent risk measure. On the other hand, VaR is not, since it violates (A2), which explains methodological advantages of CVaR-based models. Note that there are other frameworks aimed at designing an axiomatic approach to defining practical measures of risk (see Krokhmal et al. 2011, for more examples, such as deviation measures, spectral measures, etc.).

A generalization of Risk Parity approach can be achieved by selecting a coherent measure of risk in place of variance and then exploring applicability of this framework to other application domains. In this chapter, a discussion is presented on the ways to facilitate this generalization. Mathematical foundations for relevant definitions are established, some properties are explored, such as conditions for existence of the generalized Risk Parity solutions, and the types of decision making models that would be well-suited for such a framework are discussed. Throughout the chapter, we specifically focus on basing the framework as a solution to an optimization problem, hence allowing for natural expansion into more complex models. Building on results established in both finance and optimization literature, we attempt to present a unified framework stemming from both directions of research.

The rest of this chapter is organized as follows. The generalized approach to Risk Parity and CVaR-based mathematical formulation are presented in Sections 4.2. The diversification-reward stochastic optimization model and the development of the solution procedure driven from the model properties is outlined in Section 4.3. Application of our proposed methodology are presented on three realistic case studies in Section 4.4. Concluding remarks and areas for future research directions are presented in Section 4.5.

4.2 Stochastic Optimization Models Based on Risk Parity

4.2.1 Generalized Risk Parity

Let $\mathbf{x}$ be a decision vector from $\mathbb{R}^n$. Suppose that outcome X that in depends on both this decision and realization of uncertainty as defined by a random event $\omega \in \Omega$. In other words, X can be defined as a random variable representing loss (or cost) and $X = X(\mathbf{x}, \omega)$. The problem of risk-averse decision making is then to design a comprehensive approach for establishing decision preferences, i.e., a systematic way to decide between random losses.

Following risk-reward framework a function $\rho : \mathcal{X} \mapsto \mathbb{R}$ can be considered, which will be referred to as *risk measure*. Here, $\mathcal{X}$ denotes the space of random losses, for example, $\mathcal{L}$ or $\mathcal{L}^2$. Function ρ will be assumed to be a coherent measure of risk. Further, it will be assumed that the loss function X is positive homogeneous and convex. In many applications, X is linear.

The RP framework considered in this chapter can be viewed as an idea alternative to explicit minimization of the measure of risk ρ. Instead, the decision-maker is aiming at achieving "equal risk contribution" from all of the sources of uncertainty, hence ensuring maximum diversity of the decisions. It was initially proposed for financial portfolio management problem, designing a portfolio such that each asset has the same contribution to the total volatility (variance). Next, we formally define the approach, following Maillard et al. (2010), at the same time illustrating how it can be used in non-financial settings.

The goal of the decision-maker in our model is to ensure that each component of the decision vector $\mathbf{x} \in \mathbb{R}^n$ has the same contribution to the total risk, as measured by function ρ. It is then natural to make the following assumptions:

Assumption 1. *Decisions x_i are continuous.*

Assumption 2. *Decisions x_i represent similar quantities, i.e., are of the same scale and are measured in the same units.*

Note that it is, of cause, not necessary to enforce parity for all decisions at the same time. The discussion below can be trivially amended to allow for excluding some of the decisions.

Assuming sufficient differentiability of functions ρ and X, Marginal Risk Contribution (MRC) of each asset can be defined as $MRC_i = \frac{\partial \rho(X(\mathbf{x},\omega))}{\partial x_i}$ and Total Risk Contribution as $TRC_i = x_i MRC_i = x_i \frac{\partial \rho(X(\mathbf{x},\omega))}{\partial x_i}$. The intuition behind these definitions follows from the well-known result below.

Theorem 1 (Euler's Homogeneous Function Theorem). *If $f : \mathbb{R}^n \mapsto \mathbb{R}$ is continuously differentiable homogeneous function of degree τ, then*

$$f(x) = \frac{1}{\tau} \sum_{i=1}^{n} x_i \frac{\partial f}{\partial x_i}. \tag{4.1}$$

Consequently, coherency of ρ and positive homogeneity of X imply that $\rho(X(\mathbf{x},\omega)) = \sum_i TRC_i$. This then leads to RP solution, which satisfies condition $TRC_i = TRC_j$ for all

$i \neq j$, or

$$x_i \frac{\partial \rho(X(\mathbf{x}, \omega))}{\partial x_i} = x_j \frac{\partial \rho(X(\mathbf{x}, \omega))}{\partial x_j}, \text{ for all } i, j. \tag{4.2}$$

The existence and uniqueness of RP solution for a financial portfolio case with variance as the measure of risk is shown, for example, in Maillard et al. (2010).

In addition to the definition above, an equivalent representation for the variance-based RP solution has been presented in Maillard et al. (2010). The authors propose to consider the following nonlinear optimization problem.

$$\min \quad \rho(X(\mathbf{y}, \omega)) \tag{4.3a}$$

$$\text{s. t.} \quad \sum_{i=1}^{n} \ln y_i \geq c \tag{4.3b}$$

$$y \geq 0, \tag{4.3c}$$

where c is an arbitrary constant. The result in Maillard et al. (2010) showing that the normalized solution for this optimization model, i.e., $x_i^* = \frac{y_i^*}{\sum_{i=1}^n y_i^*}$, satisfies the Risk Parity condition for variance-based model, is summarized below.

Theorem 2 (Maillard et al. (2010))**.** *If* $\rho(X(\mathbf{y}, \omega)) = \sum_{ij} \sigma_{ij} y_i y_j$, *i.e., the measure of risk represents variance of a financial portfolio, then the unique optimal solution* $\mathbf{y}^*$ *to problem* (4.3) *exists, and normalized solution* $x_i^* = \frac{y_i^*}{\sum_{i=1}^n y_i^*}$ *satisfies Risk Parity (RP) condition for financial portfolio selection in* (4.2).

While this approach is natural, the definitions above directly rely on differentiability of the risk measure and loss function. While this may be a reasonable assumption if continuous stochastic model is considered, practical engineering applications usually involve discrete scenario-based models. In this case, most popular approaches, for example CVaR and VaR are not continuously differentiable. Further, existence of a generalized RP solution is also not guaranteed unless additional assumptions are made. Next, an interpretation for problem (4.3) and sufficient conditions for existence of an optimal solution are established.

For the sake of clarifying the notation, let us note that here and for the rest of the chapter, the variable vector used in problem (4.3) is denoted as $\mathbf{y}$, the true decision vector as $\mathbf{x}$ and the loss function as X.

Definition 1. Suppose that ρ is a coherent measure of risk. Then, $\mathbf{x}$ will be denoted as a *Risk Parity solution with respect to measure ρ (ρ-RP solution)* if $x_i = \frac{y_i^*}{y_1^*+\ldots+y_n^*}$, where $\mathbf{y}^*$ is an optimal solution to problem (4.3).

The next proposition establishes the relationship between ρ-RP solution and an intuitive interpretation similar to (4.2).

Proposition 1. *Suppose that ρ is a coherent measure of risk. Suppose that $\rho(X(\mathbf{y}))$ is positive homogeneous and convex as a function of $\mathbf{y}$. Then, if $\mathbf{y}^*$ is an optimal solution to problem* (4.3)*, then*

$$\cap_{i=1}^{n} y_i^* \partial_i \rho(\mathbf{y}^*) \neq \emptyset, \tag{4.4}$$

where $\partial_i f$ denotes the ith component of the subdifferential of function f.

Proof. The statement follows from KKT conditions for convex optimization problem. Indeed, following a similar arguments in Maillard et al. (2010) consider Lagrange function $\mathcal{L}(\mathbf{y}, \lambda, \lambda_c) = \rho(\mathbf{y}) - \lambda^\top \mathbf{y} - \lambda_c \Big(\sum_{i=1}^{n} \ln y_i - c \Big)$ for problem (4.3). Then a feasible solution is optimal whenever $0 \in \partial \mathcal{L}$ and complementary slackness implies $\lambda_i y_i = 0$. Clearly, $y_i = 0$ cannot be optimal, hence $\lambda_i = 0$. Therefore, at optimality

$$0 \in \partial \mathcal{L}(\mathbf{y}, \lambda, \lambda_c) = \partial_{\mathbf{y}} \rho(\mathbf{y}) - \lambda_i - \lambda_c \frac{1}{y_i} = \partial_{\mathbf{y}} \rho(\mathbf{y}) - \lambda_c \frac{1}{y_i}.$$

Thus, $\frac{\lambda_c}{y_i} \in \partial_i \rho(\mathbf{y})$ for all i. In other words, there exists a value λ_c, such that $\lambda_c \in y_i \partial_i \rho(\mathbf{y})$, which implies (4.4). □

It is easy to see that if $X(\mathbf{y}) = \sum_i r_i y_i$ and the measure of risk considered is variance, then (4.4) is equivalent to (4.2), which explains the intuition behind the definition of ρ-RP solution.

Observe that this result holds as long as $\rho(X(\mathbf{y}))$ is convex, which is true for a wide range of functions ρ and X.

Proposition 2. *Suppose that ρ is coherent and X is convex and positive homogeneous. Further, suppose that*

(i) $\rho(X(\mathbf{y}, \omega)) \geq 0$ *for all feasible* $\mathbf{y}$*, and*

(ii) $\rho(X(\mathbf{y}, \omega)) \to +\infty$*, if* $y_i \to +\infty$ *for some* i*.*

Then optimal solution to problem (4.3) *exists and is attained.*

Proof. Follows directly from the assumptions and convexity of the objective function. □

While somewhat restrictive, conditions (i) and (ii) are natural for the measures of risk. Indeed, condition (ii) states that it is impossible to create a decision of infinite value and finite risk. In the financial terms it corresponds to impossibility of an infinite investment with a finite risk. Condition (i) can be made without loss of generality if feasible region is bounded from below due to translation invariance.

The combination of Propositions 1 and 2 establishes the intuition behind using the optimization problem as the basis for generalized RP and sufficient conditions for its solution existence. In the next section, we explore how this approach can be employed with CVaR, the most widely used coherent measure of risk.

4.2.2 CVaR-Based Optimization Model

Informally, CVaR at level α of a random variable X is usually defined as the average loss in the $1-\alpha$ worst cases. Formal mathematical definition can be constructed in a variety of ways, here we rely on the so-called optimization formula (see Rockafellar and Uryasev 2002, for more details):

$$\mathsf{CVaR}_\alpha(X) = \min_\eta \eta + \frac{1}{1-\alpha}\mathsf{E}[X-\eta]_+, \tag{4.5}$$

where $\alpha \in (0,1)$, and $[t]_+ = \max\{0,t\}$. It is well-known that CVaR is coherent, and, in addition, the definition above implies that its value can be found as a solution to a linear programming problem. In other words, if X depends linearly on the decision vector $\mathbf{x}$ and the feasible region is polyhedral, then the problem of optimizing CVaR can be solved efficiently.

In view of the definition of ρ-RP, the CVaR-RP optimization problem can be constructed as

$$\min \quad \eta + \frac{1}{1-\alpha}\mathsf{E}[X(y)-\eta]_+ \tag{4.6a}$$

$$\text{s. t.} \quad \sum_{i=1}^{n} \ln y_i \geq c \tag{4.6b}$$

$$y \geq 0. \tag{4.6c}$$

From the numerical perspective, CVaR-based formulation (4.6) is a convex optimization problem that is fairly straightforward: if $X(y)$ is linear (such as in the case of portfolio optimization), then it has a single nonlinear constraint (4.6b) of a special kind. A further simplification can be obtained if a standard finite scenario model for the realizations of uncertainty is assumed. Suppose that loss function X is linear, i.e., $X(\mathbf{y}) = \boldsymbol{r}(\omega)^\top\mathbf{y}$, where ω is a random outcome taking values $\omega_1,\ldots,\omega_m$ with probabilities $p_1,\ldots,p_m$ respectively. Note that since CVaR has the property of translation invariance, additive constant in the linear function X can be ignored. Let us further denote as r_{ij} the ith component of $\boldsymbol{r}(\omega_j)$. Then problem (4.6) can be expressed as

$$\min \quad \eta + \frac{1}{(1-\alpha)}\sum_{j=1}^{m} p_j w_j \tag{4.7a}$$

$$\text{s. t.} \quad \sum_{i=1}^{n} \ln y_i \geq c \tag{4.7b}$$

$$w_j \geq \sum_{i=1}^{n} r_{ij} y_i - \eta \qquad \forall j = 1,2,...,m \tag{4.7c}$$

$$y_i \geq 0, \quad w_j \geq 0. \tag{4.7d}$$

Proposition 3. *If scenarios are such that* $\mathsf{P}(\mathbf{r}^\top \mathbf{y} > 0) > 1 - \alpha$ *for all feasible* $\mathbf{y}$*, then there exists a solution to problem* (4.7).

Proof. Observe that by properties of CVaR, the condition $\mathsf{P}(\mathbf{r}^\top \mathbf{y} > 0) > 1 - \alpha$ implies that $\mathsf{CVaR}(\mathbf{r}^\top \mathbf{y}) > 0$. By construction, it then follows that if a feasible sequence $\mathbf{y}^j$ is such that $y_i^j \to +\infty$, then $\mathsf{CVaR}(\mathbf{r}^\top \mathbf{y}^j) \to +\infty$. This, and convexity imply that optimality is attained. □

An analysis, similar to the one presented in this subsection, can be performed for other measures of risk that allow for optimization-based representation. This includes VaR, Higher Moment Coherent Measures of Risk (HMCR) and some others, see Krokhmal (2007), Vinel and Krokhmal (2017), Vinel (2015) for some suitable candidates.

Also note that the nonlinear constraint $\sum_{i=1}^n \ln y_i \geq c$ is equivalent to $\prod_{i=1}^n y_i \geq e^c$, i.e., a geometric mean of variables y_i. This, in turn, can be represented as a system of second-order cones, following for example, (Ben-Tal and Nemirovski 2001). This implies that CVaR-RP model can be solved efficiently using any of the well-established methods for second-order cone programming (SOCP).

4.3 Diversification-Reward Stochastic Optimization Model

As mentioned earlier, risk-reward framework is often the primary modeling approach in risk-averse stochastic optimization. Here, the decision maker considers a bi-objective optimization problem, minimizing risk and maximizing reward. Reward is usually measured by the expected gain, while risk can be evaluated by a number of different approaches, surveyed above. A better average performance can be achieved by placing more emphasis on the reward, while a more risk-averse decision can be preferred by selecting a more conservative risk measure. At the same time, especially in the financial portfolio selection literature, it is often hypothesized that optimal performance can be observed when decision diversification is enforced directly. The generalized RP approach described in this work can be naturally employed for this purpose.

The regular risk-reward framework provides a solution (or a family of solutions) that is aimed at achieving a certain level of average performance, yet avoids excessive risks. Since the analysis is usually performed based on historical data, this may not be enough. Indeed, especially in the case of catastrophic risk, the losses that may be encountered in the future often exceed anything present in the historical dataset. Direct enforcement of diversification could be a natural way to circumvent this issue. Hence, the following two stage approach proposed (here an analogy with two stage stochastic optimization is used): first, a set of "good" decisions is identified with the risk-reward framework. The true solution is then selected based on diversifying among these solutions only. The approach is aimed at benefiting from both risk-reward and diversification options: explicit diversification methods, such as Equally Weighted or RP approaches, cannot directly improve expected performance and instead rely on preselecting good decisions, while risk-reward framework is prone to overfitting to the stochastic model.

The following conceptual mathematical formulation can be considered for the two stage diversification-reward model:

$$
\begin{aligned}
\min \quad & \rho(X(\mathbf{x})) \\
\text{s. t.} \quad & \mathsf{E}X(\mathbf{x}) \geq r_0 \\
& \mathbf{x} \in \mathcal{C} \\
& x_i \leq z_i, \quad i = 1, \ldots, n \\
& \mathbf{z} \in \{0,1\}^n \\
& \mathbf{x} \in \mathcal{RP}^\rho(\mathbf{z}),
\end{aligned}
$$

where $\mathbf{x}, X, \rho$ are described above, and $\mathcal{RP}^\rho(\mathbf{z})$ defines a set of ρ-RP solutions on a subset of decision variables, identified by binary vector $\mathbf{z}$. Observe that in this case, $\mathbf{z}$ can be interpreted as a first stage decision, determining which variables will be considered for implementation, and the actual distribution of resources $\mathbf{x}$ is selected based on RP condition in the second stage.

A careful analysis of this framework is beyond the scope of the current work and will be investigated in a later effort. Here, let us note that the problem above can be challenging computationally. In the case studies in the next section a straightforward heuristic solution is considered, which is obtained by splitting the stages. In this case, a risk-reward problem is solved separately to identify a heuristic solution for vector $\mathbf{z}$ (i.e., which elements should be included in the final solution), and then solve ρ-RP problem for this subset only. This way we avoid the computational challenge related to mixed-integer nonlinear structure of the problem, but still obtain efficient solutions.

4.4 Experimental results: Case studies

In this section,the results of three case studies are presented. Our goal is to evaluate whether the proposed generalized RP approach and two stage diversification-reward model can lead to improved diversity in decision making. The first case study is based on a dataset for flood related insurance claims and is particularly interesting due to the presence of highly heavy-tailed distributions of the losses. The second numerical study is based on the standard financial portfolio optimization problem with real-life historical data. The third case study is based on hazardous materials shipments on the road network of Buffalo, NY. with a real dataset for exposed risk on the road segments. The Equally Weighted (EW) approach and mean-CVaR are used as benchmarks. As discussed in the introduction, EW solution is often viewed as a naive, yet effective method of achieving diversity in decision making and hence is used here as a natural base line.

In all studies, we evaluate how a solution constructed based on historical observations only (i.e., scenarios are drawn from previously observed outcomes) can perform in the future. Note that risk-reward model, e.g., mean-CVaR, explicitly promotes better average performance. On the other hand neither ρ-RP nor EW models have a built-in capability to promote average performance other than diversification of risk itself.

4.4.1 Case study 1: Flood insurance claims

Data description The study is based on a dataset from National Flood Insurance Program (NFIP) managed by a nonprofit research organization *Resources for the Future* (Cooke and Nieboer 2011). It contains flood insurance claims for 67 counties of the State of Florida from 1977 to 2006 (total of 355 months), divided by personal income estimates per county per year from the Bureau of Economic Accounts (BEA). A key feature of this dataset is its extremely heavy-tailed behavior, emphasizing the need for risk-averse approach to decision-making. Average, max and min kurtosis of the associated loss distribution for the dataset are 207.35, 353.00 (Jefferson county) and 70.55 (Lafayette county), respectively.

Problem description The decision-making problem considered in the study was selected to be deliberately simple. Since our goal is to analyze the performance of the stochastic modeling framework, a simple decision problem lets us concentrate on the risk model itself. Namely, the problem of selecting a distribution of a resource over a fixed number of counties (K below) is considered, so that the overall exposure to flood risk, as measured by flood insurance claims, is minimized. More specifically, let us denote as ℓ_{ij} the total flood insurance claims in county i under scenario j. Then, decision vector $\mathbf{x} = (x_1, \ldots, x_{67})$ is considered as a vector of weights associated with each county, and construct the problem of selecting these weights in order to reduce the overall risk exposure. The problem can be viewed as a form of portfolio selection, where the portfolio is composed of counties and the losses are due to flooding, i.e., we are interested in distributing a resource among the counties while being wary of flooding risk. Alternatively, we can view it as a way to determine a “fair” distribution of risk in the sense that each county is weighted inversely proportional to the exposure to flooding.

Methodology The dataset is split into a training and testing sets, with training comprised of the first m months (out of 355 total). The training set is used to determine optimal vector $\mathbf{x}^*$ and then actual flooding losses are observed using the testing set. The total loss is calculated as $L = \sum_{j=m+1}^{355} \sum_i \ell_{ij} x_i^*$.

A heuristic version of two stage diversification-reward framework is employed to find the resource distribution. In this case, first, K counties are identified with a minimal common insurance risk due to flood as estimated by CVaR using the following stochastic optimization model:

$$\min \quad \eta + \frac{1}{m(1-\alpha)} \sum_{j=1}^{m} w_j \tag{4.8a}$$

$$\text{s. t.} \quad w_j \geq \sum_{i=1}^{n} \ell_{ij} x_i - \eta, \quad j = 1, 2, ..., m \tag{4.8b}$$

$$\sum_{i=1}^{n} x_i \geq K \tag{4.8c}$$

$$x_i \in \{0, 1\}, \quad w_j \geq 0. \tag{4.8d}$$

We start with the solution for this problem and eliminate all counties not selected into the optimal portfolio. Then, in the second stage the actual distribution of the resource is identified by solving either CVaR-RP problem (DR-CVaR-RP) or Equally Weighted approach (DR-CVaR-EW) among K selected counties. Note that both approaches, by construction, always select all counties into the optimal solution, i.e., $x_i^{EW} \neq 0$ and $x_i^{CVaR-RP} \neq 0$ for all i.

Table 4.1 and Figure 4.1 report the performance of the approaches in terms of average loss, and standard deviation for a number of values of K, α and m. As expected, as the value of K increases, so do the average loss and its standard deviation, since it forces the first stage model to consider more flood-prone counties. Across all values of K, α and m and in terms of both average loss and standard deviation it is observed that the RP version outperforms the EW approach. While it is due to the fact that RP solution assigns lower weight to more risky counties, as it is noted above, the RP model does not have a built-in mechanism for selecting "better" solutions other than the diversification principle itself. Hence, we conclude that this experiment supports our claim that CVaR-RP solution can lead to improved performance.

Table 4.1: Comparing the performance of DR-CVaR-RP and DR-CVaR-EW in terms of average (avg) and standard deviation of loss (std) with different α_{CVaR} and testing datasets. Values are $\times 10^4$.

	m=100, $\alpha_{\text{CVaR}} = 0.95$				m=100, $\alpha_{\text{CVaR}} = 0.90$			
	DR-CVaR-RP		DR-CVaR-EW		DR-CVaR-RP		DR-CVaR-EW	
K	avg	std	avg	std	avg	std	avg	std
10	0.86	5.78	1.38	10.56	0.98	7.08	1.33	10.49
20	1.03	5.12	2.21	13.95	1.32	7.63	3.40	20.92
30	1.31	6.41	4.71	29.04	1.70	9.58	8.62	60.78
40	1.52	7.37	8.50	56.54	1.68	9.17	8.31	55.72
50	2.00	8.41	18.14	90.54	1.87	9.75	13.37	83.94
60	1.91	8.35	26.17	153.98	2.03	10.02	26.17	153.98

	m=200, $\alpha_{\text{CVaR}} = 0.95$				m=200, $\alpha_{\text{CVaR}} = 0.90$			
	DR-CVaR-RP		DR-CVaR-EW		DR-CVaR-RP		DR-CVaR-EW	
K	avg	std	avg	std	avg	std	avg	std
10	0.53	4.13	0.46	3.08	0.51	3.95	0.46	3.08
20	1.26	8.40	12.53	94.92	1.41	9.56	12.53	94.92
30	1.10	7.27	10.04	69.41	1.58	10.82	9.69	69.37
40	1.46	8.14	19.55	116.26	1.84	11.12	19.38	116.13
50	1.43	8.19	23.49	147.59	1.84	11.00	23.49	147.59
60	1.43	8.10	29.07	185.20	1.76	10.18	29.07	185.20

	m=300, $\alpha_{\text{CVaR}} = 0.95$				m=300, $\alpha_{\text{CVaR}} = 0.90$			
	DR-CVaR-RP		DR-CVaR-EW		DR-CVaR-RP		DR-CVaR-EW	
K	avg	std	avg	std	avg	std	avg	std
10	1.59	7.88	0.73	3.15	1.60	7.98	0.70	3.05
20	1.57	7.79	1.07	5.36	1.52	7.62	0.86	4.46
30	1.88	9.71	4.60	30.08	1.57	7.74	1.35	6.40
40	2.32	12.33	8.16	47.98	2.02	10.57	8.40	54.16
50	2.30	12.03	10.36	58.76	2.10	10.93	10.36	58.76
60	2.42	12.71	34.92	162.62	2.32	11.99	34.92	162.62

Figure 4.1: Comparing the performance of DR-CVaR-RP, and DR-CVaR-EW in terms of average and standard deviation of loss with different α_{CVaR} and testing datasets.

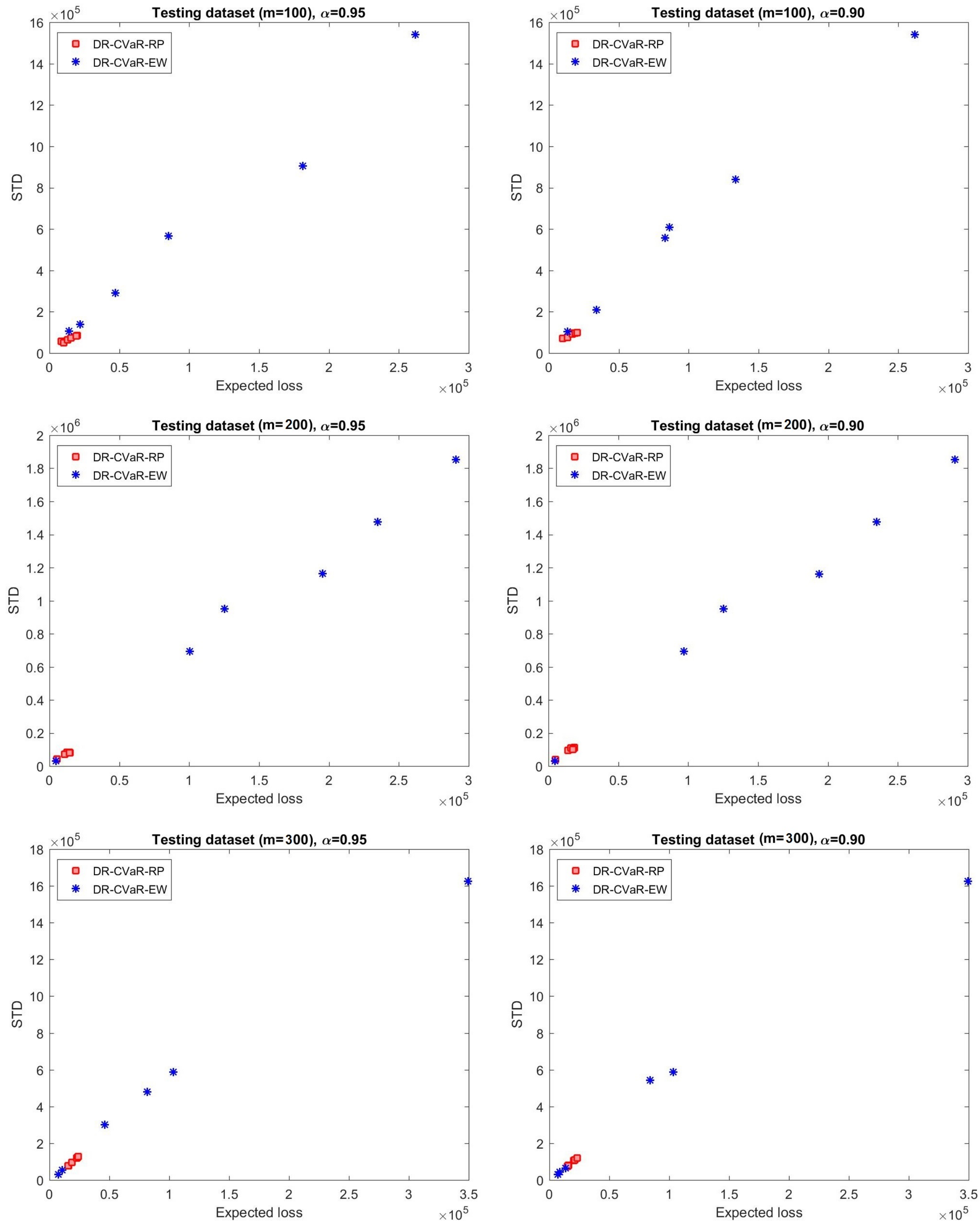

4.4.2 Case Study 2: Portfolio optimization

Data description For the second study the standard financial portfolio optimization framework is employed with historical asset returns. The data is collected through Yahoo Finance for assets in S&P500 index. Fifty assets with highest average return were selected for historical close price from September 2005 through October 2015, therefore, providing 2499 scenarios (trading days). Asset returns r_{ij} are calculated as $r_{ij} = \frac{p_{i,j} - p_{i,j-T}}{p_{i,j-T}}$, where $p_{i,j}$ is the historical close price of asset i on day j, and T represents a "delay" parameter and takes values of T = 3, 5, and 10 days. The dataset has a heavy-tailed behavior and the average kurtosis of the associated loss distribution for the datasets with T = 3, 5, and 10 are 15.39, 10.57, and 9.74, respectively.

Problem description As described in the introduction, financial portfolio selection is widely used to test risk-averse stochastic optimization models. It should be emphasized that, similarly to the first case study, since the primary goal in this study is to evaluate the modeling technique, we are not intending it to serve as a simulation of real-life trading. Our aim is to demonstrate that in the presence of heavy-tailed distributions of losses proposed models provide robust and effective diversification tools. Thus, we simplify our model to ignore some practical considerations such as transaction costs or cardinality constraints, and base the scenario model directly on the historically observed returns. A market with $n = 50$ assets is considered and assumed that $m = 1000$ scenarios for realization of random assets' returns are available, denoting as r_{ij} the return of asset i under scenario j. Portfolio weights are denoted as $\mathbf{x} = (x_1, \ldots, x_n)^\top$.

Methodology Five solution approaches are employed and the results are compared: CVaR-RP, Equally Weighted (EW), mean-CVaR, and two diversification-reward models based on Risk Parity (DR-CVaR-RP) and Equally Weighted (DR-CVaR-EW). In this case, the loss function is defined as negative portfolio return, i.e., $\sum_i -r_{ij}x_i$.

Here, the two stage diversification-reward framework is slightly different than the previous case study. Mean-CVaR is a standard solution approach. In this case, ten solutions are generated located on the efficient mean-CVaR frontier, which are denoted as P1, ..., P10. P1 corresponds to the minimum CVaR solution, and P10 is the maximum average return solution, P2, ..., P9 are selected in between by varying target average return.

Based on P1, ..., P10 we also obtain two sets of ten diversification-reward solutions for RP and EW. We start from a solution to mean-CVaR model (first stage) and eliminate all assets not selected into the optimal portfolio. Then, in the second stage the actual distribution of the budget on each asset is identified by solving either CVaR-RP problem or according to Equally Weighted approach. The resulting solutions are denoted as DR-CVaR-RP and DR-CVaR-EW respectively.

Table 4.2 shows the performance of mean-CVaR, DR-CVaR-RP, and DR-CVaR-EW in terms of average (avg), standard deviation (std) of return and the Sharpe ratio (SR). The SR, interpreted as risk-adjusted return, is calculated as the ratio between the average rate of return and the standard deviation (volatility). Figure 4.2 demonstrates the performance of above methods as well as the CVaR-RP and EW on all assets. The Sharpe ratio of these methods are compared in Figure 4.3 for different portfolios across the efficient frontier for both training and testing datasets.

Table 4.2: Comparing the performance of mean-CVaR, DR-CVaR-RP, and DR-CVaR-EW in terms of average (avg), standard deviation (std) of return, and Sharpe ratio (SR) with different α_{CVaR} and testing datasets. Values are in percentage.

	m=1000, $T=1$, $\alpha_{\text{CVaR}}=0.95$									m=1000, $T=1$, $\alpha_{\text{CVaR}}=0.90$								
	mean-CVaR			DR-CVaR-RP			DR-CVaR-EW			mean-CVaR			DR-CVaR-RP			DR-CVaR-EW		
	avg	std	SR	avg	std	SR	avg	std	SR	avg	std	SR	avg	std	SR	avg	std	SR
P1	0.04	0.70	6.03	0.04	0.71	5.66	0.04	0.71	5.53	0.04	0.72	6.13	0.05	0.76	6.14	0.05	0.77	6.00
P2	0.05	0.74	7.14	0.06	0.76	7.90	0.07	0.82	8.34	0.05	0.77	7.17	0.06	0.78	7.92	0.07	0.84	8.23
P3	0.06	0.82	7.38	0.06	0.79	7.91	0.07	0.86	8.31	0.06	0.86	7.26	0.05	0.75	7.05	0.06	0.83	7.52
P4	0.07	0.94	7.44	0.07	0.84	8.54	0.08	0.91	8.87	0.07	0.97	7.44	0.06	0.81	7.46	0.07	0.92	8.05
P5	0.08	1.11	7.62	0.06	0.91	6.76	0.07	0.98	7.25	0.08	1.11	7.56	0.06	0.76	7.61	0.07	0.85	8.20
P6	0.10	1.27	7.49	0.08	1.08	7.15	0.09	1.24	6.91	0.10	1.28	7.52	0.08	1.08	7.10	0.09	1.24	6.91
P7	0.11	1.46	7.29	0.07	1.04	6.29	0.08	1.27	6.03	0.11	1.46	7.37	0.08	1.05	7.20	0.10	1.28	7.48
P8	0.12	1.66	7.19	0.07	1.03	7.10	0.10	1.28	7.48	0.12	1.67	7.20	0.09	1.08	7.85	0.10	1.25	8.09
P9	0.13	1.88	7.00	0.08	1.08	7.83	0.10	1.25	8.09	0.13	1.88	6.99	0.08	1.05	7.20	0.10	1.28	7.48
P10	0.14	2.11	6.80	0.14	2.11	6.80	0.14	2.11	6.80	0.14	2.11	6.80	0.14	2.11	6.80	0.14	2.11	6.80

	m=1000, $T=3$, $\alpha_{\text{CVaR}}=0.95$									m=1000, $T=3$, $\alpha_{\text{CVaR}}=0.90$								
	mean-CVaR			DR-CVaR-RP			DR-CVaR-EW			mean-CVaR			DR-CVaR-RP			DR-CVaR-EW		
	avg	std	SR	avg	std	SR	avg	std	SR	avg	std	SR	avg	std	SR	avg	std	SR
P1	0.13	1.18	10.90	0.17	1.35	12.47	0.19	1.50	12.52	0.14	1.18	12.03	0.18	1.38	13.43	0.20	1.48	13.31
P2	0.16	1.23	13.17	0.21	1.42	14.77	0.24	1.57	14.97	0.18	1.28	13.84	0.20	1.34	14.55	0.22	1.47	15.06
P3	0.22	1.45	14.88	0.22	1.42	15.48	0.25	1.56	15.93	0.20	1.44	14.07	0.20	1.40	14.49	0.23	1.53	14.98
P4	0.24	1.64	14.45	0.24	1.52	15.84	0.27	1.70	16.00	0.24	1.67	14.60	0.21	1.38	15.49	0.25	1.55	16.07
P5	0.27	1.89	14.29	0.24	1.65	14.52	0.27	1.81	15.04	0.27	1.91	14.25	0.22	1.57	14.24	0.26	1.75	14.96
P6	0.31	2.19	14.00	0.29	1.89	15.31	0.31	2.03	15.46	0.31	2.20	13.89	0.29	1.87	15.30	0.31	2.03	15.46
P7	0.33	2.52	13.15	0.25	1.84	13.70	0.26	2.06	12.85	0.33	2.53	13.16	0.27	1.81	14.73	0.30	2.03	14.90
P8	0.37	2.90	12.63	0.25	1.84	13.70	0.26	2.06	12.85	0.37	2.91	12.62	0.27	1.81	14.73	0.30	2.03	14.90
P9	0.40	3.31	12.18	0.25	1.84	13.70	0.26	2.06	12.85	0.40	3.32	12.18	0.27	1.81	14.73	0.30	2.03	14.90
P10	0.43	3.71	11.58	0.43	3.71	11.58	0.43	3.71	11.58	0.43	3.71	11.58	0.43	3.71	11.58	0.43	3.71	11.58

	m=1000, $T=10$, $\alpha_{\text{CVaR}}=0.95$									m=1000, $T=10$, $\alpha_{\text{CVaR}}=0.90$								
	mean-CVaR			DR-CVaR-RP			DR-CVaR-EW			mean-CVaR			DR-CVaR-RP			DR-CVaR-EW		
	avg	std	SR	avg	std	SR	avg	std	SR	avg	std	SR	avg	std	SR	avg	std	SR
P1	0.46	2.11	21.58	0.58	2.28	25.51	0.66	2.54	25.83	0.49	2.05	23.88	0.54	2.26	23.87	0.61	2.51	24.50
P2	0.62	2.30	26.91	0.57	2.32	24.54	0.63	2.53	24.91	0.63	2.29	27.34	0.61	2.33	26.37	0.71	2.59	27.34
P3	0.74	2.68	27.69	0.66	2.42	27.47	0.76	2.66	28.59	0.75	2.65	28.13	0.66	2.40	27.70	0.79	2.75	28.55
P4	0.85	3.08	27.71	0.66	2.42	27.47	0.76	2.66	28.59	0.87	3.15	27.50	0.64	2.37	27.03	0.76	2.65	28.68
P5	0.98	3.62	27.16	0.68	2.48	27.24	0.79	2.81	28.26	0.99	3.72	26.54	0.74	2.54	29.24	0.87	2.97	29.26
P6	1.13	4.21	26.72	0.83	2.76	30.10	0.91	3.16	28.85	1.10	4.33	25.49	0.68	2.46	27.76	0.85	3.06	27.81
P7	1.23	4.84	25.36	0.87	2.80	30.90	0.98	3.23	30.46	1.23	4.97	24.65	0.85	3.27	26.03	0.99	3.79	26.20
P8	1.34	5.55	24.21	0.99	3.48	28.49	1.07	3.76	28.52	1.34	5.63	23.89	0.85	3.27	26.03	0.99	3.79	26.20
P9	1.39	6.08	22.93	1.22	4.94	24.72	1.25	5.03	24.92	1.40	6.12	22.83	1.22	4.94	24.69	1.25	5.03	24.92
P10	1.45	6.69	21.64	1.45	6.69	21.64	1.45	6.69	21.64	1.45	6.69	21.64	1.45	6.69	21.64	1.45	6.69	21.64

Figure 4.2: Comparing the performance of CVaR-RP, EW, mean-CVaR, DR-CVaR-RP, and DR-CVaR-EW in terms of average and standard deviation of return with different α_{CVaR} and testing datasets.

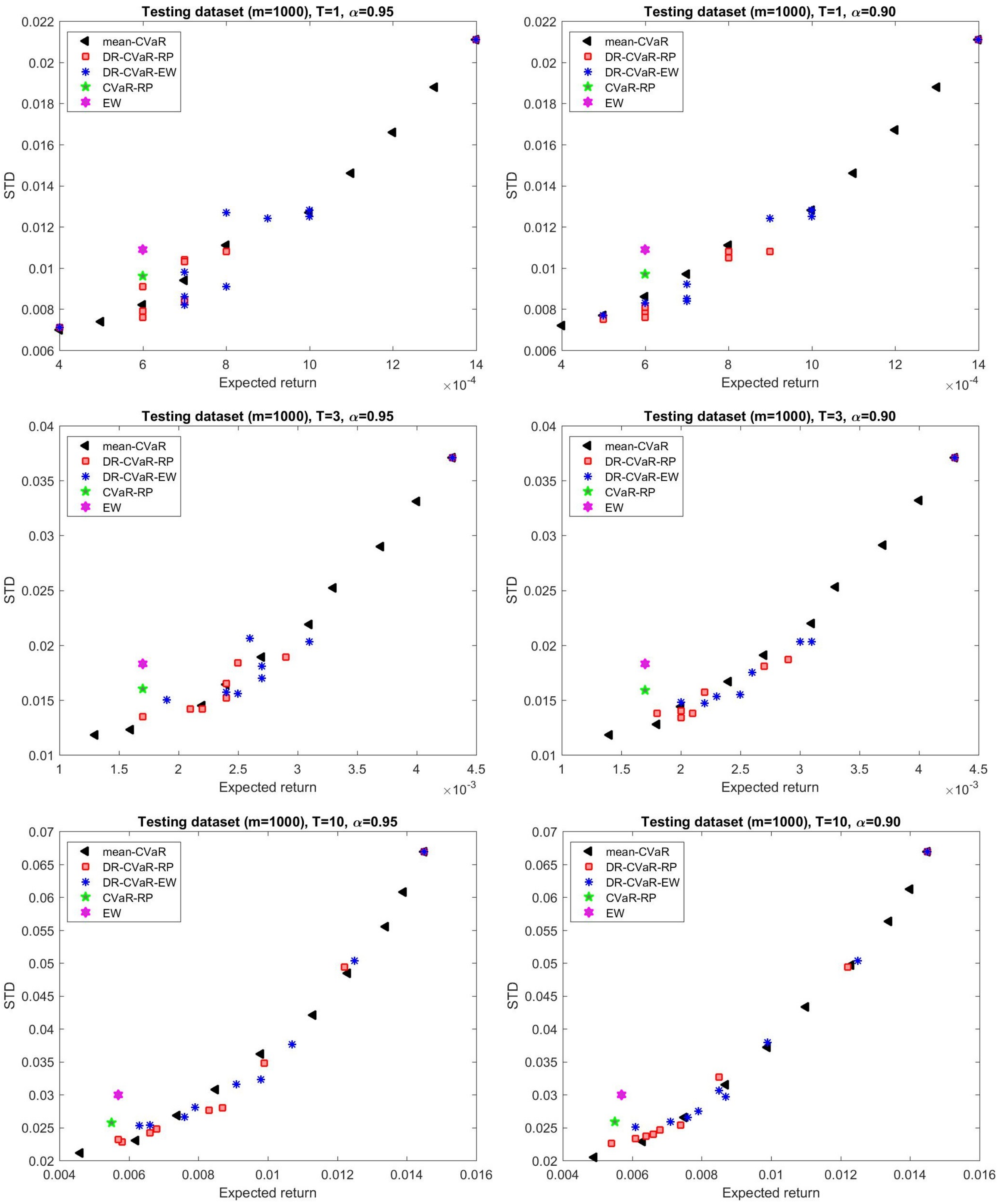

Figure 4.3: Comparing the performance of mean-CVaR, DR-CVaR-RP, and DR-CVaR-EW in terms of Sharpe ratio with $\alpha_{\text{CVaR}} = 0.95$ and different training and testing datasets.

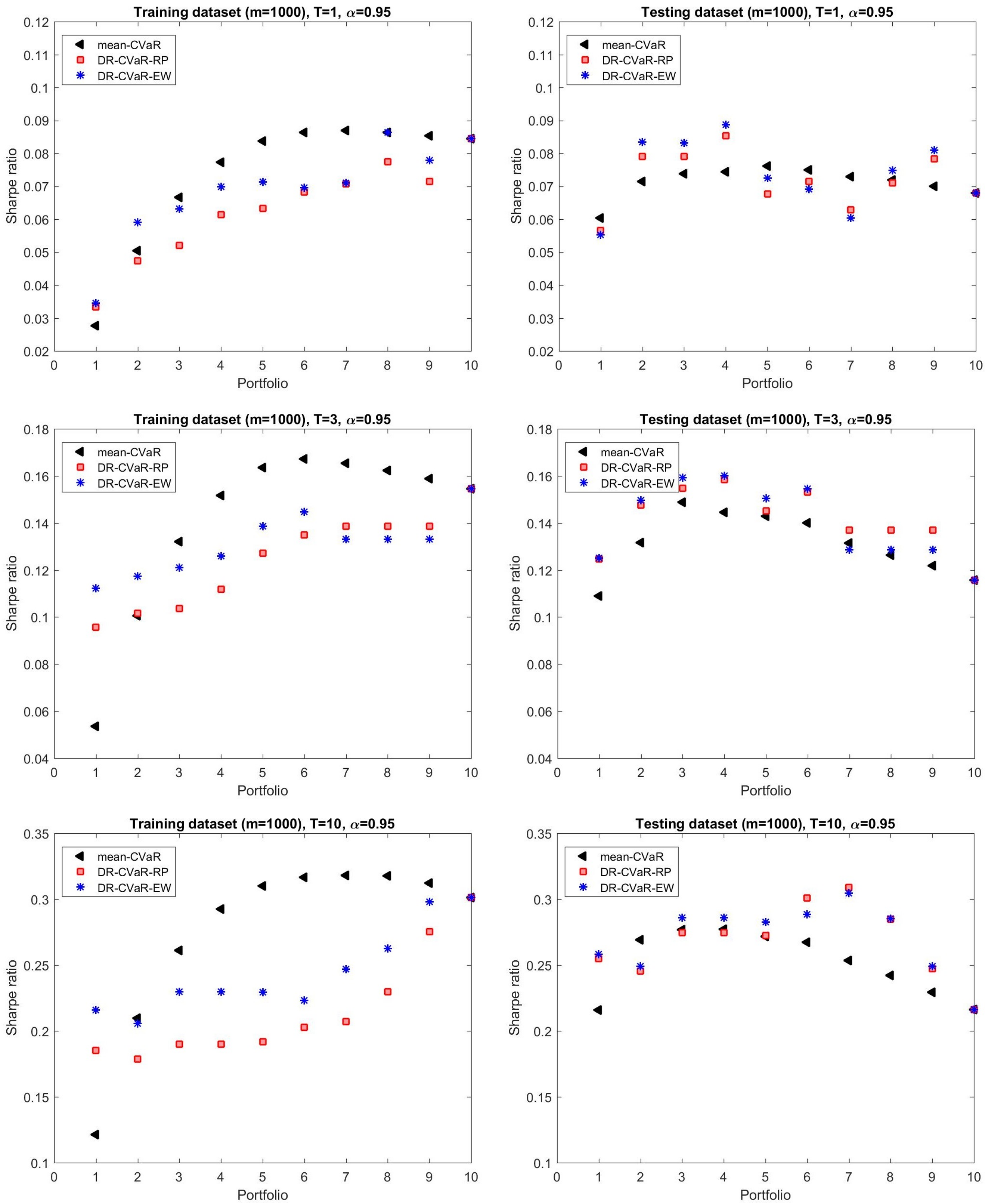

In this case, the performance improvement due to the diversification methods is moderate. Specifically, it is observed that while standard risk-reward model leads to better Sharpe ratios on the training set (the left-hand side column on Figure 4.3), either RP or EW portfolios lead to the best Sharpe ratios on the testing sets. This suggests that the improved diversity of the decisions hedges some of the risk associated with potentially inadequate selection of the testing set. It is also observed that both of the risk-diversification methods slightly improve the efficient frontier (Figure 4.2). At the same time, this improvement is at best moderate.

Note that as described in the introduction, financial portfolios are usually the primary area of application for direct diversification methods. The fact that in our experiments the proposed methods show an the best quality of improvement compared to conventional approaches for non-financial study suggest that it has a high potential to be useful in engineering and other decision-making domains. We hypothesize that the presence of extremely heavy-tailed distribution of losses is the driving force behind usefulness of the proposed RP-CVaR approach. In this case, it can be likely that a future outcome (flood-related losses) will be significantly more impactful than anything that can be learned from the past, which synergizes well with the diversification idea, and further, a more informed approach based on RP is better that the naive EW.

4.4.3 Case Study 3: Hazardous Materials Transportation

Data description The study is based on a portion of an actual road network in Buffalo, New York, which consists of 15 nodes and 21 arcs. Considering node 1 as the origin and node 14 as the destination, there are 9 possible routes to traverse the network. Thre main attributes are considered for each arc: a) length, b) accident probabilities, c) accident consequences on the λ-neighborhood of the impact zone. The risk associated with each road segment is calculated as the multiplication of accident probabilities and consequences. The nominal data is obtained from Toumazis and Kwon (2015). Hazmat accidents cause catastrophic consequences, which can be approximated with a heavy-tailed distribution. The Pareto distribution is used to generate the corresponding risk scenarios for each road segment due to heavy-tailed characteristic of the associated risk.

Problem description In hazardous material (hazmat) transportation some routes should be selected to transport products/waste on the road network. Moving hazmat raises an inherent risk for public safety and environment. Hazmat accidents cause catastrophic consequences such as fatalities, severe injuries, and property and environment damage. Using a single optimal route over time will result in overloaded hazmat traffic on specific links of the network, and lead to increase in incident probabilities and risk inequity. Our aim is to show in the presence of heavy-tailed risk distribution on the road network, the proposed models provide effective diversification approach to make routing decisions. Total $n = 9$ routes on the network from the origin to the destination with $m = 1000$ scenarios for training and another $m = 1000$ scenarios for testing are considered.

Methodology Three solution approaches are used and results are compared: DR-CVaR-RP, DR-CVaR-EW, and selecting a single path. The solution procedure is demonstrated in Figure 4.4. Yen's k-shortest algorithm (Yen 1971) is employed to finds all the paths available from the origin to the destination and sorted them based on distance. In order to select the first stage variables in the risk-reward framework, the mean-CVaR approach is applied to select best n paths. Then, the CVaR-RP model (4.9) is applied on the selected paths to find the amount of shipments on each route. Our proposed method aim to evenly distribute the risks associated with hazmat transportation among the exposed communities while making sure that overall system risk is controlled. In the benchmark the same procedure as in Figure 4.4 is used, except the Equally Weighted approach is employed to find the shipment weights on road segments.

Figure 4.4: DR-CVaR-RP solution procedure for hazmat route planning

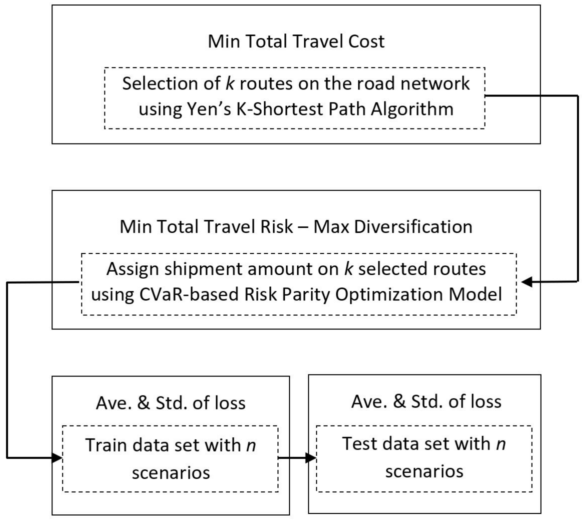

Let n and m be the number of routes and scenarios and set parameters r_{ij} as the risk on route i under scenario j. The corresponding CVaR-RP model can be formulated as follow:

$$\begin{aligned} \min \quad & \eta + \frac{1}{m(1-\alpha)} \sum_{j=1}^{m} w_j \\ \text{s. t.} \quad & \sum_{i=1}^{n} ln(y_i) \geq c \\ & w_j \geq \sum_{i=1}^{n} r_{ij} y_i - \eta, \quad \forall j = 1, 2, ..., m \\ & y_i \geq 0; \quad w_j \geq 0; \end{aligned} \tag{4.9}$$

In model (4.9), y_i indicates the weight of shipments on each route i. First, the average loss and standard deviation of selecting a single path to ship the hazmat through the road network are presented in Table 4.3. The routes are sorted based on the distance, meaning that route 1 is shorter than route 2 and so on. On the contrary, shortest path does not mean lower risk exposure. According to the results, in case of selecting only a single path, route 3 is the best choice in terms of average risk. On the other hand, routes 7, 8 and 9 appear to be less attractive having higher risk exposure.

Table 4.3: Comparing single path selection for hazmat shipments. Values are $\times 10^{-3}$.

	Single path								
	1	2	3	4	5	6	7	8	9
avg	0.64	1	0.36	0.74	3.1	2.2	3.6	3.5	3.3
std	6.7	7.9	2.2	4.8	15.5	14.1	16.7	17.9	16.9

Table 4.4 presents the route selection and the associated weights of hazmat shipments assigned to each route in case of $\alpha_{\text{CVaR}} = 0.99$ and $\alpha_{\text{CVaR}} = 0.95$. According to the results presented in Table 4.4, the model selects route 3 in case of choosing only one path to transport all the hazmat from the origin to the destination. The reason is that this route has lower corresponding risk. In case of shipping on two paths, routes 1 and 3 are selected and share close weights of shipments. As discussed earlier, routes 7, 8 and 9 are less attractive and are added to the route selection after other available routes. They also have low weights of shipment assigned. The last column in the table presents the hazmat weights on nine available routes, aiming to evenly distribute the risk through the road network. These weights can also be interpreted as a threshold for the allowance of the amount of hazmat products and waste shipments regulated by the governments and local authorities; meaning that the authorities can restrict the proportion of shipments on highly populated road segments to guarantee the risk equity on the network.

Table 4.4: Shipment weights on each route based on selecting n best routes.

	Number of n selected routes, $\alpha_{\text{CVaR}} = 0.99$								
Route	1	2	3	4	5	6	7	8	9
1	-	0.4458	0.3792	0.3065	0.2891	0.2693	0.2626	0.2641	0.2601
2	-	-	-	0.1498	0.1335	0.1287	0.1242	0.1191	0.1147
3	1.0000	0.5542	0.4051	0.3785	0.3552	0.3300	0.3292	0.3181	0.3194
4	-	-	0.2157	0.1652	0.1460	0.1411	0.1374	0.1290	0.1249
5	-	-	-	-	-	0.0574	0.0458	0.0371	0.0318
6	-	-	-	-	0.0762	0.0736	0.0616	0.0592	0.0578
7	-	-	-	-	-	-	-	0.0381	0.0321
8	-	-	-	-	-	-	0.0393	0.0353	0.0331
9	-	-	-	-	-	-	-	-	0.0259

	Number of n selected routes, $\alpha_{\text{CVaR}} = 0.95$								
Route	1	2	3	4	5	6	7	8	9
1	-	0.4115	0.3393	0.2740	0.2567	0.2442	0.2380	0.2330	0.2265
2	-	-	-	0.1492	0.1361	0.1291	0.1250	0.1209	0.1176
3	1.0000	0.5885	0.4341	0.3972	0.3729	0.3539	0.3423	0.3358	0.3307
4	-	-	0.2266	0.1796	0.1631	0.1544	0.1488	0.1438	0.1406
5	-	-	-	-	-	0.0000	0.0398	0.0368	0.0330
6	-	-	-	-	0.0711	0.0674	0.0652	0.0573	0.0560
7	-	-	-	-	-	0.0508	0.0409	0.0379	0.0331
8	-	-	-	-	-	-	-	0.0345	0.0326
9	-	-	-	-	-	-	-	-	0.0299

Table 4.5 presents the DR-CVaR-RP and DR-CVaR-EW models results for different selection of routes associated with the assigned weights. In this Table, n refers to the number of paths that are selected by mean-CVaR model in the first stage. The same results are also presented in Figure 4.5.

Table 4.5: Comparing the performance of DR-CVaR-RP and DR-CVaR-EW in terms of average (avg) and standard deviation of loss (std) with $\alpha_{\text{CVaR}} = 0.99$. Values are $\times 10^{-3}$.

	m=1000, Training dataset, $\alpha_{\text{CVaR}} = 0.99$				m=1000, Testing dataset, $\alpha_{\text{CVaR}} = 0.99$			
	DR-CVaR-RP		DR-CVaR-EW		DR-CVaR-RP		DR-CVaR-EW	
n	avg	std	avg	std	avg	std	avg	std
1	0.38	3.2	0.38	3.2	0.36	2.2	0.36	2.2
2	0.47	2.4	0.48	2.4	0.48	3.3	0.5	3.6
3	0.55	2.6	0.59	2.9	0.55	3	0.58	3
4	0.6	2.8	0.69	3.5	0.6	3.5	0.69	4.1
5	0.72	3	0.99	4.5	0.72	3.9	1	5.3
6	0.88	3.2	1.4	5.5	0.87	4	1.4	5.6
7	0.95	3.3	1.7	7.2	0.93	4.1	1.7	6.6
8	1	3.6	2	8.7	1	4	1.9	6.6
9	1.1	3.8	2.2	10.4	1	4.1	2.1	7.4

	m=1000, Training dataset, $\alpha_{\text{CVaR}} = 0.95$				m=1000, Testing dataset, $\alpha_{\text{CVaR}} = 0.95$			
	DR-CVaR-RP		DR-CVaR-EW		DR-CVaR-RP		DR-CVaR-EW	
n	avg	std	avg	std	avg	std	avg	std
1	0.38	3.2	0.38	3.2	0.36	2.2	0.36	2.2
2	0.46	2.4	0.48	2.4	0.47	3.2	0.5	3.6
3	0.54	2.7	0.59	2.9	0.54	2.9	0.58	3
4	0.6	2.9	0.69	3.5	0.6	3.4	0.69	4.1
5	0.71	3	0.99	4.5	0.71	3.7	1	5.3
6	0.87	3.1	1.5	5.5	0.86	3.6	1.4	5.1
7	0.95	3.3	1.7	7.5	0.93	3.7	1.7	5.9
8	1	3.6	2	8.7	1	3.9	1.9	6.6
9	1.1	3.9	2.2	10.4	1	4	2.1	7.4

Figure 4.5: Comparing DR-CVaR-RP, DR-CVaR-RP and single path solutions for hazmat case.

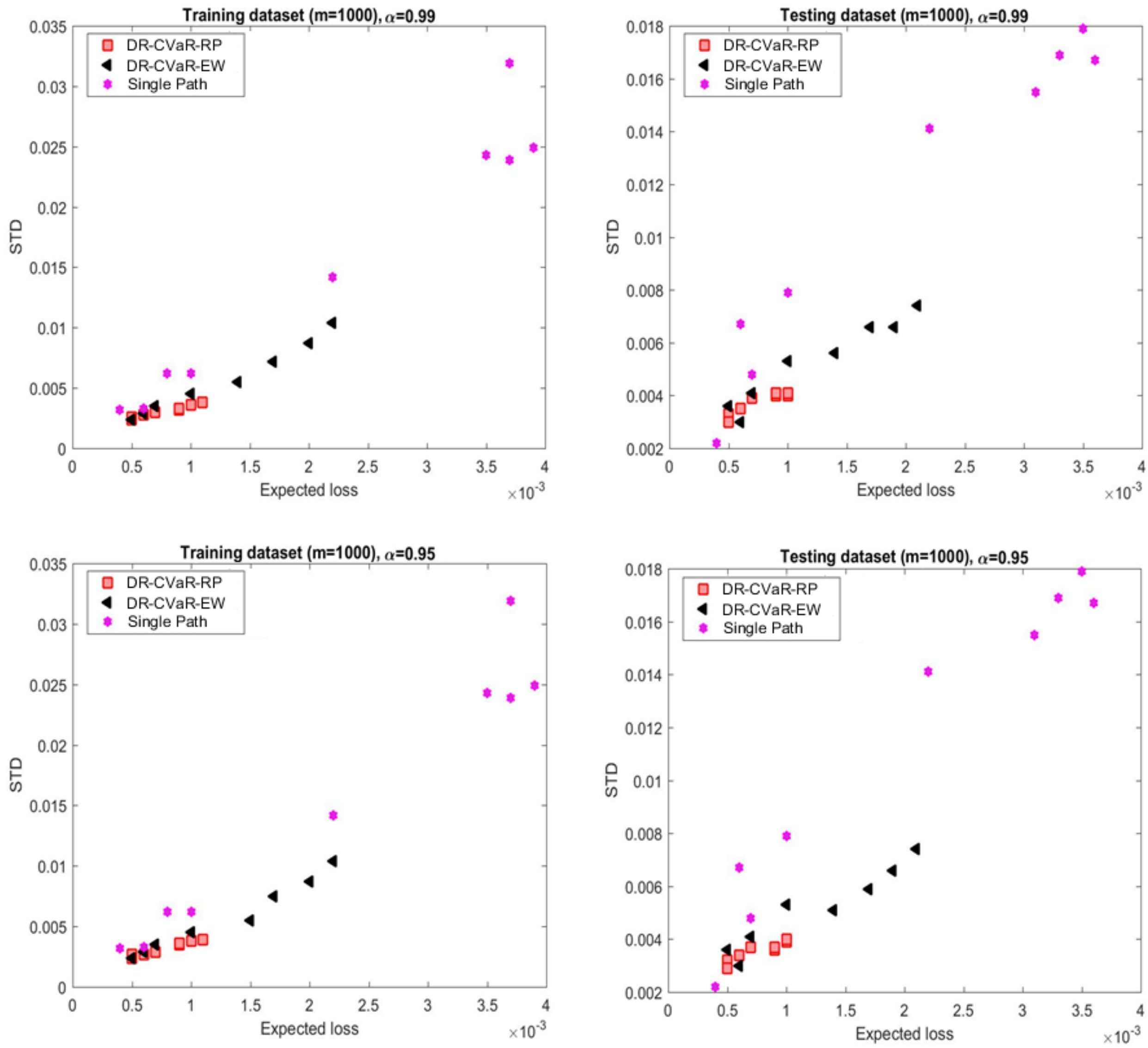

The computational results presented in Table 4.5 indicate that proposed risk-reward diversification framework outperforms Equally Weighted method in all cases of multiple route selections for hazmat shipments. The reason is that DR-CVaR-RP adjusts the shipment weights in a way that all involved routes have the same risk exposure. These results emphasize the effectiveness of proposed models in the presence of heavy-tailed risk distribution. The proposed risk diversification method ensures that the risks associated with hazmat transportation are evenly distributed through the involved road segments.

4.5 Conclusion

In this chapter, we aim at providing a mathematical programming framework for risk-averse decision making under uncertainty using both the concept of Risk Parity and coherent measures of risk. In this regard, we studied the mathematical foundation of general Risk Parity framework and presented a nonlinear convex optimization formulation for obtaining CVaR-based Risk Parity model. We also, developed a two stage diversification-risk framework aimed at combining the advantages of both Risk Parity and standard risk-reward optimization. We evaluated the performance of suggested methods by conducting three case studies. These case studies are based on historical data in flood insurance claims, financial asset returns, and hazardous materials transportation, respectively. We used the Equally Weighted approach and mean-CVaR as benchmarks to show effectiveness of our proposed models. Diversity-based solutions show promising results in all studies and we observe that the experiment based on non-financial data show particular potential. We conclude then that the considered approach could lead to improved decision-making in the presence of heavy-tailed distributions.

In addition to diversification of risk, the results can be interpreted through the concept of fairness. Here, a system can be outlined here which will be subjected to risk through the decisions. We may then be interested in assigning these decisions to parts of the system in such a way that none of them are overexposed. The hazardous materials routing and supply chain network design problems are examples for such system. Employing the proposed models in this chapter on the hazmat supply chain network design problem will be investigated in more details in a future study. Such models can be beneficial for making routing decisions in hazmat network design. Governments can regulate the hazmat transportation with respect to risk equity, while carriers can wisely select the shipment routes to follow the regulations while reducing their transportation costs.

Chapter 5

Summary and Future Research

This chapter summarizes the contributions of this dissertation and elaborates on relevant research questions that can be further addressed in future studies. In this dissertation, the hazardous materials routing and supply chain network design problems are studied. Risk-averse stochastic programming and robust optimization models are proposed to improve multiobjective decisions making processes. The goal of this dissertation is to propose policies which are not only interesting for the network regulators such as governments and local authorities in terms of hazmat risk mitigation but also are economically feasible to the hazmat carriers.

The transportation of hazmat has significant implications for public health and environmental safety, as accidents in the transportation of these materials affects not only the vehicles involved but also those communities in the surrounding vicinity. Chapters 2 is devoted to present a novel multiobjective integer programing model for the hazmat closed-loop supply chain problem which combines forward and reverse flows of hazmat products and waste to help making optimal strategical, tactical and operational decisions in the system. Considering cost factors and risks inherent in hazmat transportation, the developed model assists with optimal route selection, quantity of hazmat to be shipped, and locating the facility and emergency response teams. The model is applied to a case study with real data based on Albany road network in NY. Using the two-phase method, all the Pareto optimal solutions are extracted for various instances of the problem. The results indicate how slight increases in the cost of building the system can help reduce a significant amount of risk exposure. An interesting extension to this work would be to refine the risk assessment objective function such that it accounts other aspects that affect risk exposure such as traffic, weather condition, and driver's performance. Another interesting future direction is to achieve equity in distributing the risk among the different road segments by employing Risk Parity and risk-averse models.

In Chapter 3, the hazmat closed-loop supply chain network design problem is also investigated by taking into account various uncertainty sources, such as customers' demand and return. Two approaches are considered to deal with such uncertainty. First, it is assumed that the distributions of demand and return are known and a two-stage stochastic model is developed to provide centers' location and capacity decisions in the first stage and shipment and routing decision in the second stage after realization of the uncertainty sources. The proposed two-stage model minimized the total cost and risk on average, meaning that for a fixed placement decisions, the average of the cost and risk over many scenarios of uncertainty source converges to the expected value, where the Pareto solutions are optimal on average. Second, we considered a case where there is not enough data to estimate the distribution of demand and return. A robust framework is presented to hedge the optimization model in case of data uncertainty. The performance of both models are evaluated based on the Albany road network dataset and results demonstrate the decision-making process under uncertainty when there exists a likelihood of catastrophic or risky circumstances. A beneficial extension would be to allow risk uncertainty in the model since in many cases there is not enough historical data for hazmat accident and consequence probabilities. This not only expands the applicability of the model in practice, but also is likely to improve the routing and placement decisions in terms of the associated risk. Another suggested extension of this model is to consider reliability of centers in managing supply chain vulnerability, and generate corresponding models that can guarantee efficiency of the supply chain under potential disruptions.

In the hazmat transportation problem, a number of routes should be selected to ship products and waste. Hazmat carriers tend to select shorter routes to minimize their operational costs. Such routes might pass through heavily populated areas, in which accident occurrences can affect a larger number of people and cause catastrophic consequences. On the other hand, network regulators are more concerned about the risk mitigation in the road network and try to set enforcements for carriers to avoid certain areas. To address these challenges in hazmat transportation, risk-averse mathematical models are developed in Chapter 4 using Risk Parity concept in conjunction with coherent risk measures. We assessed the properties of the proposed frameworks for decision-making under uncertainty with heavy-tailed distribution of losses. The proposed frameworks enable the development of diversified routes, where it can be ensured that the risks associated with hazmat transportation are distributed fairly among the exposed communities, while the overall system risk is controlled. A beneficial extension, however, would be to study the mathematical formulation properties in more details and consider larger datasets for hazmat case study. Another interesting future work is to employ developed frameworks in the hazmat closed-loop supply chain network design problem to assist and improve risk equity in routing decisions.

Bibliography

Aboutahoun, A., 2012. Combined distance-reliability model for hazardous waste transportation and disposal. Life Sciences Journal 9 (2), 1286–1295.

Alumur, S., Kara, B. Y., 2007. A new model for the hazardous waste location-routing problem. Computers & Operations Research 34 (5), 1406–1423.

Amaldi, E., Bruglieri, M., Fortz, B., 2011. On the hazmat transport network design problem. In: International Conference on Network Optimization. Springer, pp. 327–338.

Ardjmand, E., Young, W. A., Weckman, G. R., Bajgiran, O. S., Aminipour, B., Park, N., 2016. Applying genetic algorithm to a new bi-objective stochastic model for transportation, location, and allocation of hazardous materials. Expert systems with applications 51, 49–58.

Artzner, P., 1997. Applebaum, d.(2004). lévy processes and stochastic calculus (cambridge university press). artzner, p., delbaen, f., eber, j.-m. and heath, d.(1997). thinking coherently, risk 10, pp. 68–71. Risk 10, 68–71.

Artzner, P., Delbaen, F., Eber, J.-M., Heath, D., 1999. Coherent measures of risk. Mathematical finance 9 (3), 203–228.

Asefi, H., Lim, S., Maghrebi, M., Shahparvari, S., 2019. Mathematical modelling and heuristic approaches to the location-routing problem of a cost-effective integrated solid waste management. Annals of Operations Research 273 (1-2), 75–110.

Asgari, N., Rajabi, M., Jamshidi, M., Khatami, M., Farahani, R. Z., 2017. A memetic algorithm for a multi-objective obnoxious waste location-routing problem: a case study. Annals of Operations Research 250 (2), 279–308.

Ben-Tal, A., Nemirovski, A., 2000. Robust solutions of linear programming problems contaminated with uncertain data. Mathematical programming 88 (3), 411–424.

Ben-Tal, A., Nemirovski, A., 2001. On polyhedral approximations of the second-order cone. Math. Oper. Res. 26 (2), 193–205.
URL http://dx.doi.org/10.1287/moor.26.2.193.10561

Berglund, P. G., Kwon, C., 2014. Robust facility location problem for hazardous waste transportation. Networks and spatial Economics 14 (1), 91–116.

Berman, O., Verter, V., Kara, B. Y., 2007. Designing emergency response networks for hazardous materials transportation. Computers & operations research 34 (5), 1374–1388.

Bertsimas, D., Sim, M., 2004. The price of robustness. Operations research 52 (1), 35–53.

Bianco, L., Caramia, M., Giordani, S., 2009. A bilevel flow model for hazmat transportation network design. Transportation Research Part C: Emerging Technologies 17 (2), 175–196.

Bianco, L., Caramia, M., Giordani, S., Piccialli, V., 2015. A game-theoretic approach for regulating hazmat transportation. Transportation Science 50 (2), 424–438.

Birge, J. R., Louveaux, F., 1997. Introduction to Stochastic Programming. Springer, New York.

Birge, J. R., Louveaux, F., 2011. Introduction to stochastic programming. Springer Science & Business Media.

Boudt, K., Carl, P., Peterson, B. G., 2012. Asset allocation with conditional value-at-risk budgets.

Boyer, O., Sai Hong, T., Pedram, A., Mohd Yusuff, R. B., Zulkifli, N., 2013. A mathematical model for the industrial hazardous waste location-routing problem. Journal of Applied Mathematics 2013.

Bruder, B., Roncalli, T., 2012. Managing risk exposures using the risk budgeting approach.

Cappanera, P., Gallo, G., Maffioli, F., 2003. Discrete facility location and routing of obnoxious activities. Discrete Applied Mathematics 133 (1-3), 3–28.

Cesarone, F., Colucci, S., Apr 2017. Minimum risk versus capital and risk diversification strategies for portfolio construction. Journal of the Operational Research Society.
URL https://doi.org/10.1057/s41274-017-0216-5

Cesarone, F., Tardella, F., 2016. Equal risk bounding is better than risk parity for portfolio selection. Journal of Global Optimization, 1–23.

Charnes, A., Cooper, W. W., Symonds, G. H., 1958. Cost horizons and certainty equivalents: An approach to stochastic programming of heating oil. Management Science 4 (3), 235–263.
URL http://www.jstor.org/stable/2627328

Chaves, D. B., Hsu, J. C., Li, F., Shakernia, O., 2011. Risk parity portfolio vs. other asset allocation heuristic portfolios. Journal of Investing 20 (1), 108–118.

Chaves, D. B., Hsu, J. C., Li, F., Shakernia, O., 2012. Efficient algorithms for computing risk parity portfolio weights. Journal of Investing 21, 150–163.

Cherny, A., Orlov, D., 2011. On two approaches to coherent risk contribution. Mathematical Finance 21 (3), 557–571.

Choueifaty, Y., Froidure, T., Reynier, J., 2013. Properties of the most diversified portfolio. Journal of Investment Strategies 2 (2), 49–70.

Cooke, R. M., Nieboer, D., 2011. Heavy-tailed distributions: Data, diagnostics, and new developments. Resources for the Future Discussion Paper (11-19).

Current, J., Ratick, S., 1995. A model to assess risk, equity and efficiency in facility location and transportation of hazardous materials. Location Science 3 (3), 187–201.

Duffie, D., Pan, J., 1997. An overview of value-at-risk. Journal of Derivatives 4, 7–49.

Emek, E., Kara, B. Y., 2007. Hazardous waste management problem: The case for incineration. Computers & Operations Research 34 (5), 1424–1441.

Erkut, E., Alp, O., 2007a. Designing a road network for hazardous materials shipments. Computers & Operations Research 34 (5), 1389–1405.

Erkut, E., Alp, O., 2007b. Integrated routing and scheduling of hazmat trucks with stops en route. Transportation Science 41 (1), 107–122.

Erkut, E., Gzara, F., 2008. Solving the hazmat transport network design problem. Computers & Operations Research 35 (7), 2234–2247.

Esfandeh, T., Batta, R., Kwon, C., 2017. Time-dependent hazardous-materials network design problem. Transportation Science.

Esfandeh, T., Kwon, C., Batta, R., 2016. Regulating hazardous materials transportation by dual toll pricing. Transportation Research Part B: Methodological 83, 20–35.

Falit-Baiamonte, A., Osleeb, J. P., 2000. An equity model for locating environmentally hazardous facilities. Geographical Analysis 32 (4), 351–368.

Fan, J., Yu, L., Li, X., Shang, C., Ha, M., 2019. Reliable location allocation for hazardous materials. Information Sciences.

Feng, Y., Palomar, D. P., 2015. Scrip: Successive convex optimization methods for risk parity portfolio design. IEEE Transactions on Signal Processing 63 (19), 5285–5300.

Feng, Y., Palomar, D. P., 2016. Portfolio optimization with asset selection and risk parity control. In: Acoustics, Speech and Signal Processing (ICASSP), 2016 IEEE International Conference on. IEEE, pp. 6585–6589.

Fisher, G. S., Maymin, P., Maymin, Z., 2012. Risk parity optimality. Available at SSRN 2188574.

Fontaine, P., Minner, S., 2018. Benders decomposition for the hazmat transport network design problem. European Journal of Operational Research 267 (3), 996–1002.

Giannikos, I., 1998. A multiobjective programming model for locating treatment sites and routing hazardous wastes. European Journal of Operational Research 104 (2), 333–342.

Griveau-Billion, T., Richard, J.-C., Roncalli, T., 2013. A fast algorithm for computing high-dimensional risk parity portfolios.

Gzara, F., 2013. A cutting plane approach for bilevel hazardous material transport network design. Operations Research Letters 41 (1), 40–46.

Haimes, Y., 1971. On a bicriterion formulation of the problems of integrated system identification and system optimization. IEEE transactions on systems, man, and cybernetics 1 (3), 296–297.

Hamouda, G., Saccomanno, F., Fu, L., 2004. Quantitative risk assessment decision-support model for locating hazardous materials teams. Transportation research record 1873 (1), 1–8.

Hatefi, S., Jolai, F., 2014. Robust and reliable forward–reverse logistics network design under demand uncertainty and facility disruptions. Applied Mathematical Modelling 38 (9-10), 2630–2647.

Haugh, M., Iyengar, G., Song, I., 2015. A generalized risk budgeting approach to portfolio construction.

Helander, M. E., Melachrinoudis, E., 1997. Facility location and reliable route planning in hazardous material transportation. Transportation science 31 (3), 216–226.

Holeczek, N., 2019. Hazardous materials truck transportation problems: A classification and state of the art literature review. Transportation Research Part D: Transport and Environment 69, 305–328.

Hu, H., Li, X., Zhang, Y., Shang, C., Zhang, S., 2019a. Multi-objective location-routing model for hazardous material logistics with traffic restriction constraint in inter-city roads. Computers & Industrial Engineering 128, 861–876.

Hu, Q., Mehdizadeh, A., Mohabbati Kalejahi, N., Yazdi, M., Cai, M., Vinel, A., Rigdon, S., Davis, K., Megahed, F., 2019b. Bridging the gap between the different research streams of crash risk modeling: areview and perspective on the divide between statistical and optimization approaches. Under review.

Jacobs, T. L., Warmerdam, J. M., 1994. Simultaneous routing and siting for hazardous-waste operations. Journal of urban planning and development 120 (3), 115–131.

Jorion, P., 1997. Value at Risk: The New Benchmark for Controlling Market Risk. McGraw-Hill.

JP Morgan, 1994. Riskmetrics. JP Morgan, New York.

Kang, Y., Batta, R., Kwon, C., 2014. Generalized route planning model for hazardous material transportation with var and equity considerations. Computers & Operations Research 43, 237–247.

Kara, B. Y., Verter, V., 2004. Designing a road network for hazardous materials transportation. Transportation Science 38 (2), 188–196.

Keyvanshokooh, E., Ryan, S. M., Kabir, E., 2016. Hybrid robust and stochastic optimization for closed-loop supply chain network design using accelerated benders decomposition. European Journal of Operational Research 249 (1), 76–92.

Kolm, P. N., Tütüncü, R., Fabozzi, F. J., 2014. 60 years of portfolio optimization: Practical challenges and current trends. European Journal of Operational Research 234 (2), 356–371.

Krokhmal, P., Zabarankin, M., Uryasev, S., 2011. Modeling and optimization of risk. Surveys in Operations Research and Management Science 16 (2), 49 – 66.

Krokhmal, P. A., 2007. Higher moment coherent risk measures. Quant. Finance 7 (4), 373–387. URL http://dx.doi.org/10.1080/14697680701458307

Lee, D.-H., Dong, M., 2008. A heuristic approach to logistics network design for end-of-lease computer products recovery. Transportation Research Part E: Logistics and Transportation Review 44 (3), 455–474.

Li, Z., Ding, R., Floudas, C. A., 2011. A comparative theoretical and computational study on robust counterpart optimization: I. robust linear optimization and robust mixed integer linear optimization. Industrial & engineering chemistry research 50 (18), 10567–10603.

List, G., Mirchandani, P., 1991. An integrated network/planar multiobjective model for routing and siting for hazardous materials and wastes. Transportation Science 25 (2), 146–156.

List, G. F., Turnquist, M. A., 1998. Routing and emergency-response-team siting for high-level radioactive waste shipments. IEEE Transactions on Engineering Management 45 (2), 141–152.

Lohre, H., Opfer, H., Orszag, G., 2014. Diversifying risk parity. Journal of Risk 16 (5), 53–79.

Ma, C., He, R., Pan, F., 2015. Emergency facilities location optimisation for hazardous materials transportation under the background of counterterrorism. International Journal of Computing Science and Mathematics 6 (4), 354–365.

Ma, H., Li, X., 2018. Closed-loop supply chain network design for hazardous products with uncertain demands and returns. Applied Soft Computing 68, 889–899.

Mahmoudabadi, A., 2015. Developing a chaotic pattern of dynamic risk definition for solving hazardous material routing-locating problem. Journal of Loss Prevention in the Process Industries 37, 1–10.

Mahmoudabadi, A., Farokhi, R., Fattahi, A.-A., 2016. Developing a tolerated risk model for solving routing-locating problem in hazardous material management. Journal of Intelligent Transportation and Urban Planning 4 (1), 53–61.

Mahmoudabadi, A., Seyedhosseini, S. M., 2014. Developing a bi-level objective model of risk-cost trade-off for solving locating-routing problem in transportation of hazardous material. International journal of transportation Engineering 1 (3), 173–182.

Maillard, S., Roncalli, T., Teïletche, J., 2010. The properties of equally weighted risk contribution portfolios. The Journal of Portfolio Management 36 (4), 60–70.

Marcotte, P., Mercier, A., Savard, G., Verter, V., 2009. Toll policies for mitigating hazardous materials transport risk. Transportation Science 43 (2), 228–243.

Mausser, H., Romanko, O., 2014. Computing equal risk contribution portfolios. IBM Journal of Research and Development 58 (4), 5–1.

Meiyi, W., Xiang, L., Lean, Y., 2015. Time-dependent fuzzy random location-scheduling programming for hazardous materials transportation. Transportation Research Part C: Emerging Technologies 57, 146–165.

National Transportation Statistics, U.S. Department of Transportation, B. o. T. S., 2018. Tech. rep. URL `https://www.bts.gov/browse-statistical-products-and-data/national-transportation-statistics/national-transportation-6`

Nema, A., Gupta, S., 2003. Multiobjective risk analysis and optimization of regional hazardous waste management system. Practice Periodical of Hazardous, Toxic, and Radioactive Waste Management 7 (2), 69–77.

Nema, A. K., Gupta, S., 1999. Optimization of regional hazardous waste management systems: an improved formulation. Waste Management 19 (7-8), 441–451.

Parragh, S. N., Tricoire, F., 2018. Branch-and-bound for bi-objective integer programming. arXiv preprint arXiv:1809.06823.

Pflug, G. C., 2000. Some remarks on the value-at-risk and the conditional value-at-risk. In: Probabilistic constrained optimization. Springer, pp. 272–281.

PHMSA, 2018. Yearly incident summary report. Tech. rep.
URL `https://hip.phmsa.dot.gov/analyticsSOAP/saw.dll?Dashboard.[Online;accessed28-February-2018`

Pishvaee, M. S., Farahani, R. Z., Dullaert, W., 2010. A memetic algorithm for bi-objective integrated forward/reverse logistics network design. Computers & operations research 37 (6), 1100–1112.

Prékopa, A., 1995. Stochastic Programming. Kluwer Academic Publishers.

Qian, E., 2005. Risk parity portfolios: Efficient portfolios through true diversification. Panagora Asset Management.

Rabbani, M., Heidari, R., Farrokhi-Asl, H., Rahimi, N., 2018. Using metaheuristic algorithms to solve a multi-objective industrial hazardous waste location-routing problem considering incompatible waste types. Journal of Cleaner Production 170, 227–241.

Rabbani, M., Heidari, R., Yazdanparast, R., 2019. A stochastic multi-period industrial hazardous waste location-routing problem: Integrating nsga-ii and monte carlo simulation. European Journal of Operational Research 272 (3), 945–961.

ReVelle, C., Cohon, J., Shobrys, D., 1991. Simultaneous siting and routing in the disposal of hazardous wastes. Transportation Science 25 (2), 138–145.

Rockafellar, R. T., Uryasev, S., 2000. Optimization of conditional value-at-risk. Journal of Risk 2, 21–41.

Rockafellar, R. T., Uryasev, S., 2002. Conditional value-at-risk for general loss distributions. Journal of Banking and Finance 26 (7), 1443–1471.

Roncalli, T., 2013. Introduction to risk parity and budgeting. CRC Press.

Roncalli, T., Weisang, G., 2016. Risk parity portfolios with risk factors. Quantitative Finance 16 (3), 377–388.

Saccomanno, F., Allen, B., 1987. Locating emergency response capability for dangerous goods incidents on a road network. Transportation of Hazardous Materials, 1.

Samanlioglu, F., 2013. A multi-objective mathematical model for the industrial hazardous waste location-routing problem. European Journal of Operational Research 226 (2), 332–340.

Sattarzadeh, A., 2015. Hazmat Network Design Considering Risk and Cost Equity. State University of New York at Buffalo.

Shapiro, A., Dentcheva, D., Ruszczyński, A., 2014. Lectures on stochastic programming, 2nd Edition. Vol. 9 of MOS-SIAM Series on Optimization. Society for Industrial and Applied Mathematics (SIAM), Philadelphia, PA; Mathematical Optimization Society, Philadelphia, PA, modeling and theory.

Soyster, A. L., 1973. Convex programming with set-inclusive constraints and applications to inexact linear programming. Operations research 21 (5), 1154–1157.

Stefanovits, D., 2010. Equal contributions to risk and portfolio construction. Masters thesis, ETH Zürich.

Stidsen, T., Andersen, K. A., 2018. A hybrid approach for biobjective optimization. Discrete Optimization 28, 89–114.

Stidsen, T., Andersen, K. A., Dammann, B., 2014. A branch and bound algorithm for a class of biobjective mixed integer programs. Management Science 60 (4), 1009–1032.

Stowers, C. L., Palekar, U. S., 1993. Location models with routing considerations for a single obnoxious facility. Transportation Science 27 (4), 350–362.

Sun, L., Karwan, M. H., Kwon, C., 2015. Robust hazmat network design problems considering risk uncertainty. Transportation Science 50 (4), 1188–1203.

Sun, L., Karwan, M. H., Kwon, C., 2016. Implications of cost equity consideration in hazmat network design. Transportation Research Record: Journal of the Transportation Research Board (2567), 67–77.

Taslimi, M., Batta, R., Kwon, C., 2017. A comprehensive modeling framework for hazmat network design, hazmat response team location, and equity of risk. Computers & Operations Research 79, 119–130.

Tavakkoli-Moghaddam, R., Abolghasem, A., Mahmoudabadi, A., 2015. Comparison between combined and separate approaches for solving a location-routing problem in hazardous materials transportation. International Journal of Transportation Engineering 3 (1), 67–77.

Toumazis, I., 2015. Hazmat data.
URL http://toumiak.com/research.php

Toumazis, I., Kwon, C., 2015. Worst-case conditional value-at-risk minimization for hazardous materials transportation. Transportation Science 50 (4), 1174–1187.

Toumazis, I., Kwon, C., Batta, R., 2013. Value-at-risk and conditional value-at-risk minimization for hazardous materials routing. In: Handbook of OR/MS Models in Hazardous Materials Transportation. Springer, pp. 127–154.

Ulungu, E. L., Teghem, J., 1995. The two phases method: An efficient procedure to solve bi-objective combinatorial optimization problems. Foundations of Computing and Decision Sciences 20 (2), 149–165.

Verter, V., Kara, B. Y., 2008. A path-based approach for hazmat transport network design. Management Science 54 (1), 29–40.

Vinel, A., 2015. Mathematical programming techniques for solving stochastic optimization problems with certainty equivalent measures of risk. Ph.D. thesis, The University of Iowa.

Vinel, A., Krokhmal, P. A., 2017. Certainty equivalent measures of risk. Annals of Operations Research 249 (1), 75–95.
URL http://dx.doi.org/10.1007/s10479-015-1801-0

Wang, J., Kang, Y., Kwon, C., Batta, R., 2012. Dual toll pricing for hazardous materials transport with linear delay. Networks and Spatial Economics 12 (1), 147–165.

Wei, M., Yu, L., Li, X., 2015. Credibilistic location-routing model for hazardous materials transportation. International Journal of Intelligent Systems 30 (1), 23–39.

Xin, C., Qingge, L., Wang, J., Zhu, B., 2015. Robust optimization for the hazardous materials transportation network design problem. Journal of Combinatorial Optimization 30 (2), 320–334.

Xu, J., Gang, J., Lei, X., 2013. Hazmats transportation network design model with emergency response under complex fuzzy environment. Mathematical Problems in Engineering 2013.

Yen, J. Y., 1971. Finding the k shortest loopless paths in a network. management Science 17 (11), 712–716.

Yilmaz, O., Kara, B. Y., Yetis, U., 2017. Hazardous waste management system design under population and environmental impact considerations. Journal of environmental management 203, 720–731.

Yin, H., Sun, H., Peng, S., Wu, J., Ge, Y.-e., Chen, Y., 2019. Designing a safe and fair network for hazmat road transportation. Journal of Transportation Safety & Security, 1–19.

Yu, H., Solvang, W., 2016. An improved multi-objective programming with augmented ε-constraint method for hazardous waste location-routing problems. International journal of environmental research and public health 13 (6), 548.

Zhang, M., Ma, Y., Weng, K., 2005. Location-routing model of hazardous materials distribution system based on risk bottleneck. In: Proceedings of ICSSSM'05. 2005 International Conference on Services Systems and Services Management, 2005. Vol. 1. IEEE, pp. 362–368.

Zhao, J., Huang, L., Lee, D.-H., Peng, Q., 2016. Improved approaches to the network design problem in regional hazardous waste management systems. Transportation research part E: logistics and transportation review 88, 52–75.

Zhao, J., Ke, G. Y., 2017. Incorporating inventory risks in location-routing models for explosive waste management. International Journal of Production Economics 193, 123–136.

Zhao, J., Verter, V., 2015. A bi-objective model for the used oil location-routing problem. Computers & Operations Research 62, 157–168.

Zhao, J., Zhu, F., 2016. A multi-depot vehicle-routing model for the explosive waste recycling. International Journal of Production Research 54 (2), 550–563.

Zhao, R., Liu, Y., Zhang, N., Huang, T., 2017. An optimization model for green supply chain management by using a big data analytic approach. Journal of Cleaner Production 142, 1085–1097.

Zografos, K., Samara, S., 1989. A combined location-routing model for hazardous waste transportation and disposal. Transportation Research Record 1245, 52–59.

Zografos, K. G., Androutsopoulos, K. N., 2008. A decision support system for integrated hazardous materials routing and emergency response decisions. Transportation Research Part C: Emerging Technologies 16 (6), 684–703.